Underwater Acoustic Monitoring of the Tappan Zee Bridge Pile Installation Demonstration Project

Comprehensive Report

Submitted to:
AECOM

Authors:
Bruce Martin
Alexander MacGillivray
Jeff MacDonnell
Jonathan Vallarta
Terry Deveau
Graham Warner
David Zeddies

2012 July 7

P001171-001
Document 00355
Version 1.1

JASCO Applied Sciences
Suite 202, 32 Troop Ave.
Dartmouth, NS, B3B 1Z1, Canada
Phone: +1.902.405.3336
Fax: +1.902.405.3337
www.jasco.com

Suggested citation:

Martin, B., A. MacGillivray, J. MacDonnell, J. Vallarta, T. Deveau, G. Warner, and D. Zeddies. 2012. *Underwater Acoustic Monitoring of the Tappan Zee Bridge Pile Installation Demonstration Project: Comprehensive Report*. JASCO Document 00355, Version 1.1. Technical report for AECOM by JASCO Applied Sciences.

Contents

Figures

Tables

Executive Summary

JASCO measured underwater sound from pile driving as part of the Tappan Zee Bridge Pile Installation Demonstration Project (PIDP). The purpose of the hydroacoustic monitoring project was to record underwater noise levels generated by the PIDP pile driving operations and evaluate the effectiveness of these five noise attenuation systems (NASs):

- Unconfined Single-Tier Air Bubble Curtain
- Unconfined Multi-Tier Air Bubble Curtain
- Hard Bubble Noise Attenuation System
- Isolation Casing and Bubble System
- Two-Stage Confined Bubble Curtain System

We compared noise level measurements from the PIDP with pre-program model estimates of the distances at which impact pile driving sound levels fell below the National Marine Fisheries Service (NMFS) physiological and behavioral threshold criteria.

During the PIDP, vibratory and impact pile driving were used to install seven cylindrical steel piles at four test sites:

- Site 1 (West side of river channel): two 4-foot piles in 9-foot deep water.
- Site 2 (West side of river channel): two 4-foot piles in 11-foot deep water.
- Site 3 (West side of river channel): one 4-foot and one 8-foot pile in 16-foot deep water.
- Site 4 (East side of river channel): one 10-foot pile in 16-foot deep water.

Previous modeling of sound levels assumed that noise attenuation systems (NASs) could reduce sound exposure levels (SELs) from impact hammer pile driving by 10 dB. The PIDP evaluated the above listed NASs against the 10 dB SEL criterion.

JASCO measured sound levels at a nominal range of 33 feet from the test piles and used autonomous acoustic recorders to collect data at ranges of 1000–10,000 feet from the piles. By comparing the measurements to the sound levels previously modeled by JASCO, we offer an opinion of the accuracy of the modeled results for predicting the effects of the bridge construction pile driving. The test pile installation differed from the previously modeled scenarios in that the contractor used more vibratory hammer driving and less impact hammer driving, and that construction barges with drafts between six and eight feet surrounded the test piles, which obstructed sound transmission.

Measured propagation losses for impact pile driving were 30 to 40 $\log_{10} r$, much stronger than the losses of approximately 20 $\log_{10} r$ the model predicted. Therefore, we found that distances to the peak SPL, rms SPL, and cSEL thresholds were smaller than predicted in the Draft Environmental Impact Statement (DEIS) and the Biological Opinion. We applied linear regression analysis to the acoustic data to estimate distances where impact pile driving exceeded the NMFS physiological and behavioral thresholds (Table 1 - Table 3).

Table 1. Measured versus modeled distances to the 206 dB re 1 µPa peak SPL physiological threshold for unmitigated and mitigated impact pile driving.

		206 dB re 1 µPa Peak SPL	
Pile Diameter (ft)	Location	Modeled distance (ft)	Max. measured distance (ft)
Unmitigated (no NAS)			
4	PLT2	31	42
8	PLT3	146	101
10	PLT4	573	71
Mitigated (with NAS)			
4	PLT2	<10	20
8	PLT3	101	38
10	PLT4	166	14

Table 2. Measured versus modeled distances to the 187 dB re 1 µPa^{2}s cSEL physiological threshold for unmitigated and mitigated impact pile driving. The total number of impact hammer blows is indicated in parentheses.

		187 dB re 1 µPa^{2}s cSEL	
Pile Diameter (ft)	Location	Modeled distance[1] (ft)	Max. measured distance (ft)
Unmitigated (no NAS)			
4	PLT2	1263 (15400)	192 (1394)
8	PLT3	3238 (3400)	351 (2181)
10	PLT4	5013 (3000)	282 (1031)
Mitigated (with NAS)			
4	PLT2	825 (15400)	114 (1394)
8	PLT3	1950 (3400)	190 (2181)
10	PLT4	3275 (3000)	125 (1031)

[1] Assumed equal to 50% of the north-south extent of the 187 dB contour from the Biological Opinion, dated 7 March, 2012.

Table 3. Measured versus modeled distances to the 150 dB re 1 µPa rms SPL behavioral threshold for unmitigated and mitigated impact pile driving.

		150 dB re 1 µPa rms SPL	
Pile Diameter (ft)	Location	Modeled distance[1] (ft)	Max. measured distance (ft)
Unmitigated (no NAS)			
4	PLT2	2000	452
8	PLT3	6350	809
10	PLT4	9500	822
Mitigated (with NAS)			
4	PLT2	1250	306
8	PLT3	4600	462
10	PLT4	6750	429

[1] Assumed equal to 50% of the north-south extent of the 150 dB contour from the Biological Opinion, dated 7 March, 2012.

Data from the current study indicate the modeled effects of pile driving are conservative with respect to expected sound levels during actual bridge construction. We believe the main reason for the large difference between modeled and measured sound propagation was the presence of construction barges surrounding the piles. The barges likely acted as barriers that prevented sound from transmitting outside the barge area, thereby decreasing the long-range peak SPL, rms SPL, and cSEL. If construction plans call for barges to surround each pile during bridge replacement, we expect the barges will attenuate the sound as measured during the PIDP.

All the tested NASs met the criterion of 10 dB SEL attenuation. Based on short-range measurements, acoustic attenuations of the five NASs were:

- 12.2–17.0 dB reduction in peak SPL
- 10.8–16.1 dB reduction in rms SPL
- 9.9–13.7 dB reduction in SEL/cSEL

We cannot comment on the stability of NASs with respect to river currents because the experimental results were inconclusive. Each test pile required less than two hours of impact pile driving and the river conditions were stable throughout each event. Therefore, we do not have sufficient data for any of the test piles to compare NAS performance in high-current and low-current conditions. Nonetheless, we expect the performance of the confined NASs would be more stable in running current than the unconfined NASs.

The pile driving contractor is expected to dredge large channels at the construction site to simplify barge movements. On the west side of the river the channel design is 16-feet deep, 500-feet wide and 7000-feet long channel. The channel sides will be armored with rock. Sound levels will likely be higher in the dredged channel because in deeper water pile vibrations couple better to the water column and sound generally propagates to greater distances. During the PIDP, sound levels were highest at locations where the mean water depth was 16 feet. Sound levels from pile driving in a dredged channel should be comparable to sound levels at these locations, which were below the modeled levels.

1. Introduction

JASCO performed hydroacoustic monitoring of the Tappan Zee Bridge Pile Installation Demonstration Project (PIDP) for AECOM in support of the Tappan Zee Bridge/I-287 Environmental Review. This report presents hydroacoustic measurements of the installation of seven PIDP test piles from 28 April through 18 May 2012. The purpose of the hydroacoustic monitoring program was to record underwater noise levels generated by PIDP pile driving operations and to evaluate the effectiveness of the noise attenuation systems (NASs) employed.

1.1. Test Piles

Vibratory and impact hammers were used to drive seven cylindrical steel test piles at four locations along the proposed bridge span (Figure 1). Each of the test piles consisted of two separate segments (top and bottom). Vibratory hammers were used to drive the bottom segments. A combination of vibratory and impact hammers were used to drive the top segments. Table 4 lists the specifications for each test pile monitored. The bottom segments of Test Piles 2A, 2B, and 3B were not monitored.

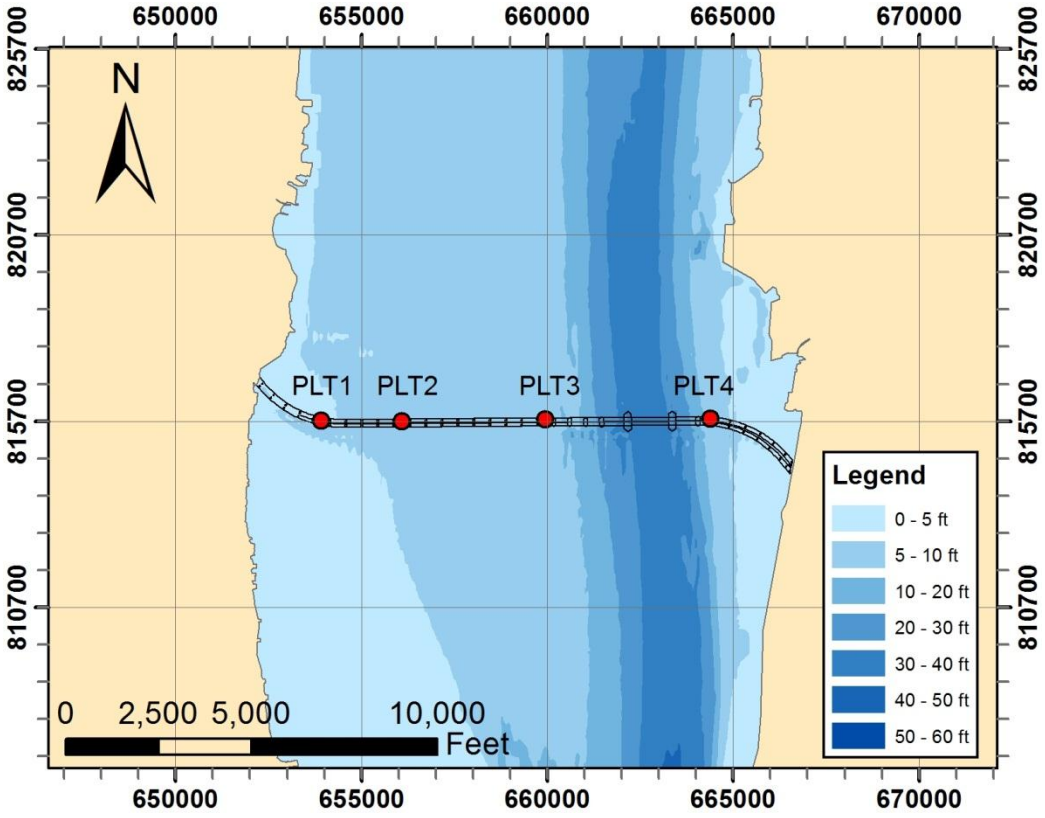

Figure 1. PIDP test pile locations (red circles), in relation to the existing Tappan Zee bridge span. Coordinates are NY State Plane East (NAD83).

Table 4. Specifications of test piles driven during the Tappan Zee Bridge Pile Installation Demonstration Project.

Test pile	Location	Diameter (ft)	Wall thickness (in)	Segment	Vibratory Driver	Impact Hammer	Length (ft)	Date (2012)	Mean water depth (ft)
1A	PLT1	4	1 5/8	Bottom	ICE 66	–	160	02-May	9
				Top	–	MHU 270T	140	05-May	9
1B	PLT1	4	1 5/8	Bottom	ICE 66	–	160	02-May	9
				Top	ICE 66	MHU 270T	140	05-May	9
2A	PLT2	4	1 1/4	Top	ICE 66, Super Kong 600	MHU 270T	140	16-May	11
2B	PLT2	4	1 1/4	Top	ICE 66, Super Kong 600	MHU 270T	140	16-May	11
3A	PLT3	4	1 1/8	Bottom	ICE 66	–	140	28-Apr	16
				Top	–	MHU 800S	80	08-May	16
3B	PLT3	8	2	Top	Super Kong 600	MHU 800S	80	18-May	16
4A	PLT4	10	1 3/4	Bottom	Super Kong 600	–	80	09-May	16
				Top	Super Kong 600	MHU 800S	60	12, 14 May	16

1.2. Pile Drivers

Two vibratory hammers and two impact hammers were used during the PIDP (Table 5, Table 6, Figure 2, Figure 3). Appendix E contains pile driving logs as well as details about the hammers and drivers provided by the construction contractor.

Table 5. Vibratory pile driver specifications.

Model	Max. vibrations per minute	Eccentric moment (in-lb)	Weight (tons)
ICE 66 vibratory driver	1800	6,600	13.1
Super Kong 600 vibratory hammer	1400	20,000	34

Table 6. Hydraulic impact hammer specifications.

Model	Max. hammer energy (kips-foot)	Ram weight (tons)	Total hammer weight (tons)
MENCK MHU 800S	605	50	87.7
MENCK MHU 270T	221	17.9	34.0

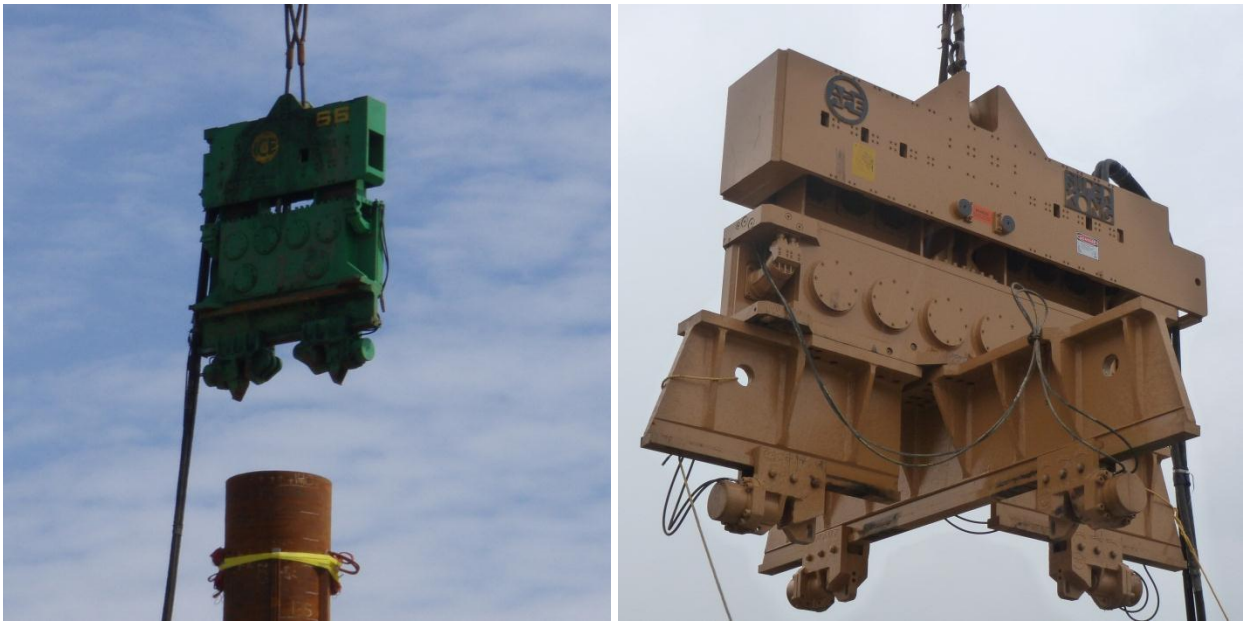

Figure 2. (Left) ICE 66 vibratory driver lowering onto Test Pile 3A during driving on 28 April 2012. (Right) Super Kong 600 vibratory hammer during driving on 9 May 2012.

Figure 3. (Left) MENCK MHU 800S hydraulic impact hammer being lowered onto Test Pile 4A on 14 May 2012. (Right) MENCK MHU 270T hydraulic impact hammer being lowered onto Test Pile 1A on 5 May 2012.

1.3. Noise Attenuation Systems

Five different noise attenuation systems (NASs) were tested during the PIDP. The NASs reduce underwater sound levels produced by impact hammer pile driving. Logs of noise attenuation airflow settings are given in Appendix F.

1.3.1. Unconfined Single-Tier Air Bubble Curtain

An Unconfined Single-Tier Air Bubble Curtain NAS was employed at Test Pile 1A on 5 May 2012 (Figure 4) and at Test Pile 4A on 9 and 12 May 2012. This system employs a single air distribution manifold, which consists of an annular ring of tubing deployed around the base of the pile on the river bottom. Large compressors provide a continuous supply of air to the distribution ring via several hoses. Air is released through small holes in the distribution ring to create a curtain of bubbles around the pile. The curtain of air bubbles inhibits transmission of pile driving sound to the surrounding water.

Figure 4. Base of Test Pile 1A showing air bubbles from the Unconfined Single-Tier Air Bubble Curtain, 5 May 2012.

1.3.2. Unconfined Multi-Tier Air Bubble Curtain

An Unconfined Multi-Tier Air Bubble Curtain NAS was used at Test Pile 3A on 8 May 2012 and Test Pile 2A on 16 May 2012. This system employs multiple air distribution manifolds, which consist of an annular ring of tubing deployed around the pile on the river bottom. Large compressors provide a continuous supply of air to the distribution rings via several hoses. Air is released through small holes in the distribution rings to create a curtain of bubbles around the pile. The curtain of air bubbles inhibits transmission of pile driving sound to the surrounding water. The turbidity curtain was the only enclosure we put around the bubble curtain to prevent the river current from disrupting the bubbles.

1.3.3. Hard Bubble Noise Attenuation System

A Gunderboom Hard Bubble NAS was used at Test Pile 1B on 5 May 2012. The Hard Bubble NAS consists of different sizes of air-filled rigid plastic balls inside a fabric sheath suspended around the pile (Figure 5). The larger balls are pressurized to adjust their resonant vibration frequencies, which alters the attenuation characteristics of the Hard Bubble NAS.

Figure 5. Photo of the base of Test Pile 1B showing the containment curtain for the Hard Bubble Noise Attenuation System (yellow and gray) and the turbidity curtain top floats (orange).

1.3.4. Isolation Casing and Bubble System

An Isolation Casing and Bubble NAS was used at Test Pile 2B on 16 May 2012 (Figure 6). This system employs a single air distribution manifold, which is an annular ring of tubing deployed around the pile on the river bottom. A solid steel isolation casing surrounds the pile and air distribution manifold to protect the bubbles from river currents. Large compressors provide a continuous supply of air to the distribution rings via several hoses. Air is released through small holes in the distribution rings to create a curtain of air bubbles around the pile. The curtain of air bubbles inhibits transmission of pile driving sound to the surrounding water.

Figure 6. Photo inside the isolation casing at Test Pile 2B showing the air bubbles from the Isolation Casing and Bubble System, 16 May 2012.

1.3.5. Two-Stage Confined Bubble Curtain System

A Two-Stage Confined Bubble Curtain NAS was used at Test Pile 3B on 18 May 2012 and Test Pile 4A on 14 May (Figure 7).

This system consists of two principal noise attenuation elements:

- A single tier of perforated aeration pipes that rest on the river bottom and discharge compressed air to the water column through bubble release holes.
- A full water column barrier through which compressed air flows, providing further noise attenuation.

The curtain of air bubbles inhibits transmission of pile driving sound to the surrounding water. Air is an excellent hydroacoustic barrier because it is highly compressible compared to water; it and therefore conducts sound poorly. The enclosure around the bubble curtain prevents the river current from dispersing the bubbles.

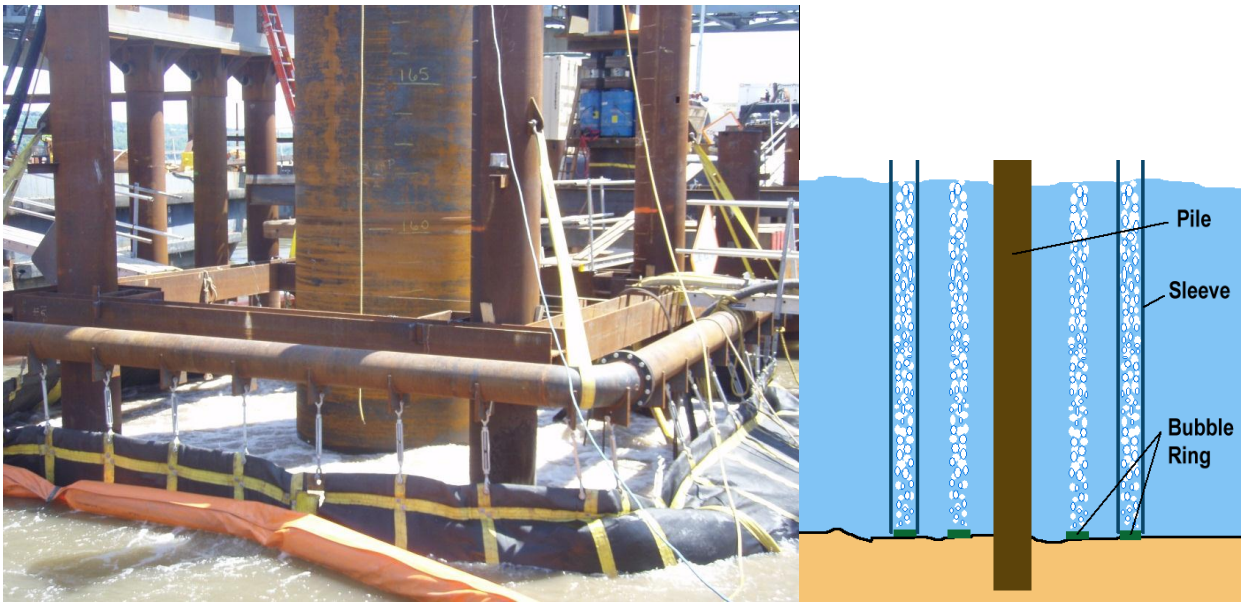

Figure 7. Base of Test Pile 3B showing air bubbles from the Two-Stage Confined Bubble Curtain System, 18 May 2012.

1.4. Pile Driving Equipment Barges

The pile-driving contractor, Trevcon, deployed several barges at each test pile site. Trevcon used these barges as a platform for heavy equipment (cranes, generators, and air compressors) and as a staging area for construction materials. Engineering testing, including short-range hydroacoustic monitoring, was also carried out from the Trevcon barges. The barges almost entirely surrounded the test piles (Figure 8). The barges had drafts between 6 and 10 feet, which occupied a considerable portion of the water column.

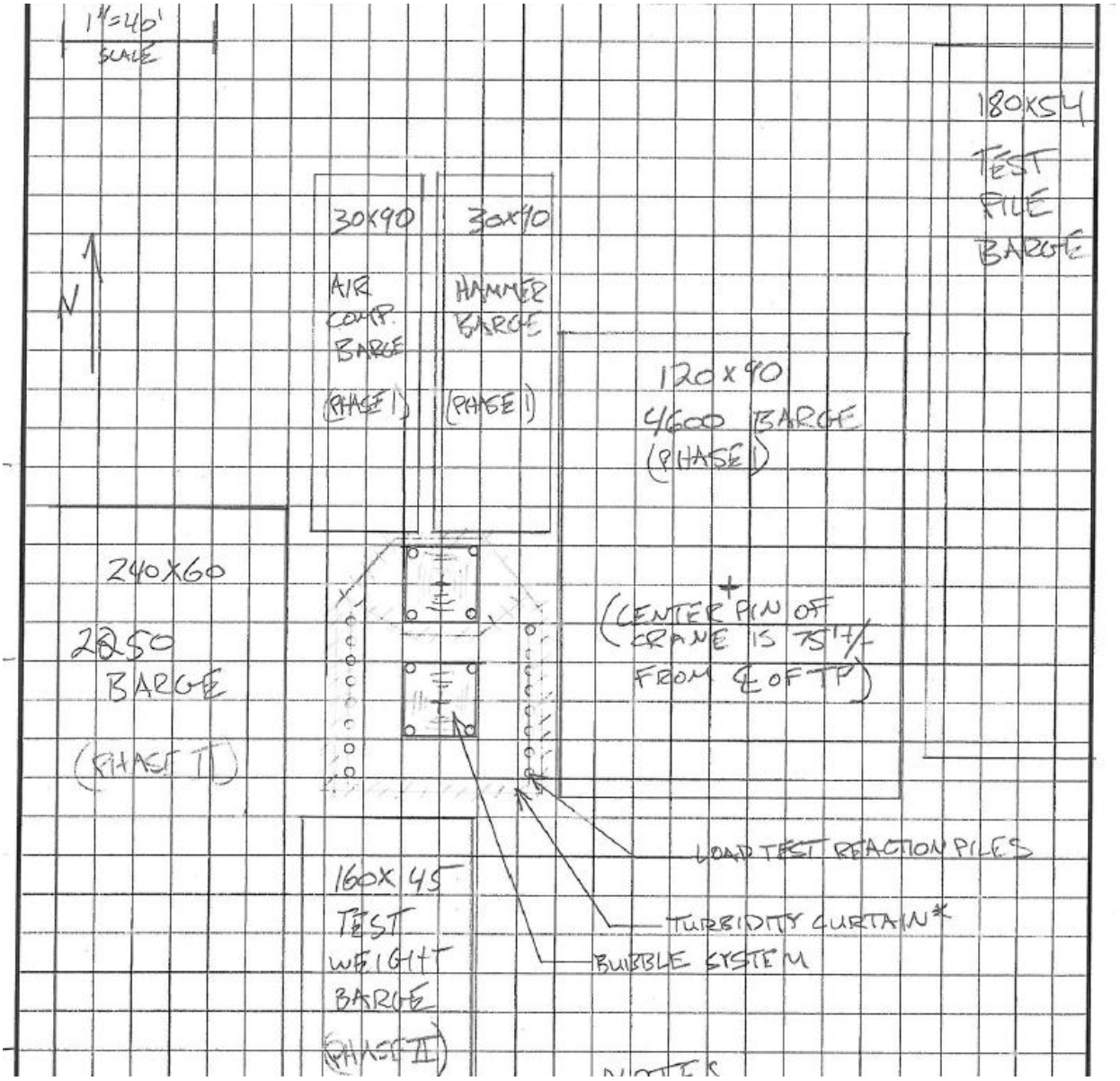

Figure 8. Planned barge arrangement around Test Piles 3A and 3B.

2. Methods

2.1. Hydroacoustic Monitoring

This section describes the equipment used for short and long-range hydroacoustic monitoring during the PIDP.

2.1.1. Short-range monitoring

JASCO performed real-time acoustic monitoring at short ranges to the test piles from the noise attenuation barge. The short-range hydroacoustic measurements were performed with two JASCO Acoustic Data Acquisition and Monitoring Systems (ADAMSs, Figure 9), which monitor and record acoustic information in real time. The acoustic signal can be viewed as it is received with SpectroPlotter, JASCO's custom software, which detects acoustic events by displaying the signal amplitude and spectrum while it continuously processes the data. The incoming acoustic signal is also recorded as WAV files, which provides data for a comprehensive post-analysis.

Each ADAMS streamed acoustic data from both a high- and low-sensitivity hydrophone to a laptop onboard the barge. We used a RESON TC4034 low-sensitivity hydrophone to sample the high sound levels generated by impact and vibratory pile driving, and a RESON TC4032 high-sensitivity hydrophone to sample the lower background sound levels during period between pile driving. The hydrophones of both ADAMS were affixed to a mounting plate deployed on the river bottom at a nominal distance of 10 m (33 ft) from the center of the test pile (Figure 10).

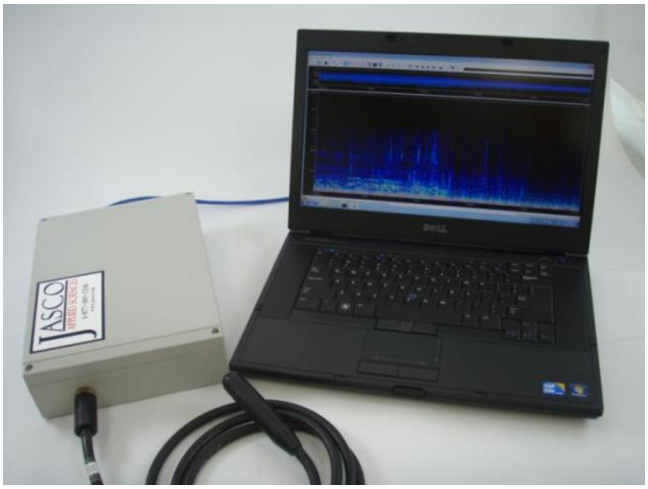

Figure 9. The JASCO Acoustic Data Acquisition and Monitoring System (ADAMS), shown with one hydrophone and a laptop, used for real-time monitoring and acquiring short-range measurements.

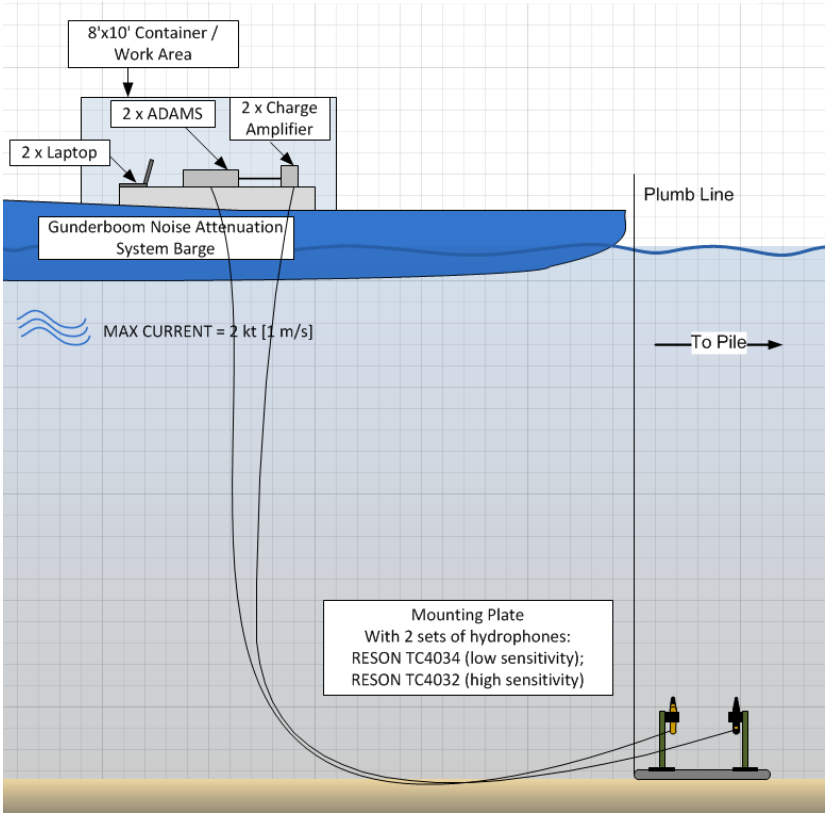

Figure 10. The two short-range hydroacoustic monitoring apparatuses, each consisting of two hydrophones secured to a single mounting plate, extension cables, charge amplifier, ADAMS, and laptop. Figure is not to scale.

Each ADAMS continuously sampled the TC4034 and TC4032 hydrophone channels at 64,000 samples per second. The total acoustic recording bandwidth was 5 Hz to 31 kHz, which is within the linear frequency range of both hydrophones (±3 dB). The ADAMS specifications are as follows:

- Input channel gain: 0 dB
- Input channel range: ±2.5 V
- Broadband dynamic range: 104 dB
- Broadband noise floor and peak level of low-sensitivity channel: 132 dB re 1 µPa
- Broadband noise floor, and peak level of high-sensitivity channel: 72 dB re 1 µPa

The RESON TC4032 high-sensitivity hydrophone has a built-in preamplifier, whereas the RESON TC4034 low-sensitivity hydrophone uses a RESON EC6067 programmable charge amplifier to condition the hydrophone signal (Table 7). The charge amplifier was configured as a −10 dB attenuator to permit sampling of high-level signals on the low-sensitivity hydrophone (up to 238 dB re 1 µPa peak level). Both hydrophones were connected to the ADAMS with a 50 m shielded cable.

Table 7. Nominal sensitivity of the low- and high-sensitivity hydrophones used for short-range hydroacoustic monitoring.

Hydrophone	Source targeted	Sensitivity (dB re 1 V/µPa)	Amplifier gain (dB)	Max. signal level (dB re 1 µPa)
TC4034	Impact and vibratory pile driving	−218	−10	236
TC4032	Background noise	−170	0	176

A steel mounting plate, which keeps the hydrophones precisely located with respect to one another during deployment, allows researchers to accurately identify where the hydrophones are relative to the pile. From the deck of the barge, the mounting plate was lowered to a specified location on the riverbed using a system of bridle lines. Once the mounting plate was on the riverbed, the location of the hydrophones was determined with a vertical plumb line affixed to the plate. A Leica DISTO D5 digital laser range finder (0.1 ft accuracy) was used to determine the distance from the measurement point to the pile wall.

The hydrophone mount (Figure 11) is designed to minimize resonant vibrations of the hydrophones by the following means:

- Rotating the U-channels 90° for each post to eliminate preferred vibration directions.
- Coupling all the posts together to increase their effective mass and reduce the resonant frequency and magnitude of induced vibrations.
- Decreasing the number of mounting components that could vibrate against one another.

Figure 11. The hydrophone mounting plate prepared for deployment for short-range hydroacoustic monitoring. The smaller RESON TC4034 low-sensitivity hydrophones are top left and bottom right; the larger RESON TC4032 high-sensitivity hydrophones are bottom left and top right. Each pair of hydrophones is connected to a JASCO ADAMS for monitoring in real time and recording.

Two ADAMSs recorded sound at short ranges from the seven test piles between 28 April and 18 May 2012 (Table 8).

Table 8. Summary of short-range monitoring measurements.

Test Pile	Segment	Date (2012)	Hammer type	NAS	Distance to pile wall
1A	Bottom	2 May	Vibratory	-	32’8”
	Top	5 May	Vibratory then Impact	Unconfined Single-Tier Bubble Curtain	33’1”, 59’10”
1B	Bottom	2 May	Vibratory	Hard Bubble System deployed but inactive	33’10”
	Top	5 May	Vibratory then Impact	Hard Bubble System	30’10”
2A	Top	16 May	Vibratory then Impact	Unconfined Multi-Tier Bubble Curtain	33’2”
2B	Top	16 May	Vibratory then Impact	Isolation Casing and Bubble System	33’5”
3A	Bottom	28 Apr	Vibratory	-	45’10”
	Top	8 May	Impact	Unconfined Multi-Tier Bubble Curtain	37’8”
3B	Top	18 May	Vibratory Impact	Two-Stage Confined Bubble Curtain	36’9” 29’8”
4A	Bottom	9 May	Vibratory	-	30’0”
	Top	12 May	Vibratory	-	31’5”
		14 May	Impact	Two-Stage Confined Bubble Curtain	29’7”

2.1.2. Long-range monitoring

JASCO used 12 Autonomous Multichannel Acoustic Recorders (AMARs) for long-range acoustic monitoring. We deployed one AMAR at each monitoring station. Table 9 lists the AMAR stations and the associated deployment and retrieval times; Figure 12 maps the AMAR stations.

Each AMAR continuously recorded at least one channel of acoustic data using an M8K hydrophone with nominal sensitivity of −212 dB re V/µPa. The AMARs at Stations 1 and 10 recorded two channels of acoustic data: one channel with an M8K hydrophone, the other channel with an M8E hydrophone (nominal sensitivity −164.7 dB re V/µPa). The AMARs recorded 24-bit samples at 64,000 samples per second. The total acoustic recording bandwidth was 5 Hz to 31 kHz, which is within the linear frequency range of both hydrophones (±3 dB). The AMAR specifications are as follows:

- Input channel gain: 0 dB
- Input channel range: ±2.5 V
- Broadband dynamic range: 104 dB
- Broadband noise floor and peak level with the M8K hydrophone: 116 dB re 1 µPa
- Broadband noise floor and peak level with the M8E hydrophone: 67 dB re 1 µPa

Table 9. Locations (datum NAD83) and deployment times (UTC) of the long-range monitoring AMAR stations deployed in Tappan Zee Reach.

Station	Latitude	Longitude	Deployment time	Retrieval time
1	41°02′41.99″ N	73°52′46.57″ W	2012-04-23 15:38	2012-05-19 13:58
2	41°03′32.08″ N	73°52′46.37″ W	2012-04-23 19:52	2012-05-19 22:34
3	41°03′56.07″ N	73°52′47.11″ W	2012-04-23 15:58	2012-05-19 20:50
4	41°04′21.72″ N	73°54′33.55″ W	2012-04-23 21:07	2012-05-19 16:30
5	41°04′21.71″ N	73°53′53.98″ W	2012-04-23 20:42	Not recovered
6	41°04′23.35″ N	73°53′18.81″ W	2012-04-23 20:28	2012-05-19 15:09
7	41°04′23.20″ N	73°52′39.44″ W	2012-04-23 20:07	2012-05-19 14:39
8	41°04′41.37″ N	73°54′32.69″ W	2012-04-23 17:47	2012-05-19 18:53
9	41°04′41.08″ N	73°52′59.39″ W	2012-04-23 16:11	2012-05-19 20:26
10	41°05′05.96″ N	73°54′33.02″ W	2012-04-23 17:32	2012-05-19 16:53
11	41°05′05.14″ N	73°52′58.98″ W	2012-04-23 16:39	2012-05-19 20:04
12	41°05′51.72″ N	73°52′59.28″ W	2012-04-23 16:58	2012-05-19 19:31

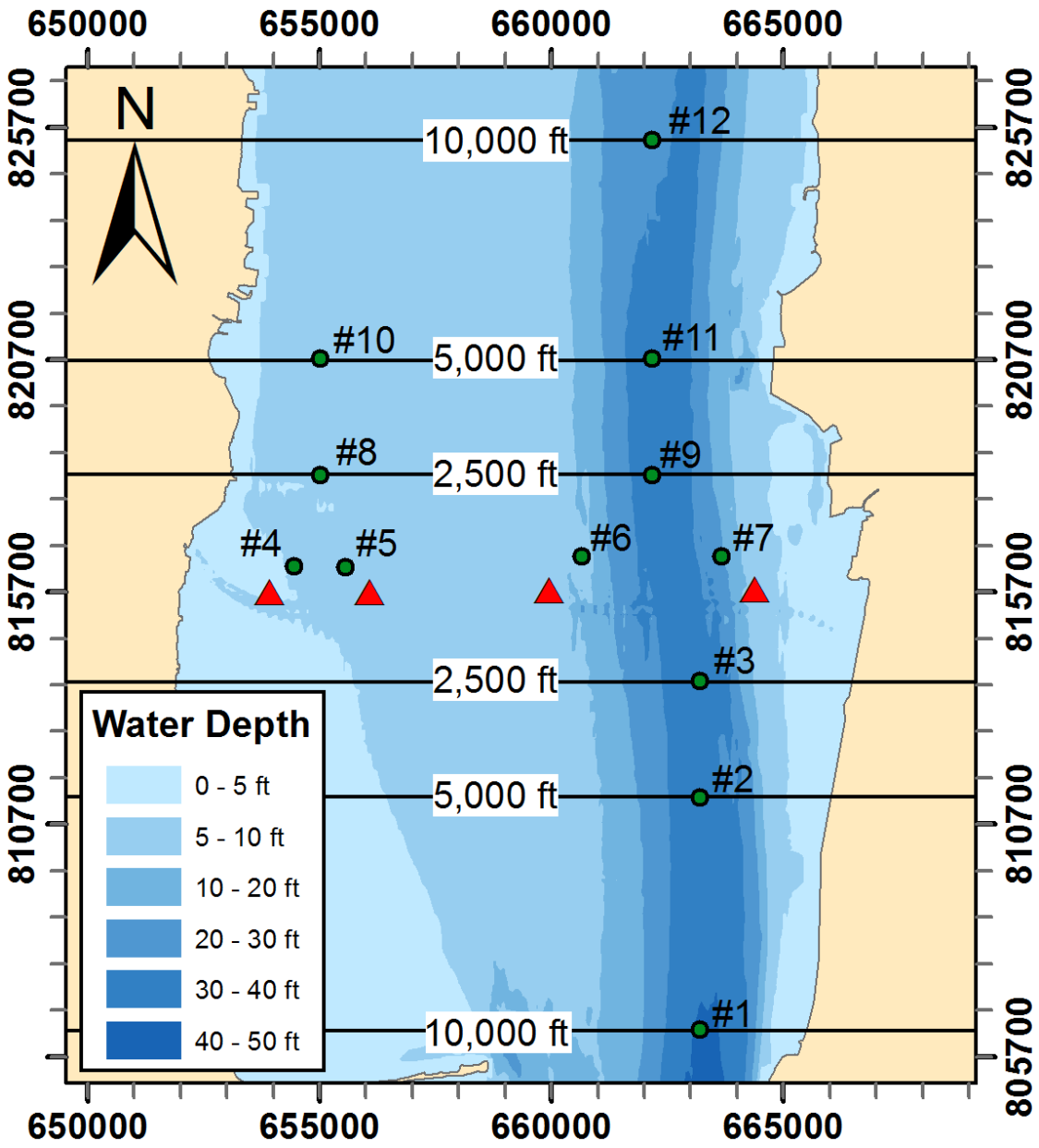

Figure 12. AMAR stations (white circles) and pile locations (red squares) in Tappan Zee Reach. Distances shown on the map are measured upriver and downriver from the test piles. Coordinates are NY State Plane East (NAD83).

Each AMAR was lowered to the river bottom from the *M/V George*. The location of the AMAR was recorded with a handheld GPS accurate to 10 ft. The AMAR was mounted on a mooring plate, which was connected to an anchor with at least 250 ft of ground line (Figure 13).

The AMARs were retrieved from the *M/V George* by grappling the ground line and using a winch to bring the AMAR and anchor onboard.

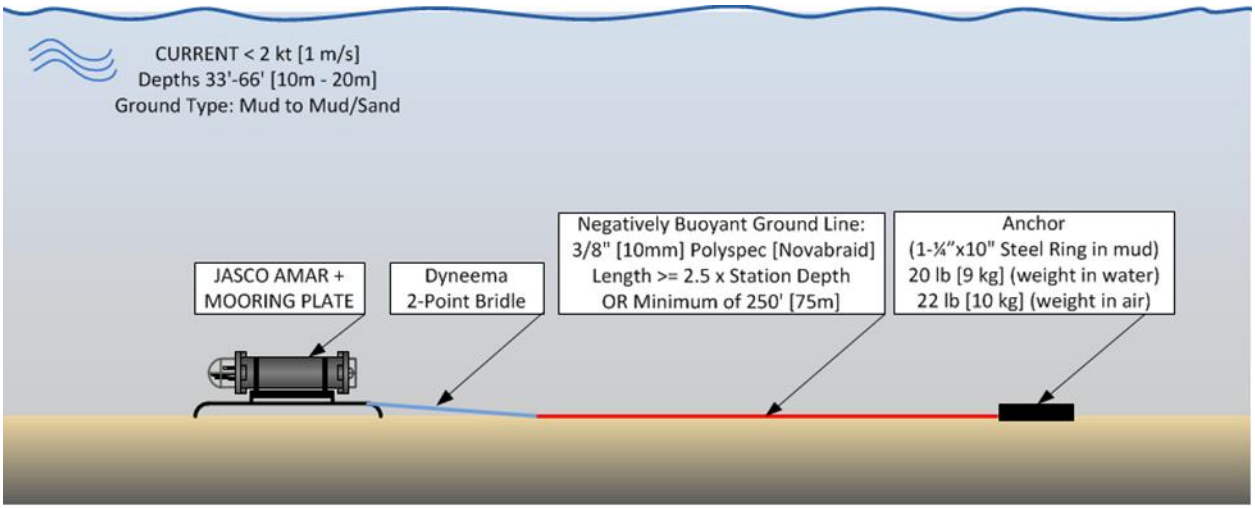

Figure 13. AMAR mooring configuration for long-range measurements.

2.1.3. Hydrophone calibrations

A GRAS 42AC pistonphone calibrator, which is NIST traceable, was used to verify the sensitivity of the recording apparatus as a whole, i.e., the hydrophone, pre-amplifier, and ADAMS for both lab and field calibrations. Single-frequency calibrations of each hydrophone channel were performed in the lab before mobilization and in the field before each deployment. The pistonphone produces a known pressure signal on the hydrophone element (a 250 Hz sinusoid) which verifies the pressure response of the recording system. Each hydrophone model has a custom-fit adapter that couples it to the pistonphone (Figure 14). Ambient atmospheric pressure was measured with a Garmin GPSMap 76CX (at left of Figure 14) to compensate for deviations in ambient pressure (from the nominal 1 atm) and increase the accuracy of the calibrations.

Figure 14. Example of a GRAS pistonphone calibrator on a RESON TC4032 hydrophone. The RESON hydrophones—TC4032 and TC4034—used for short-range monitoring, and the M8E and M8K hydrophones, used for long-range monitoring, require different adaptors (not shown).

2.2. Environmental Monitoring

Profiles of salinity and temperature with depth were obtained during pile driving with a Minos X conductivity-temperature-depth (CTD) profiler. The CTD profiler uses conductivity, temperature, and pressure sensors to measure temperature and salinity versus depth. The temperature and salinity data were used to derive the speed of sound in water as a function of depth. Appendix C shows the results of the CTD measurements.

River currents were measured with two Teledyne Workhorse Sentinel 1200 kHz acoustic Doppler current profilers (ADCPs). The ADCP uses the Doppler shift of backscattered sound from microscopic particles in the water to measure the water current. The ADCPs were generally only deployed when noise attenuation systems were used. The two ADCPs were typically deployed north (upstream) of the pile and south (downstream) of the pile to characterize the influence of river currents on the NAS performance. Appendix D contains the ADCP measurements.

Levelogger Gold self-contained pressure and temperature recorders (Figure 15) measured the total water and atmospheric pressure at Stations 1 and 10 (Figure 12). Two self-contained barometric pressure loggers mounted in the acoustics monitoring container (Figure 10) provided the reference pressure. The pressure loggers have a maximum error of 0.1% full scale (FS), which is approximately ±0.03 m with the sensor range selected to match the mooring deployment depth. The barometric pressure loggers are also accurate to 0.1% FS, which corresponds to a typical offset of 0.001 m depth equivalent in water pressure. For the whole long-term monitoring period, the loggers took a measurement every 5 minutes. We obtained the water depth, which correlates to the tidal state, with the Levelogger software by subtracting the barometric pressure from the water pressure.

Figure 15. Levelogger Gold pressure and temperature recorder.

2.3. Fish Tag Acoustic Monitoring Receivers

JASCO used four VEMCO VR2W 69 kHz Acoustic Monitoring Receivers (Figure 16) to log the presence of tagged fish. We attached the receivers to the long-range acoustic recorders at Stations 4, 5, 6, and 7 (Figure 12). On retrieval, we downloaded the tag detection logs from the receivers and sent the logs to the clients and to VEMCO. VEMCO provided contact information for the tag owners. JASCO traded the receiver logs with the tag owners, who identified species for each tag detected. JASCO plotted the number of fish present at each logger as a function of time.

Figure 16. Acoustic recorder (gray) and VR2W 69 kHz Acoustic Monitoring Receiver (black) at Station 4 before deployment.

2.4. Rock Drilling Monitoring

JASCO monitored rock drilling at Test Pile 3B on 12 June 2012 (Figure 17). The drilling contractor lowered a 60-inch diameter auger into the pile casing and slowly rotated the bit to drill the rock socket. JASCO visually estimated the rotation rate at 12 revolutions per minute. JASCO recorded the rock drilling sounds using the short-range monitoring system described in Section 2.1.1. The *M/V William M* deployed the short-range system 231 ft from Test Pile 3B.

Figure 17. (Left) 60-inch auger bit at Test Pile 3B, 12 June 2012. (Right) Drill inside casing of Test Pile 3B.

JASCO monitored one of the drilling sequences. The drill was lowered into the casing at 15:34 (UTC) and removed at 15:50. When drilling ceased, the bit depth was 10 ft below the bottom of the pile casing.

2.5. Data Analysis

2.5.1. Piling sound levels

Sound levels for short-range and long-range data were computed with JASCO's custom acoustic analysis software application, SpectroPlotter. The impact pile driving strikes were automatically detected, and for each strike the broadband SPL, broadband SEL, and 1/3–octave band SELs were computed. The cumulative broadband SEL since the start of recording was also computed. During the long-range data analysis, JASCO analysts adjusted the thresholds for our auto-detection system for each station and each pile driving event.

The acoustic data were continuously processed to compute the 1-second average 1/3-octave band SPLs for vibratory pile driving and the 1-minute average 1/3-octave band SPLs of the background noise. Definitions of the standard acoustic metrics employed and flowcharts of the data processing are provided in Appendix B.

2.5.2. Percentiles statistics for NAS attenuation calculations

We computed the SPL and SEL percentile statistics for vibratory and impact hammer pile driving. The sound level statistics quantify the observed distribution of recorded sound levels and

characterize the effectiveness of the NAS attenuation. Following standard acoustical practice, the *n*th percentile level (L_n) is the SPL or SEL exceeded by *n*% of the data. We computed sound level statistics at the following standard percentiles:

- L_{max}, the maximum recorded sound level
- L_5, the sound level exceeded 5% of the time
- L_{25}, the sound level exceeded 25% of the time
- L_{50}, the median sound level
- L_{75}, the sound level exceeded 75% of the time
- L_{95}, the sound level exceeded 95% of the time

We computed the mean sound levels (L_{mean}) as the linear arithmetic mean of the sound power, which can be significantly different from the median sound level (L_{50}).

We calculated the SPL and SEL percentiles for vibratory and impact hammer pile driving for each configuration of pile driver and NAS settings. For instance, one set of percentiles was computed with the NAS off, and another set with the NAS operating at a steady 22 scfm/lf airflow rate. We measured NAS effectiveness by comparing the SPL and SEL percentiles for different NAS settings against control conditions with the NAS off. We present the sound level statistics in 1/3-octave bands.

2.5.3. Distances to impact thresholds

We applied linear regression to the sound level data to estimate the distances at which pile driving noise exceeded the NMFS physiological and behavioral thresholds. The data were fit to the simplified geometrical propagation loss equation:

$$\mathrm{RL}(r) = \mathrm{SL} - A\log_{10}(r)$$

In this equation, RL is the received sound level, SL is the source level, and *A* is the spreading law coefficient. Typical values of *A* are between 10 (cylindrical spreading) and 20 (spherical spreading).

Based on the linear regression analysis, we computed threshold distances to the Fisheries Hydroacoustic Working Group interim criteria for onset of physiological effects:

- Peak SPL: 206 dB re 1 µPa
- cSEL: 187 dB re 1 µPa2s (for fishes above 2 grams)

We computed threshold distances for the NMFS criterion for onset of behavioral effects:

- 150 dB re 1 µPa rms SPL

For peak and rms SPL threshold distances, we computed a mean, minimum, and maximum value. These are based on the L_{mean}, L_{95}, and L_{max} values measured for each test pile and recorder. We used mean single-strike SEL and the total number of pile driving strikes ($N_{strikes}$) to calculate the cumulative SEL that each station would have received with and without the NAS active. Cumulative SEL was computed by adding $10\log_{10}(N_{strikes})$ to the mean SEL measured at each station during periods when the NAS was on and when the NAS was off.

3. Results

3.1. Summary of Data Collected

JASCO collected all of the acoustic and non-acoustic data required to study the short-range acoustic levels during pile driving of seven test piles, which includes:

- 56.9 h of acoustic data
- 38 CTD casts
- 461 h of ADCP data

Logs of pile driving and noise attenuation system activities, as provided by New York State Department of Transportation (NYSDOT), are given in Appendix E and Appendix F, respectively. The CTD and ADCP measurements are given in Appendix C and Appendix D, respectively.

We retrieved 11 of the 12 long-range AMARs on May 19. All retrieved AMARs successfully recorded from 23 April to 19 May except the AMAR from Station 1, which calibrated correctly on-site, however it only recorded electronic noise. Despite 26 grapple attempts and 3 hours of side-scan sonar surveying of the area, JASCO could not find the recorder from Station 5. The side-scan sonar detected a fresh anchor scar through Station 5, indicating that the recorder was likely dragged away by a barge or vessel during the monitoring period (Figure 18). Subsequent side-scan sonar surveys along the anchor scar did not detect the lost AMAR.

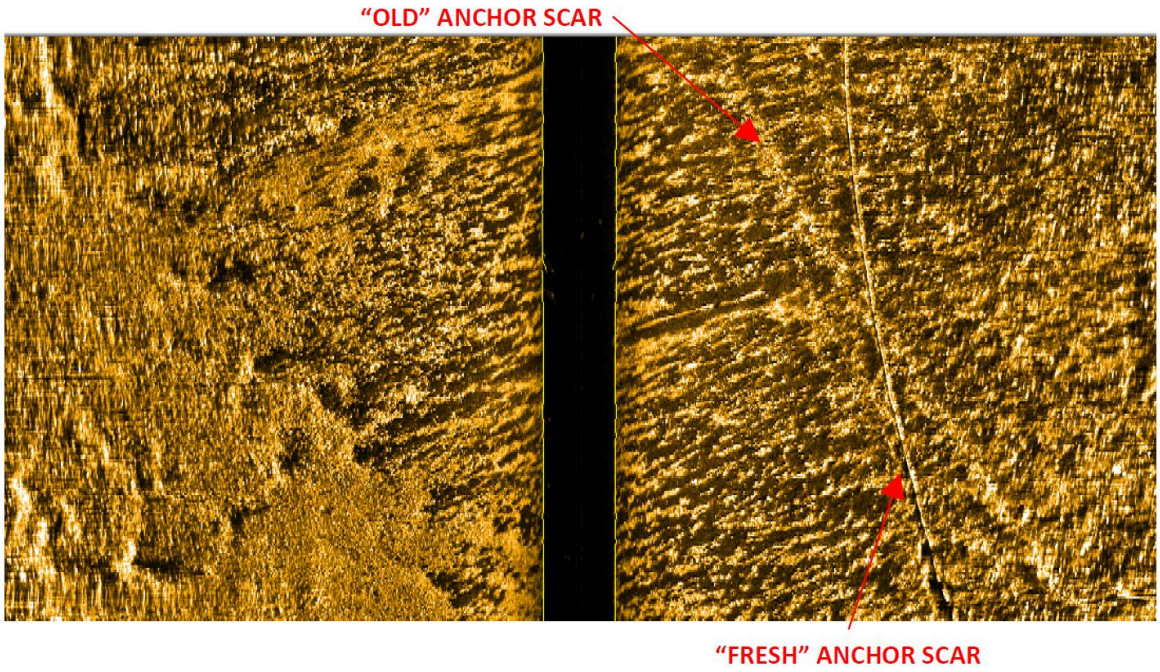

Figure 18. Side-scan sonar image of anchor scars at Station 5.

The VEMCO VR2W acoustic monitoring receivers attached to Stations 4, 6, and 7 recorded throughout the project and detected many sturgeon vocalizations.

The Leveloggers successfully sampled water depth and temperature at 5-minute intervals from 23 April to 19 May 2012 at Stations 1 and 10.

3.2. Environmental Conditions

River temperature and salinity profiles measured at each test pile location were uniform during the PIDP, indicating that the waters were well mixed. Based on this information, the temperature and salinity profiles at the long-range recorders would likely be similar to those measured at the piles. Figure 19 shows average water temperature from each CTD cast, and the riverbed water temperature and water depth recorded by the Leveloggers for Stations 1 and 10, clearly showing the influence of the tides throughout the PIDP. Detailed CTD cast results are given in Appendix C.

Air temperature, wind speed, and rainfall at a nearby weather station in Tarrytown, NY are shown in Figure 20.

Water temperature, which increased from approximately 55 to 65 °F during the PIDP, was positively correlated with air temperature. Riverbed water temperature was also correlated with the tide, becoming colder at high tides.

Salinity and river current velocity were more variable with time because they were influenced by tides; however, at any given time they were fairly uniform. Salinity varied between 1 and 7 ppt over the duration of the PIDP. Current velocity measurements are shown in Appendix D.

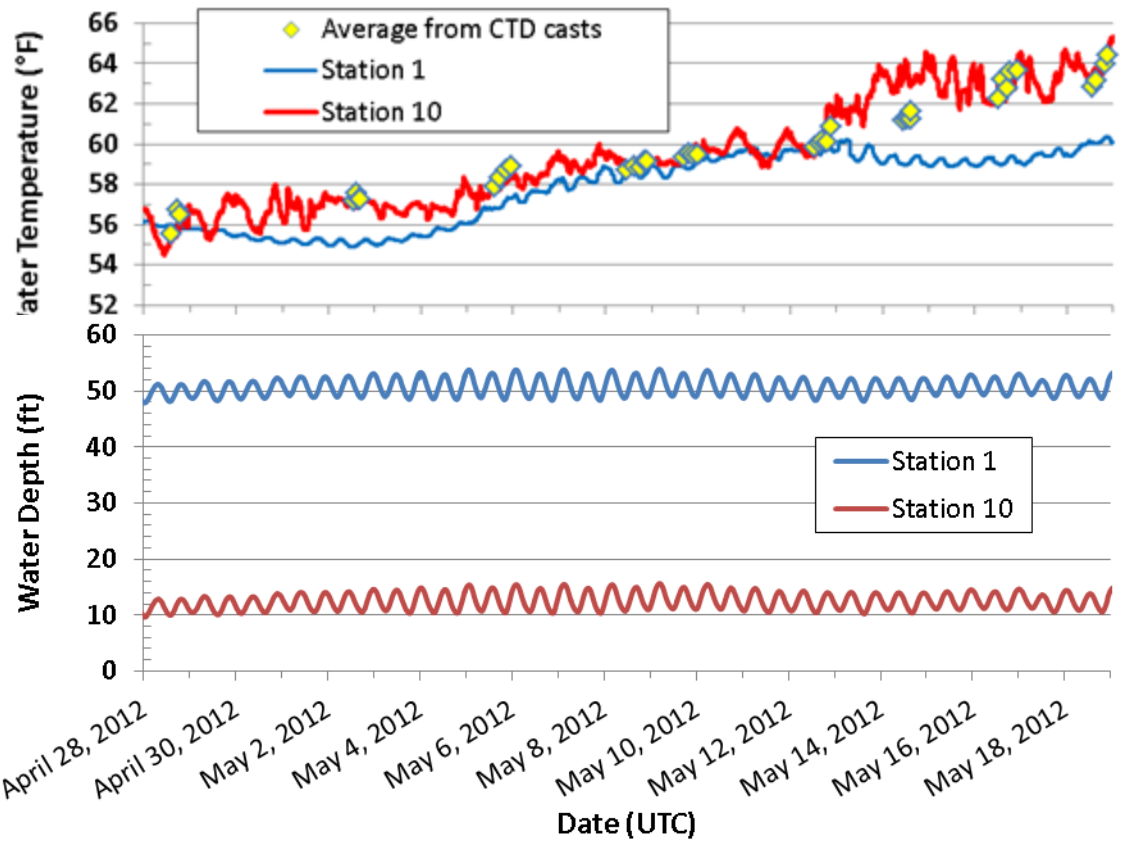

Figure 19. (Top) Water temperature from each CTD cast and the Leveloggers at Stations 1 and 10. (Bottom) Water depth, corrected for atmospheric pressure, measured with the Leveloggers at Stations 1 and 10.

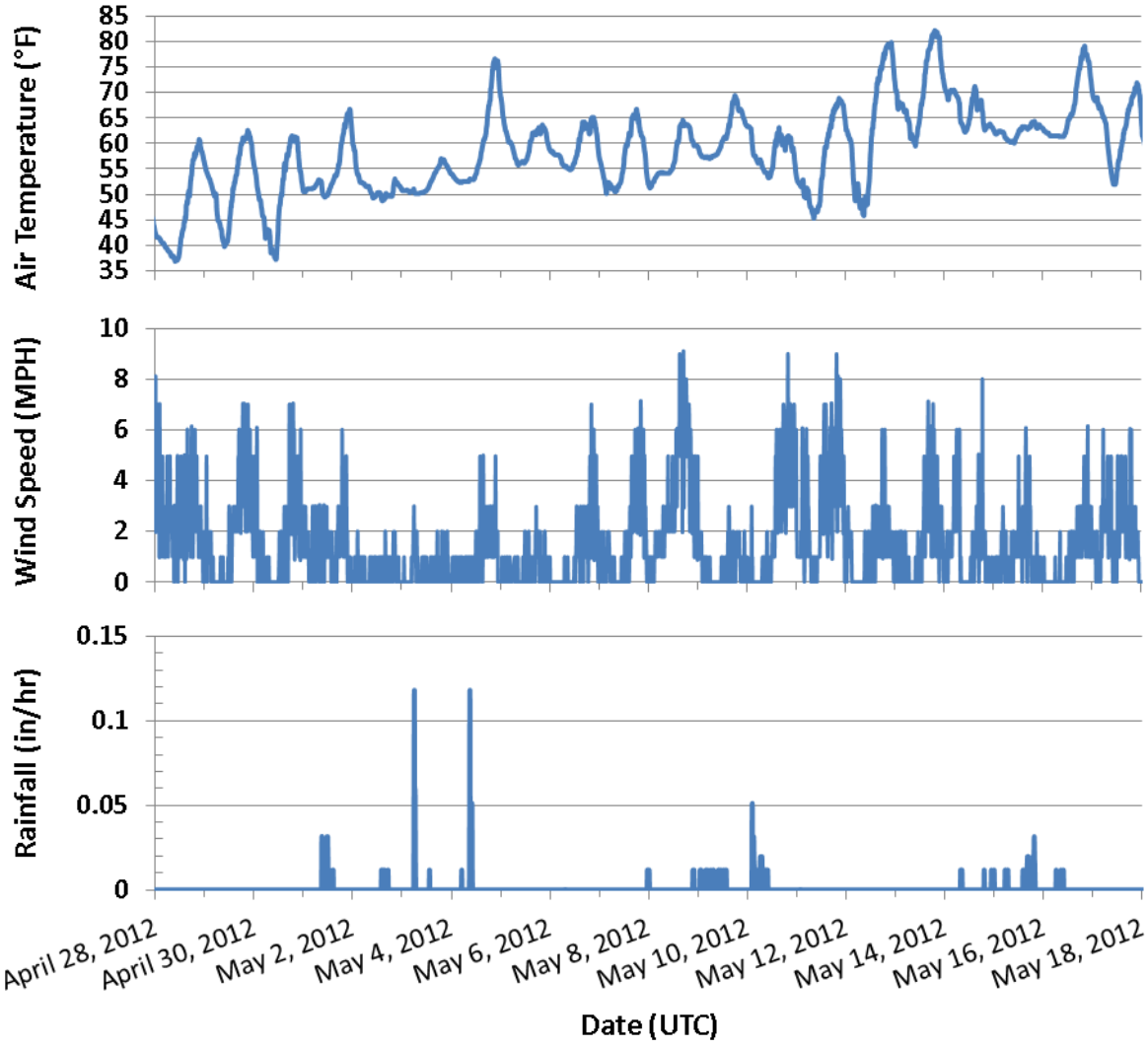

Figure 20. Air temperature, wind speed, and rainfall at Tarrytown, NY.

3.3. Impact Pile Driving

3.3.1. Maximum sound levels

Tables 10–13 contain the maximum peak SPLs, maximum 90% rms SPLs, SELs, and cumulative SELs based on short- and long-range data for each of the recording stations, except Stations 1 and 5.. The metrics were computed from all valid pile driving detections for each event. Cells with two dashes (--) indicate the manual analysis did not find measureable pile driving. The minimum measureable rms SPL was 110–114 dB re 1 µPa, depending on the noise levels at the station. This noise floor is 40 dB below the 150 dB re 1 µPa behavior disturbance threshold for sturgeon. Appendix G provides plots of the received levels and 1/3-octave percentile distributions for all detected impact pile driving.

Table 10. Maximum peak SPL (dB re 1 µPa) measured during impact piling at each station for each test pile during the Tappan Zee Bridge PIDP. Dashes (--) indicate the manual analysis did not detect pile driving. The short-range measurements were made at a nominal distance of 33 feet from the pile center.

Station	Pile 1A	Pile 1B	Pile 2A	Pile 2B	Pile 3A	Pile 3B	Pile 4A
Short-range	201.6	188.3	209.4	209.7	214.2	224.7	219.1
2	--	--	--	--	--	--	142.3
3	--	--	--	--	--	--	149.1
4	148.9	140.5	161.6	159.2	--	136.4	--
6	--	--	--	146.1	160.4	171.1	156.7
7	--	--	--	--	149.2	149.1	160.4
8	137.1	134.8	140.0	139.1	--	--	--
9–12	--	--	--	--	--	--	--

Table 11. Maximum 90% rms SPL (dB re 1 µPa) measured during impact piling at each station for each test pile during the Tappan Zee Bridge PIDP. Dashes (--) indicate the manual analysis did not detect pile driving. The short-range measurements were made at a nominal distance of 33 feet from the pile center.

Station	Pile 1A	Pile 1B	Pile 2A	Pile 2B	Pile 3A	Pile 3B	Pile 4A
Short-range	185.0	170.8	193.5	194.1	197.1	208.5	202.5
2	--	--	--	--	--	--	121.6
3	--	--	--	--	--	--	131.5
4	131.0	129.2	134.6	132.4	--	114.5	--
6	--	--	--	119.6	143.7	151.7	131.8
7	--		--	--	125.5	120.7	143.5
8	124.5	119.7	116.6	116.2	--	--	--
9–12	--	--	--	--	--	--	--

Table 12. Maximum single-strike SEL (dB re 1 $\mu P^2 \cdot s$) measured during impact piling at each station for each test pile during the Tappan Zee Bridge PIDP. Dashes (--) indicate the manual analysis did not detect pile driving. The short-range measurements were made at a nominal distance of 33 feet from the pile center.

Station	Pile 1A	Pile 1B	Pile 2A	Pile 2B	Pile 3A	Pile 3B	Pile 4A
Short-range	174.7	162.1	183.1	184.3	186.9	195.8	192.0
2	--	--	--	--	--	--	119.2
3	--	--	--	--	--	--	128.1
4	125.0	123.7	126.7	125.0	--	111.3	--
6	--	--	--	113.9	134.9	139.8	127.5
7	--	--	--	--	118.5	117.6	136.1
8	115.4	114.3	113.6	112.8	--	--	--
9–12	--	--	--	--	--	--	--

Table 13. Cumulative SEL (dB re 1 µPa^2·s) of detected impact pile driving measured at each station for each test pile during the Tappan Zee Bridge PIDP. Dashes (--) indicate the manual analysis did not detect pile driving. The short-range measurements were made at a nominal distance of 33 feet from the pile center.

Station	Pile 1A	Pile 1B	Pile 2A	Pile 2B	Pile 3A	Pile 3B	Pile 4A
Short-range	202.8	192.8	205.0	206.1	210.3	222.5	212.8
2	--	--	--	--	--	--	145.8
3	--	--	--	--	--	--	156.3
4	153.1	152.7	150.2	154.7	--	141.7	--
6	--	--	--	142.3	160.5	168.8	153.9
7	--	--	--	--	145.2	148.1	163.5
8	144.5	145.3	136.2	142.2	--	--	--
9–12	--	--	--	--	--	--	--

3.3.2. Noise attenuation system performance

Table 14 contains estimates of the attenuation provided by each noise attenuation system based on short- and long-range data. The long-range attenuations were computed from the mean SEL of the received SELs with and without the NAS.

In some cases, the levels measured with the NAS on were slightly higher than the levels measured the NAS off. This is attributed to variations in sound emissions due to changes in the hammer energy and driving conditions.

Table 14. SEL/cSEL attenuation (dB) measured at each station for each noise attenuation system/test pile during the Tappan Zee Bridge PIDP. Dashes (--) indicate the manual analysis did not detect pile driving.

Station	Unconfined Single-Tier Air Bubble Curtain		Unconfined Multi-Tier Air Bubble Curtain	Hard Bubble System	Isolation Casing and Bubble System	Two-Stage Confined Bubble Curtain	
	Pile 1A	Pile 2A	Pile 3A	Pile 1B	Pile 2B	Pile 3B	Pile 4A
Short-range	11.4	10.0	11.6	12.2	9.9	13.7	12.9
2	--	--	--	--	--	--	1.7
3	--	--	--	--	--	--	-0.2
4	-0.5	4.8	--	-0.9	5.1	*	--
6	--	--	6.9	--	4.7	7.4	11
7	--	--	5.8	--	--	5.2	6.2
8	-0.4	-0.1	--	-2.5	2.0	--	--
9–12	--	--	--	--	--	--	--

* Impact piling with the NAS active was not detected.

3.3.3. Distances to sound level thresholds

Table 15 summarizes the calculated distances from the test piles that the sound levels were above the regulatory thresholds. The cumulative SEL distances are based on the mean measured single-strike SEL multiplied by the number of strikes used during the PIDP at each test pile. The

peak SPL and rms SPL distances are based on the maximum measured values at each test pile. Appendix H contains plots of the regressions for each test pile with the NAS on and with the NAS off. Table 15 contains ratios for each test pile of the area that is above the threshold with NAS on, compared to the area with NAS off.

Table 15. Distances (ft) to the physiological and behavioral thresholds from the Biological Opinion, dated 7 March, 2012, for each test pile with the NAS off and on. The ratio (%) of the NAS On area to the NAS Off area is given in parenthesis and assumes a circular impact area.

Test Pile	206 dB re 1 µPa max. peak SPL		187 dB re 1 µPa^2·s cumulative SEL		150 dB re 1 µPa rms SPL	
	NAS Off	NAS On	NAS Off	NAS On	NAS Off	NAS On
1A	29.2	8.3 (8.1%)	137.3	75.0 (26.0%)	405.3	294.1 (52.7%)
1B	25.2	7.5 (8.9%)	122.6	66.6 (%)	314.5	146.5 (21.7%)
2A	42.0	19.6 (21.8%)	109.6	72.4 (43.6%)	394.4	289.6 (53.9%)
2B	42.4	17.0 (16.1%)	191.5	114.0 (35.4%)	452.2	306.0 (45.8%)
3A	62.7	16.0 (6.5%)	216.0	105.0 (23.6%)	749.4	332.1 (19.6%)
3B	100.8	37.8 (14.1%)	351.2	189.9 (29.2%)	807.8	461.8 (32.7%)
4A	70.6	14.4 (4.1%)	281.5	125.2 (19.8%)	821.8	428.5 (27.2%)

3.4. Vibratory Pile Driving

The next series of tables contain the maximum peak SPLs, maximum 90% rms SPLs, and cumulative SELs for short-range and long-range data by recording stations during vibratory driving (except for Station 5, which was not recovered). The metrics were computed from all valid pile driving detections for each event. Cells with two dashes (--) indicate the manual analysis did not find measureable pile driving. The minimum measureable rms SPL was 110–114 dB re 1 µPa, depending on the noise levels at the station. Appendix I provides plots of the received levels for all detected vibratory driving.

The Super Kong 600 vibratory hammer produced the highest peak SPL, rms SPL, and cSELs measured by the long-range recorders. The highest peak SPL was 138.8 dB re 1 µPa at Station 7 while driving Test Pile 4A. The maximum rms SPL was 129.8 dB re 1 µPa measured at Station 4 while driving Test Pile 2B, and at Station 6 while driving Test Pile 3B. The highest cSEL was 154.7 dB re 1 µPa^2·s measured at Test Pile 4 while driving Test Pile 2B.

Table 16. Summary of maximum peak SPLs (dB re 1 µPa) measured during vibratory pile driving at each station for each pile during the Tappan Zee Bridge PIDP. The short-range measurements were made at a nominal distance of 33 feet from the pile center.

Station	Pile 1A Bottom, ICE 66	Pile 1B Bottom, ICE 66	Pile 1B Top, ICE 66	Pile 2A Top, ICE 66	Pile 2A Top, Super Kong 600	Pile 2B Top, ICE 66	Pile 2B Top, Super Kong 600	Pile 3A Bottom, ICE 66	Pile 3B, Top, Super Kong 600	Pile 4A, Bottom, Super Kong 600
Short-range	177.1	177.1	169.6	172.9	185.2	182.4	177.2	173.1	182.3	177.1
2	--	--	--	--	--	--	--	--	--	--
3	--	--	--	--	--	123.4	122.6	--	124.7	134.7
4	127.1	135.8	125.5	132.9	137.4	136.2	137.4	--	126.7	--
6	--	--	--	120.8	123.3	127.5	126.1	126.7	137.1	124.9
7	--	--	--	--	--	--	--	--	--	138.8
8	120.1	122.7	121.9	123.7	127.7	124.4	131.3	--	--	--
9	--	--	--	--	--	--	--	125.0	130.5	126.7
10-12	--	--	--	--	--	--	--	--	--	--

Table 17. Summary of maximum 90% rms SPLs (dB re 1 µPa) measured during vibratory pile driving at each station for each pile during the Tappan Zee Bridge PIDP. The short-range measurements were made at a nominal distance of 33 feet from the pile center.

Station	Pile 1A Bottom, ICE 66	Pile 1B Bottom, ICE 66	Pile 1B Top, ICE 66	Pile 2A Top, ICE 66	Pile 2A Top, Super Kong 600	Pile 2B Top, ICE 66	Pile 2B Top, Super Kong 600	Pile 3A Bottom, ICE 66	Pile 3B, Top, Super Kong 600	Pile 4A, Bottom, Super Kong 600
Short-range	164.6	158.3	161.6	160.8	169.2	165.3	160.2	161.6	171.4	164.8
2	--	--	--	--	--	--	--	--	--	--
3	--	--	--	--	--	106.3	112.0	--	112.8	125.0
4	115.0	120.7	118.0	122.6	127.6	123.3	129.8	--	114.2	--
6	--	--	--	111.6	111.2	111.1	118.6	119.7	129.8	112.9
7	--	---	--	--	--	--	--	--	--	127.4
8	111.2	111.9	112.5	116.0	118.9	116.0	120.1	--	--	--
9	--	--	--	--	--	--	--	113.0	122.6	118.1
10-12	--	--	--	--	--	--	--	--	--	--

Table 18. Summary of cumulative SEL (dB re 1 µPa^2·s) of detected vibratory pile driving measured at each station for each pile during the Tappan Zee Bridge PIDP. The short-range measurements were made at a nominal distance of 33 feet from the pile center.

Station	Pile 1A Bottom, ICE 66	Pile 1B Bottom, ICE 66	Pile 1B Top, ICE 66	Pile 2A Top, ICE 66	Pile 2A Top, Super Kong 600	Pile 2B Top, ICE 66	Pile 2B Top, Super Kong 600	Pile 3A Bottom, ICE 66	Pile 3B, Top, Super Kong 600	Pile 4A, Bottom, Super Kong 600
Short-range	177.6	175.4	180.8	188.5	196.1	190.4	189.0	177.7	197.4	183.5
2	--	--	--	--	--	--	--	--	--	--
3	--	--	--	--	--	128.5	133.7	--	135.4	145.5
4	138.0	137.5	135.7	150.6	153.8	147.0	154.7	--	137.1	--
6	--	--	--	136.3	137.7	135.6	137.7	132.6	154.0	130.4
7	--	--	--	--	--	--	--	--	--	148.3
8	133.0	131.6	131.4	138.5	145.1	143.2	141.4	--	--	--
9	--	--	--	--	--	--	--	129.5	142	134.2
10-12	--	--	--	--	--	--	--	--	--	--

3.5. Background Sound Levels

3.5.1. Short-range background sound levels

Marine construction sounds dominate the background sounds recorded during short-range monitoring. The sounds include workboat traffic (Figure 21), crane operations on the barges, hydraulic power packs for the cranes and pile drivers, transient impacts such as the pile drivers settling onto the piles (Figure 22) and diesel generators to provide power (Figure 23).

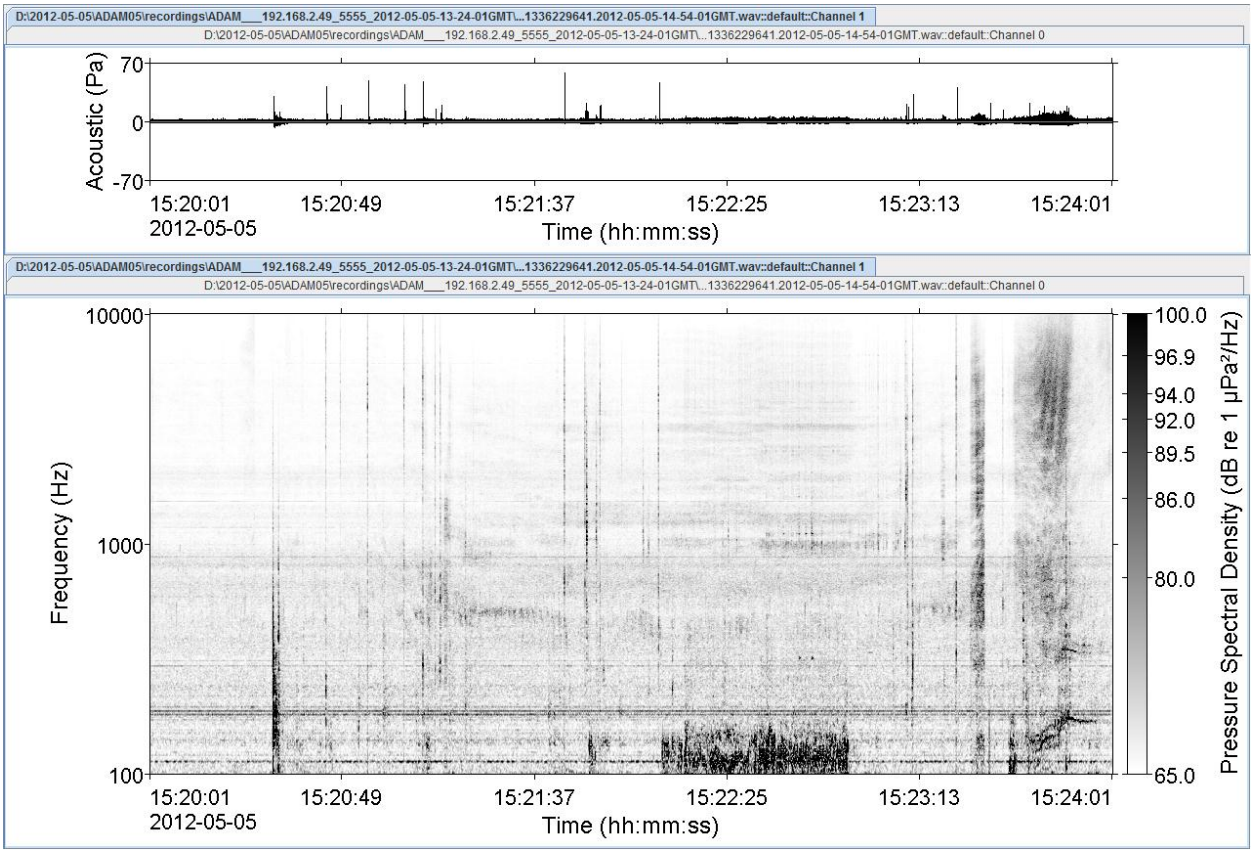

Figure 21. Time-series and spectrogram of a workboat arriving at the construction barges on 5 May 2012 during preparations for piling of Test Piles 1A and 1B.

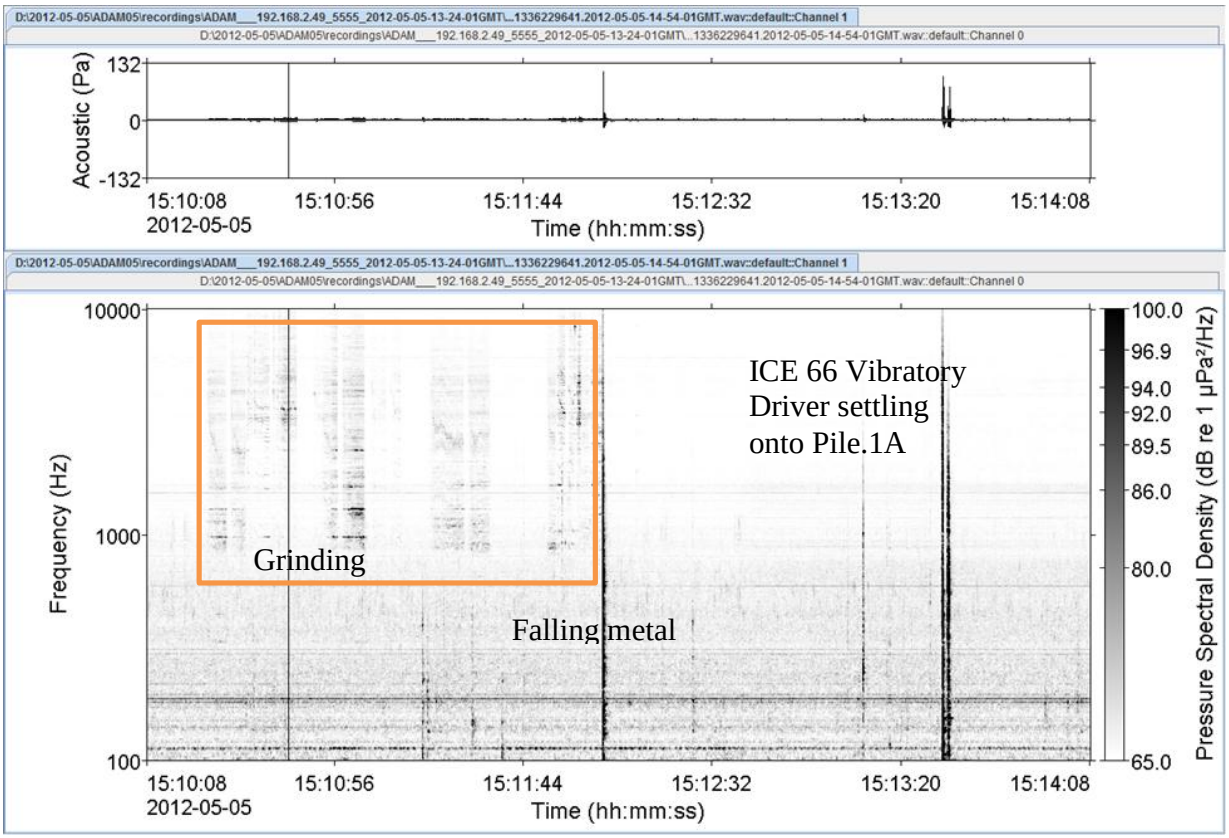

Figure 22. Time-series and spectrogram of grinding and the noise spike that occurred when the ICE 66 vibratory driver settled onto Test Pile 1A on 5 May 2012.

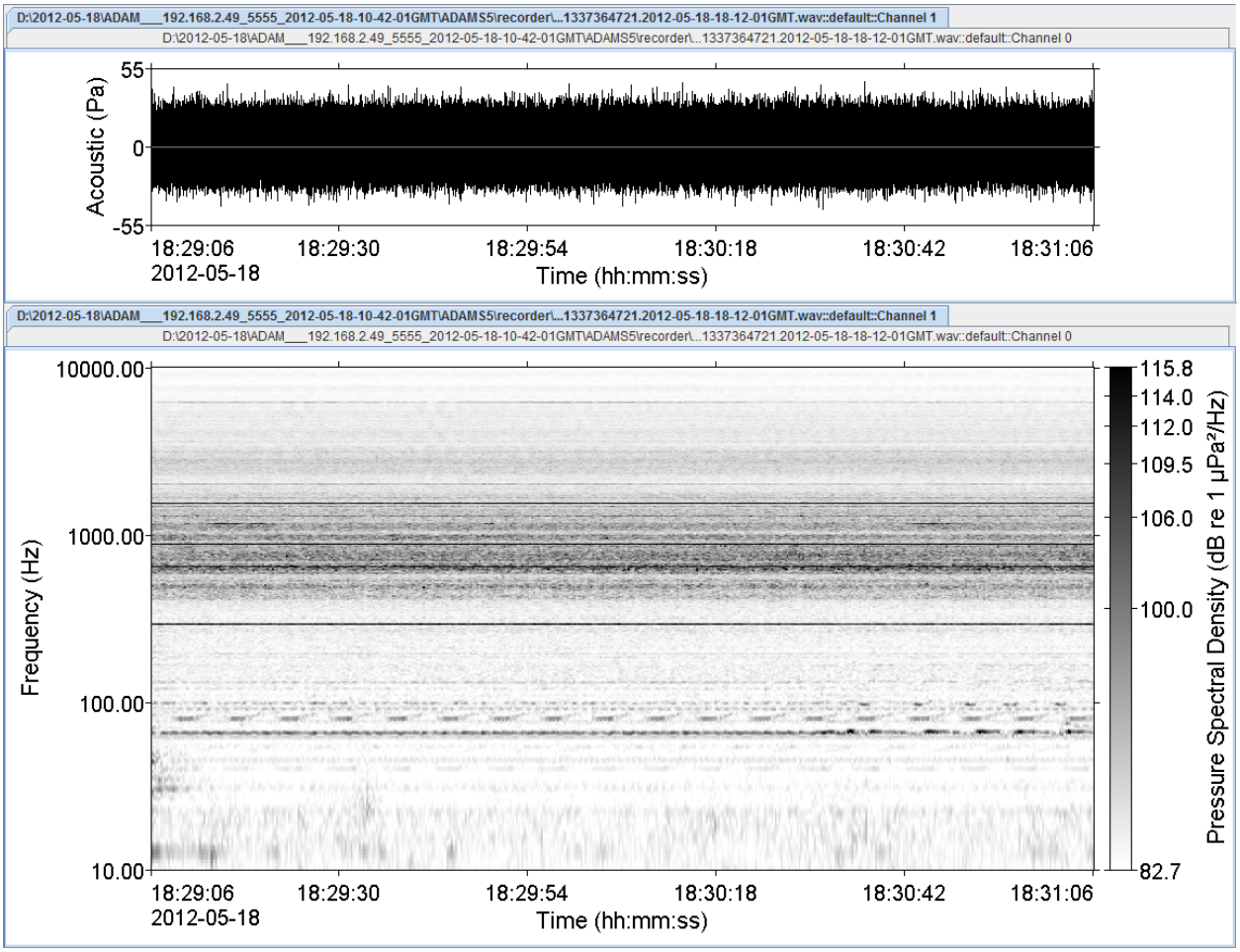

Figure 23. Time-series and spectrogram from 18 May 2012 showing the 60 Hz fundamental and its harmonics from diesel power generators as well as tonal frequencies from the air compressors for the two-stage confined bubble curtain system.

The difference in background sound levels between the PIDP site (for example Figure 24) and at Station 10 (Figure 25), which represents the normal river conditions, ranged from 26.3–43 dB (Table 19).

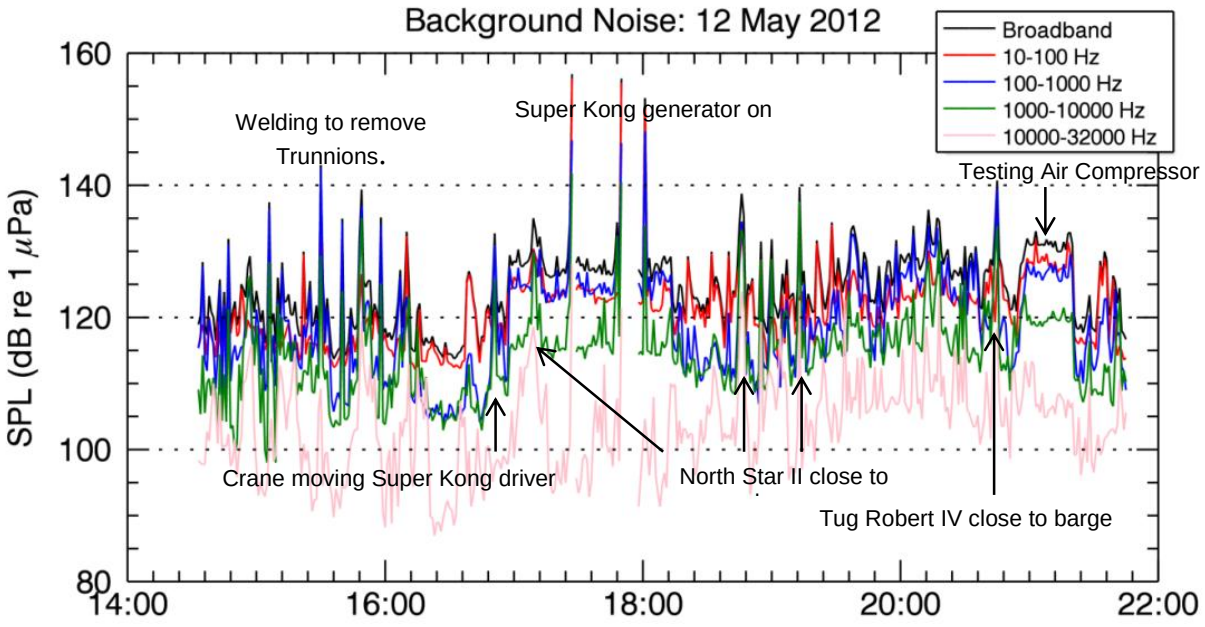

Figure 24. Background sound levels during short-range monitoring at Test Pile 4A, 12 May 2012, annotated with events from JASCO logs.

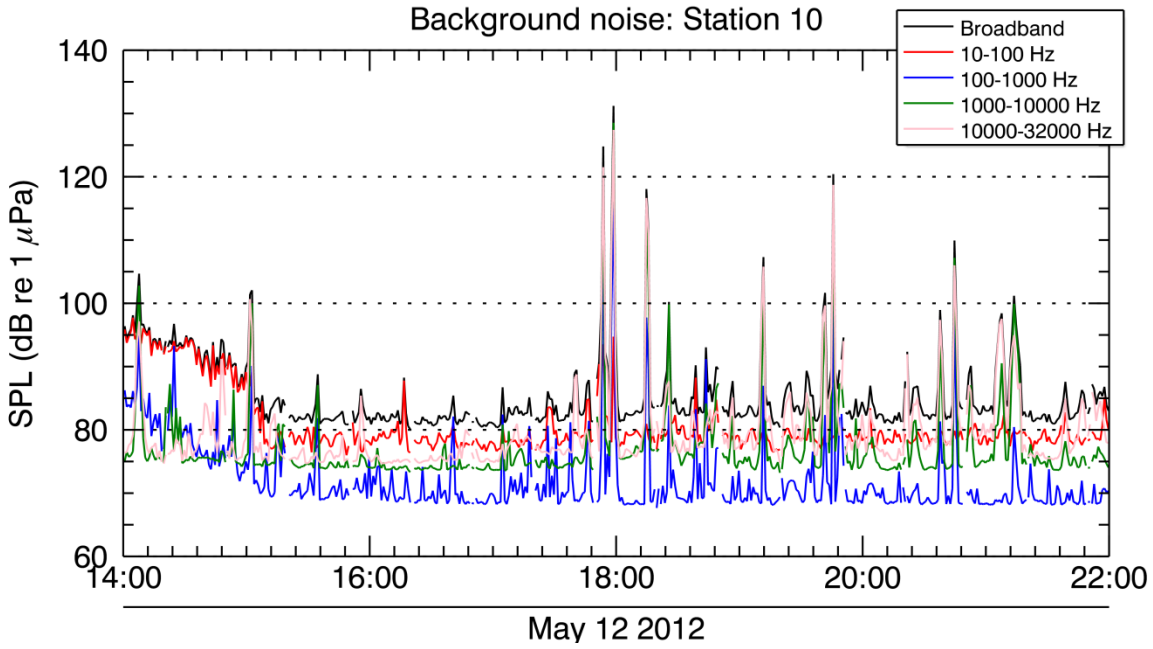

Figure 25. Sound levels at Station 10 during vibratory piling at Test Pile 4A, 12 May 2012.

Table 19. Comparison of rms SPLs during the short-range monitoring and over the same period for long-range monitoring (Station 10).

Date (UTC)	Test Pile	Median short-range rms SPL, dB re 1 µPa	Median Station 10 rms SPL, dB re 1 µPa	rms SPL Difference, dB
16:00–19:00, 28 April	3A Bottom	125.8	82.8	43.0
14:20–16:10 2 May	1A and 1B Bottom	119.1	92.1	27.0
14:10–23:15 5 May	1A and 1B Top	119.3	93.0	26.3
12:00–23:00 8 May	3A Top	127.0	97.6	29.4
17:45–23:30 9 May	4A Bottom	118.1	87.4	30.7
14:30–21:45 12 May	4A Top, Vibratory	122.6	83.6	39.0
11:40–14:45 14 May	4A Top	128.3	86.9	41.4
13:30–22:30 16 May	2A and 2B Top	122.4	86.9	35.5
--	3B Top	Insufficient background data.		

3.5.2. Long-range background sound levels

The background sound levels recorded throughout the PIDP at Station 10 were similar to the levels recorded during the ambient monitoring program in 2010.

The ranges of received levels were:

- Peak SPL: Median value of 117.2 dB re 1 µPa with a 5th percentile value of 128.6 dB re 1 µPa and a 95th percentile value of 107.8 dB re 1 µPa.
- rms SPL: Median value of 87.6 dB re 1 µPa with a 5th percentile value of 104.0 dB re 1 µPa and a 95th percentile value of 80.7 dB re 1 µPa.

The regular peaks in the band level plot (Figure 26) and the yellow spikes at low frequencies in the spectrogram (Figure 27) are due to real and pseudo-noise from tides. The percentile plot (Figure 28) shows increased sound levels in the band of 300 Hz–4 kHz which is associated with wind and wave noise. The 1/3-octave band percentile statistics show the largest variability in received SPL ranged between 100–4000 Hz.

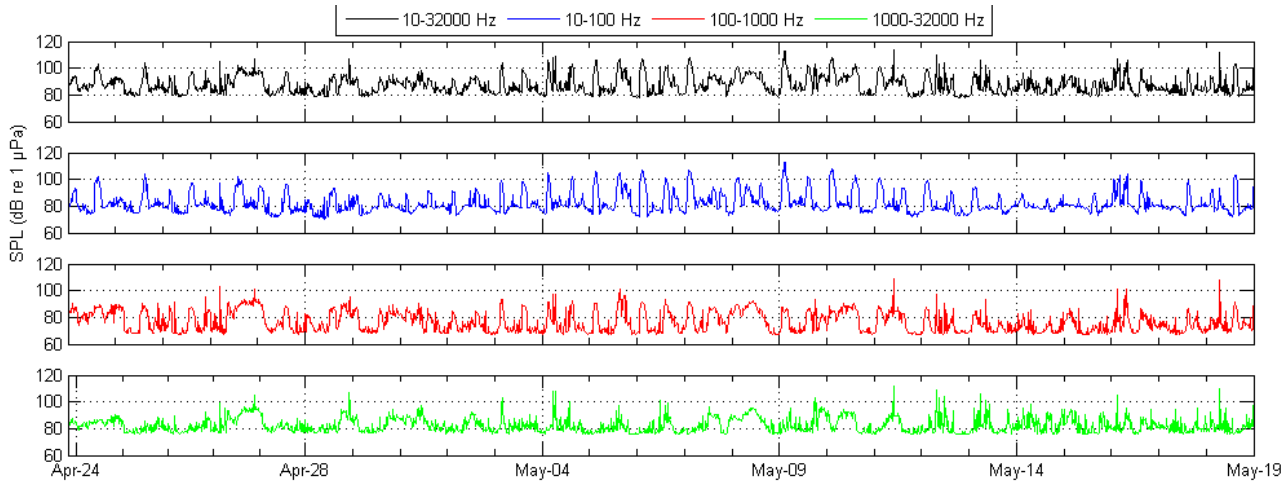

Figure 26. Background sound levels at Station 10 throughout the PIDP. All dates are UTC.

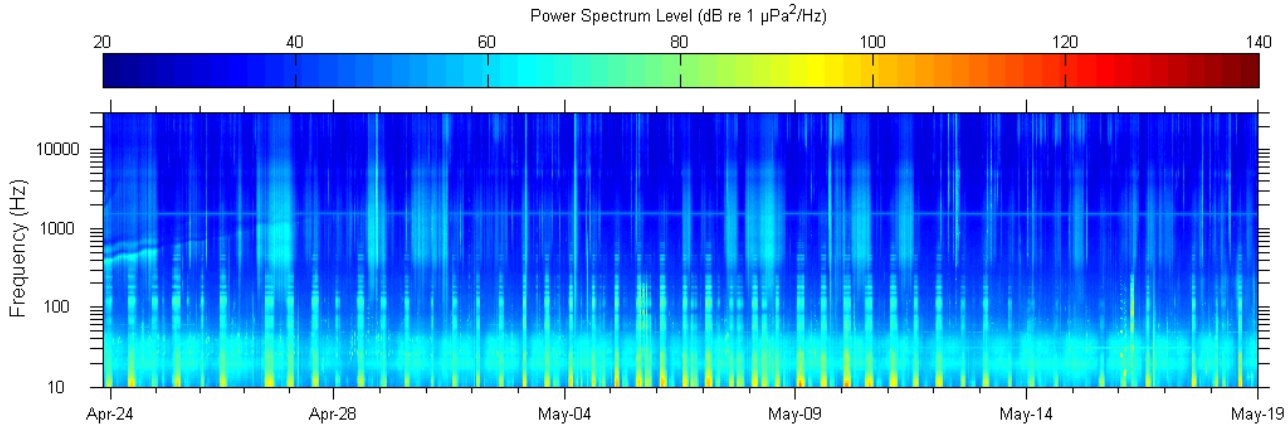

Figure 27. Spectrogram of background sound levels at Station 10 throughout the PIDP. All dates are UTC.

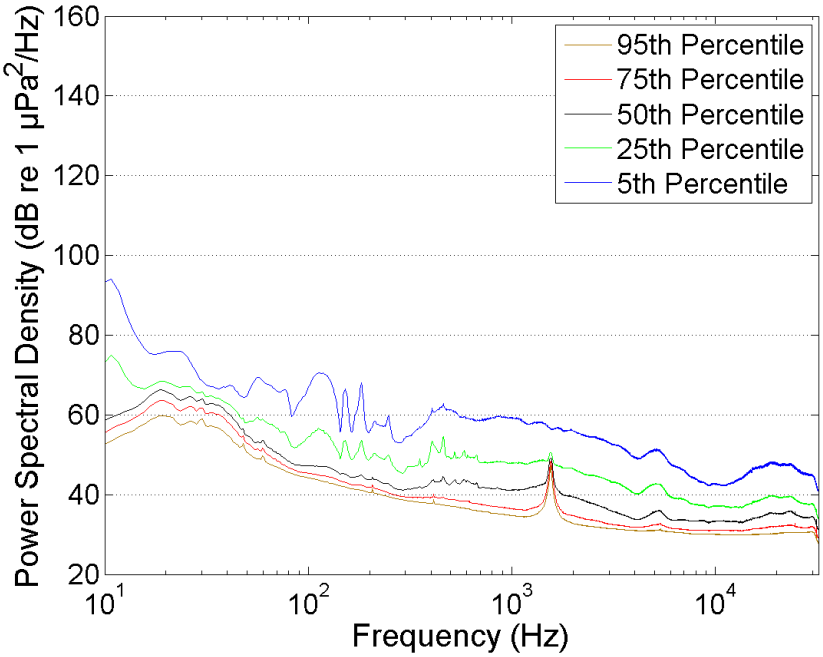

Figure 28. Percentile plot of background sound levels measured during the PIDP.

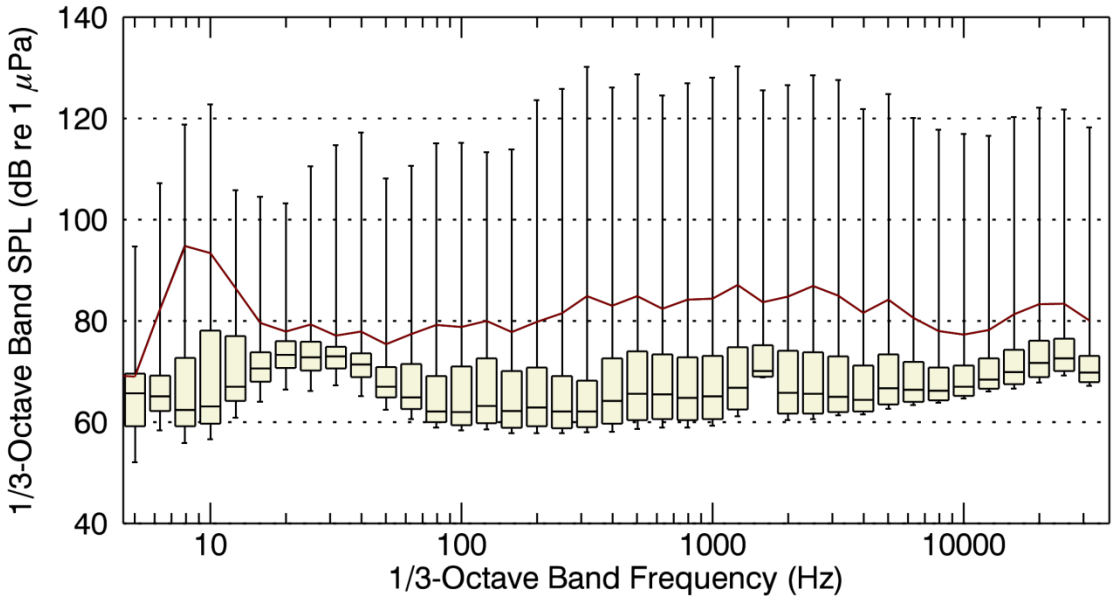

Figure 29. 1/3-octave percentile statistics for the received levels at Station 10 throughout the PIDP. Beige bars indicate the first, second, and third quartiles (L_{25}, L_{50}, and L_{75}). Upper error-bars indicate the maximum levels (L_{max}). Lower error bars indicate the 95% exceedance percentiles (L_{95}). The maroon line indicates the arithmetic mean (L_{mean}).

3.6. Fish Tag Logging Results

The VEMCO VR2W acoustic monitoring receivers at long-range Stations 4, 6, and 7 detected 195 different tags ID's. Each tag ID is a unique fish. Of the 195 tag IDs, 126 were known to be implanted in sturgeon. The detections by station were:

- Station 4: 123 detections from 4 different tags (including 2 JASCO test tags)
- Station 6: 15,838 detections from 185 different tags
- Station 7: 20,418 detections from 187 different tags

There was a significant difference between the detection rates at station 4 compared to stations 6 and 7. The deployment method for three recorders was identical (Figure 16). The VR2W recorders require line-of-sight to the tagged fish. The results suggest that the tagged fish preferred the deeper waters by the river channel to the shallows. However, the result could also be the result of poor propagation conditions for the tag pings in the shallow waters around station 4.

Figure 30 and

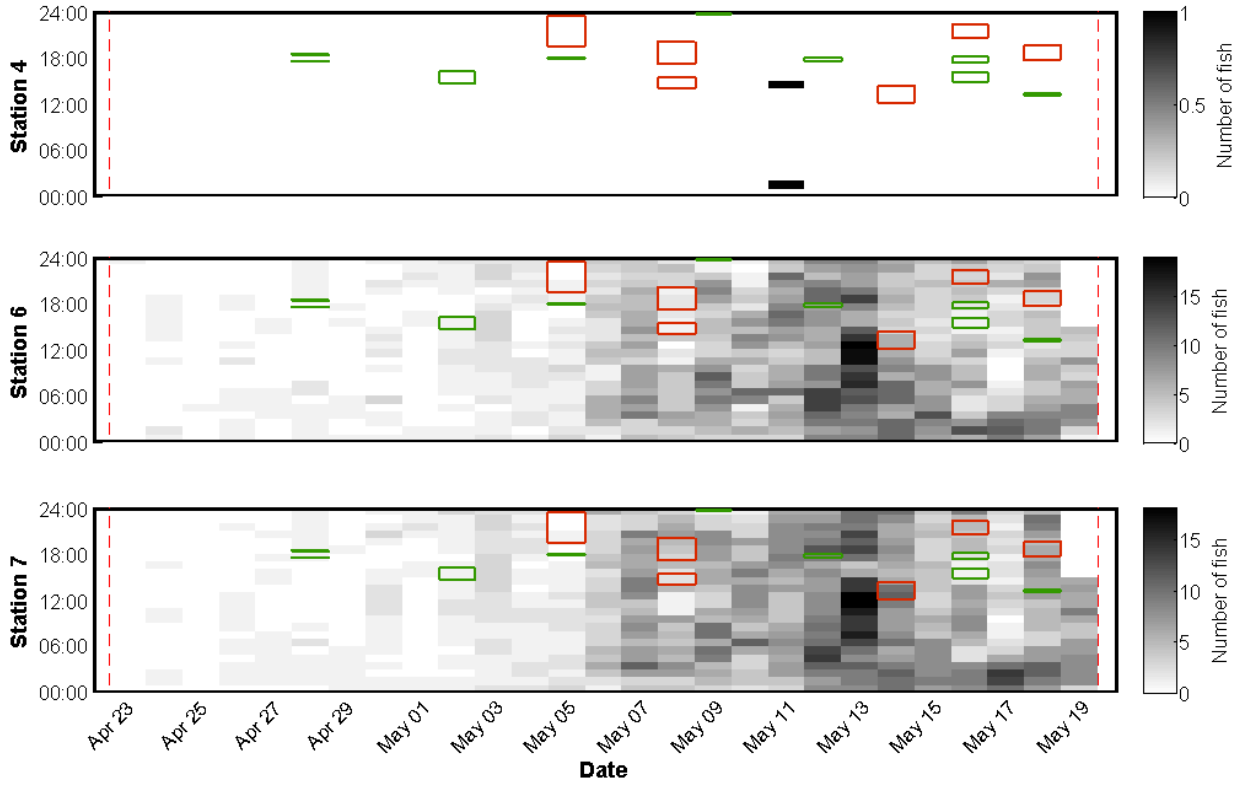

Figure 31 plot the fish detections as a function of time. The data indicate that a school of 15 - 20 fish moved through the project area the morning of 13 May, a day when no pile driving occurred. There does not appear to be any correlation between the presence of fish in the project area and the pile-driving activity.

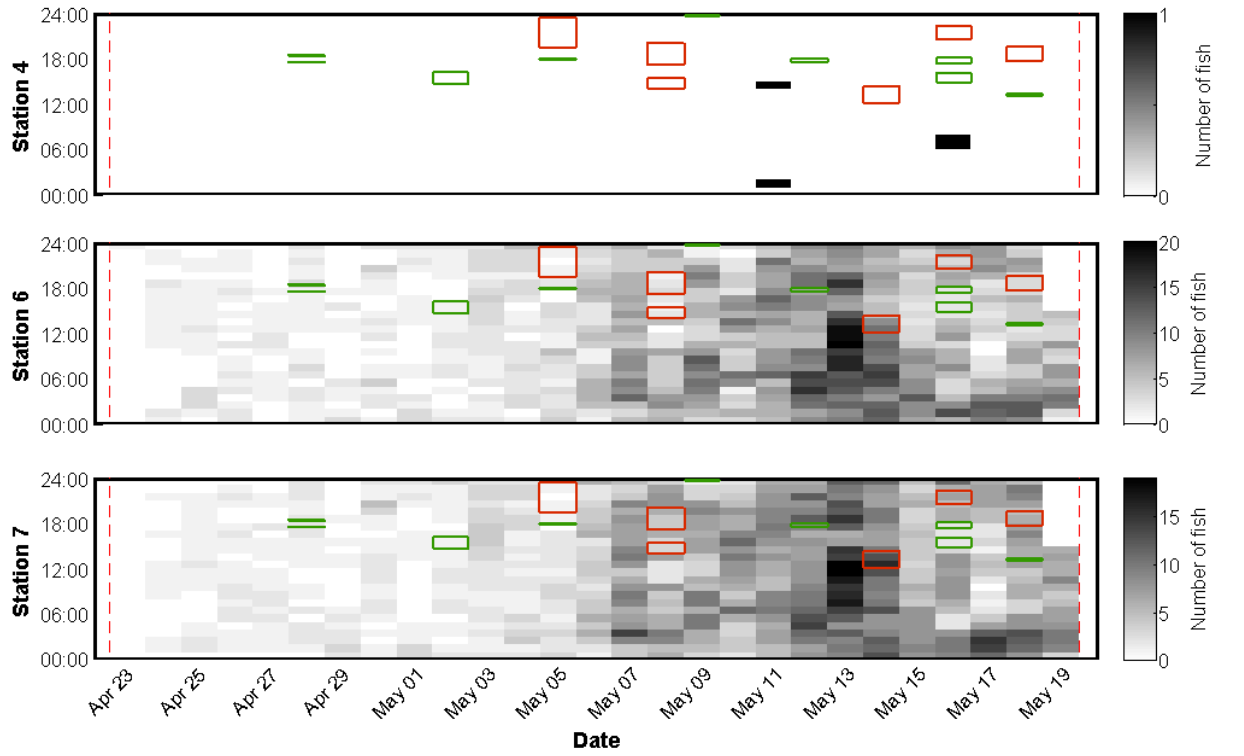

Figure 30. Presence plots for all fish detected by the VR2W acoustic monitoring receivers at Stations 4, 6, and 7 during the PIDP. Grayscale color is the number of unique fish detected per hour. All times are in UTC. The red and green boxes overlaid on the plots are the occurrence of pile driving during the PIDP.

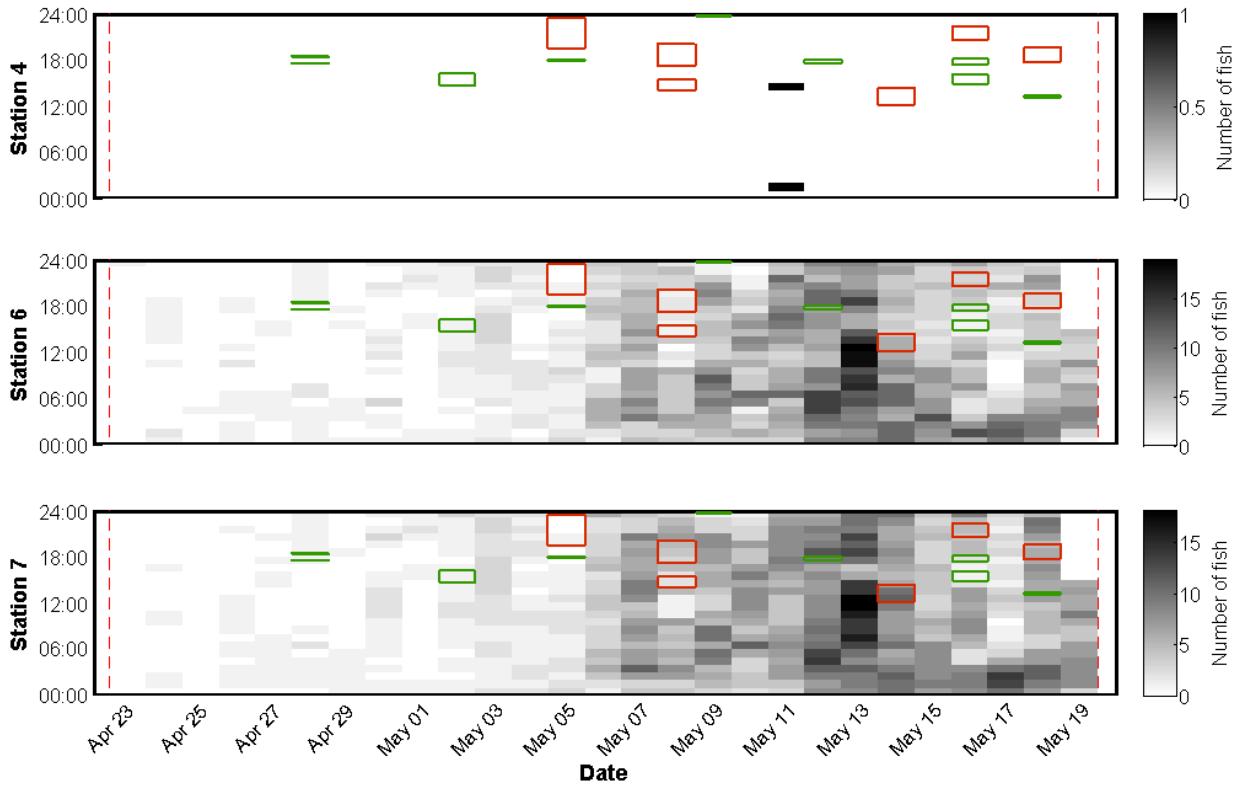

Figure 31. Presence plots for sturgeon detected by the VR2W acoustic monitoring receivers at Stations 4, 6, and 7 during the PIDP. Grayscale color is the number of sturgeon detected per hour. All times are in UTC. The red and green boxes overlaid on the plots are the occurrence of pile driving during the PIDP.

3.7. Rock Drilling Results

JASCO's field team did not notice any in-air sounds during the drilling except the sounds of the equipment on the barges. JASCO staff did not measure any broadband in-water sounds from the rock drilling (Figure 32, Table 20). The drill moved at 12 rpm, or 0.2 Hz, a very low frequency. JASCO reanalyzed the data using fast Fourier transforms with a 0.015 Hz resolution, but found no sign of the drill frequency or its harmonics.

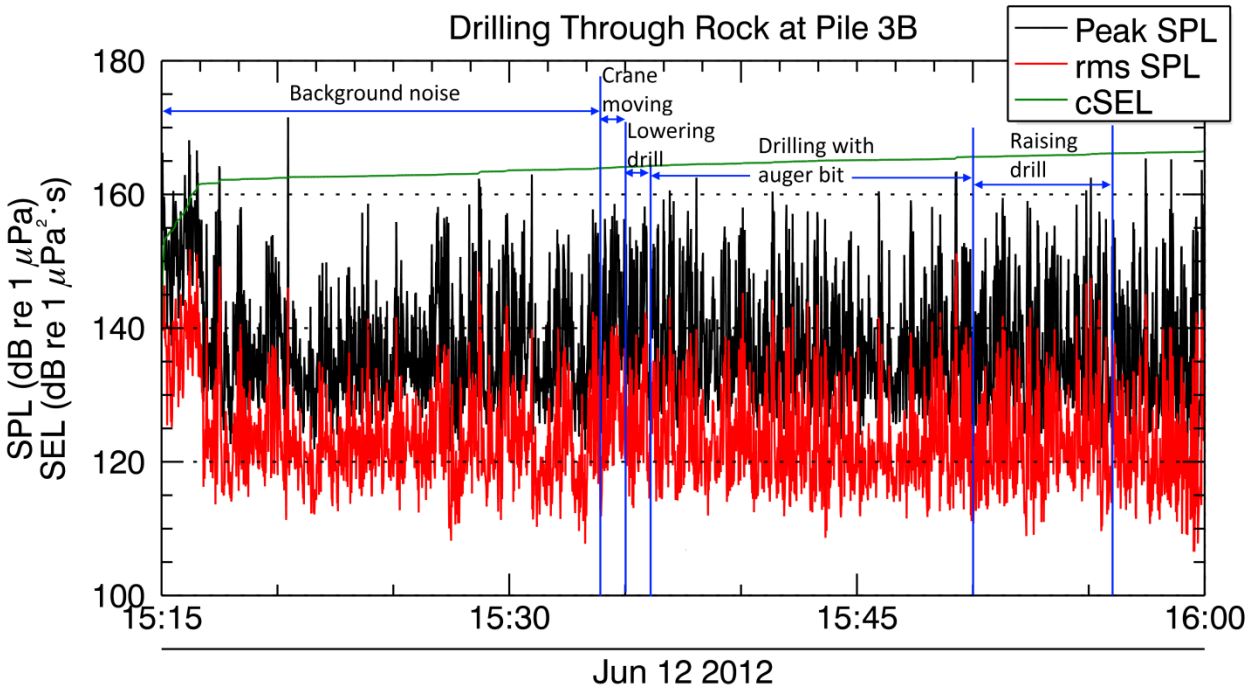

Figure 32. Background Noise and Drilling Through Rock: Peak and rms sound pressure level (SPL) and cumulative sound exposure level (cSEL) versus time (UTC) measured 231 ft from Test Pile 3B.

Table 20. Drilling Through Rock: Maximum peak and rms sound pressure levels (SPLs) and cumulative sound exposure level (cSEL) measured 231 ft from Test Pile 3B.

Max. peak SPL (dB re 1 µPa)	Max. rms SPL (dB re 1 µPa)	cSEL (dB re 1 µPa^2·s)
165.4	151.2	162.6

4. Discussion

4.1. Measured Impact Pile Driving Levels Compared to Pre-Program Modeling

JASCO performed pre-program modeling of underwater sound levels from impact pile driving associated with the PIDP (Warner and MacGillivray 2011). The methods used for the PIDP modeling were identical to those used for modeling underwater noise for the DEIS (MacGillivray et al. 2011). The PIDP modeling study estimated peak SPLs, rms SPLs, single-strike SELs, and cumulative SELs for several different pile diameters, source locations, and NAS attenuation curves. One of the goals of the PIDP hydroacoustics study was to determine whether the pre-program model estimates were conservative with respect to the NMFS physiological and behavioral threshold criteria. The measurements indicate the model accurately predicted received sound levels at short ranges (33 ft), but overestimated sound levels at long ranges (≥1000 ft). Therefore, the model predicted conservative threshold radii.

Table 19 shows comparisons of measured and modeled peak SPLs at the short-range hydrophones (33 ft range). For the unmitigated impact driving, the model slightly underestimated the levels for the 4 ft and 8 ft piles, whereas the model overestimated the levels for the 10 ft piles. In the latter case, we believe that sound levels were lower than predicted because the 10 ft pile met with less driving resistance than the other piles; the driving logs for 4A showed the impact hammer only reached 35% of its rated energy. For all piles, the mitigated impact pile driving levels were greater than the measured values. Thus, except for the 10 ft pile, the short-range sound levels were comparable to the modeled values.

Table 21. Measured and modeled short-range (33 ft) peak SPLs for unmitigated and mitigated impact pile driving.

Pile Diameter (ft)	Location	Modeled Peak SPL (dB re 1 µPa)	Max. Measured Peak SPL (dB re 1 µPa)
Unmitigated (no NAS)			
4	PLT2	205.1	209.7
8	PLT3	223.3	224.7
10	PLT4	228.0	219.1
Mitigated (with NAS)			
4	PLT2	201.1	198.1
8	PLT3	213.4	207.1
10	PLT4	220.7	198.3

Figure 33 shows the comparison of the modeled 1/3-octave band source levels with estimates derived from the unmitigated short-range measurements. These comparisons show the frequency spectrum of the impact pile driving coincided well with the model. We estimated source levels by applying back-propagation (i.e., by adding 20 dB = 10 $\log_{10}$ 10 m) to the mean 1/3-octave band SEL data for piles 2B, 3B, and 4A.

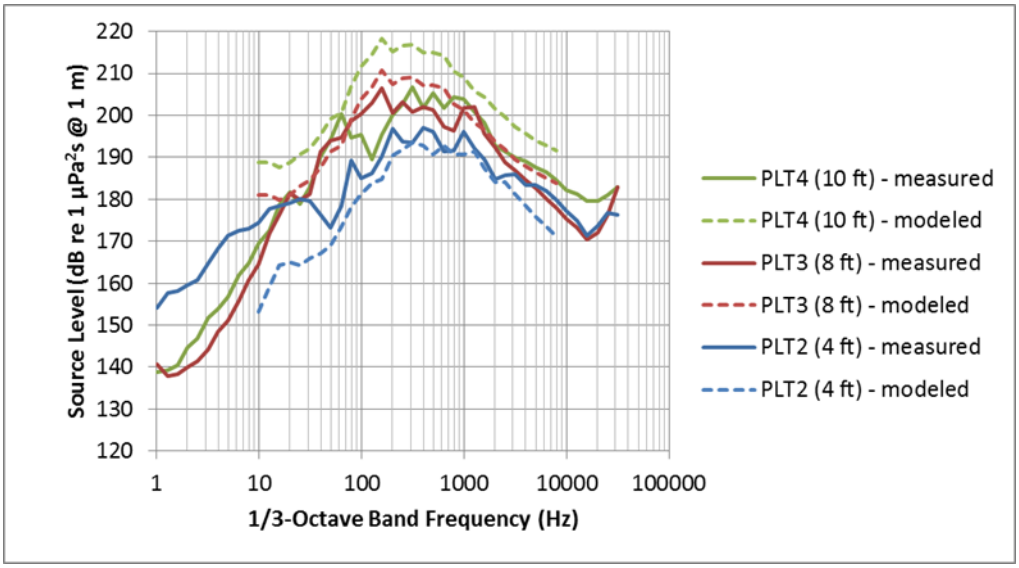

Figure 33. Measured versus modeled 1/3-octave band source levels for unmitigated impact pile driving of 4 ft, 8 ft, and 10 ft diameter piles.

Table 22 through Table 24 compare the measured and modeled distances to the three NMFS physiological and behavioral thresholds. The distances predicted by the model exceeded the measured values in all but one instance (peak SPL for Test Pile 2B). This is because the measured propagation loss between the piles and the long-range recorders was much stronger than the model predicted. Linear regression analysis of the SPL-versus-distance data indicated that the propagation loss was 30−40 log *r* (see Appendix H). This was substantially greater than the ~20 log *r* propagation loss predicted by the pre-program modeling and much greater than the 15 log *r* typically assumed by the NMFS Practical Spreading Loss model (CALTRANS, 2009).

We believe the following two factors contributed to the stronger than expected propagation loss at Tappan Zee Reach:

1. The numerous barges surrounding the piles (see Section 1.4) acted as an acoustic barrier that inhibited sound transmission away from the piles. The drafts of the barges extended 6–10 ft below the waterline and the barges completely surrounded the piles in most instances. We believe the presence of the barges increased sound attenuation beyond that predicted by the model.
2. The riverbed sediments at Tappan Zee Reach may be even more absorptive than the acoustic propagation model predicted. Although the pre-program modeling assumed the sediments were predominantly silty-clay, and therefore quite absorptive, the Tappan Zee Reach riverbed may be even more absorptive than is typical for these kinds of sediments.

Of these two factors, we believe the barges may have been the more influential one since the propagation loss was much stronger than is typically observed at other locations. However, since we did not take acoustic measurements when the barges were absent, we cannot definitively conclude which contributed more to the stronger than expected propagation loss.

Table 22. Measured versus modeled distances to the 206 dB re 1 µPa peak SPL physiological threshold for unmitigated and mitigated impact pile driving.

		206 dB re 1 µPa Peak SPL	
Pile Diameter (ft)	Location	Modeled distance (ft)	Max. measured distance (ft)
Unmitigated (no NAS)			
4	PLT2	31	42
8	PLT3	146	101
10	PLT4	573	71
Mitigated (with NAS)			
4	PLT2	<10	20
8	PLT3	101	38
10	PLT4	166	14

Table 23. Measured versus modeled distances to the 187 dB re 1 µPa^{2}s cSEL physiological threshold for unmitigated and mitigated impact pile driving. The total number of impact hammer blows is indicated in parentheses.

		187 dB re 1 µPa^{2}s cSEL	
Pile Diameter (ft)	Location	Modeled distance[1] (ft)	Max. measured distance (ft)
Unmitigated (no NAS)			
4	PLT2	1263 (15400)	192 (1394)
8	PLT3	3238 (3400)	351 (2181)
10	PLT4	5013 (3000)	282 (1031)
Mitigated (with NAS)			
4	PLT2	825 (15400)	114 (1394)
8	PLT3	1950 (3400)	190 (2181)
10	PLT4	3275 (3000)	125 (1031)

[1] Assumed equal to 50% of the north-south extent of the 187 dB contour from the Biological Opinion, dated 7 March, 2012.

Table 24. Measured versus modeled distances to the 150 dB re 1 µPa rms SPL behavioral threshold for unmitigated and mitigated impact pile driving.

		150 dB re 1 µPa rms SPL	
Pile Diameter (ft)	Location	Modeled distance[1] (ft)	Max. measured distance (ft)
Unmitigated (no NAS)			
4	PLT2	2000	452
8	PLT3	6350	809
10	PLT4	9500	822
Mitigated (with NAS)			
4	PLT2	1250	306
8	PLT3	4600	462
10	PLT4	6750	429

[1] Assumed equal to 50% of the north-south extent of the 150 dB contour from the Biological Opinion, dated 7 March, 2012.

The pile driving contractor is expected to dredge large channels at the construction site to simplify barge movements. On the west side of the river the channel design is 16-feet deep, 500-feet wide and 7000-feet long channel. The dredged channel will follow the proposed bridge span and the sides of the dredged channel will be armored with rock. Constructing a dredged channel will increase pile driving sound levels because pile vibrations couple better to the water column in deeper water. Threshold distances will be greater in the dredged channel because sound generally propagates farther in deeper water. We expect that sound levels in the dredged channel will be comparable to those measured at PLT3 and PLT4, where the mean water depth was 16 ft. We do not know what influence the armored rock wall would have on sound propagation, although we expect the effect to be minimal.

4.2. Recommended Noise Attenuation System

Table 25 shows the mean broadband acoustic attenuation (peak SPL, rms SPL, and SEL/cSEL) for the five NASs tested during the PIDP at 33 ft from the seven test piles. We found NAS performance was generally the same for different airflow/pressure settings.

JASCO's pre-program modeling assumed the NASs would achieve 10 dB of SEL attenuation. Although all of the NASs met the 10 dB SEL attenuation criterion (within experimental error), the Two-Stage Confined Bubble Curtain System provided the strongest overall attenuation. Because the duration of impact pile driving was much shorter than the tidal period at Tappan Zee Reach (usually less than two hours), we lack sufficient data to comment on the stability of the NAS performance with respect to current. Nonetheless, in running current we expect a more stable performance from the confined NASs than the unconfined NASs.

Table 25. Mean broadband NAS attenuation as measured at short-range (33 ft) from impact hammer pile driving. Attenuation levels are averaged over different airflow/pressure settings. From top to bottom, the NASs are ranked in terms of overall effectiveness at reducing physiological and behavioral threshold levels.

			Attenuation (dB)		
Rank	Pile	NAS	Peak SPL	rms SPL	SEL/cSEL
1	3B	Two-Stage Confined Bubble Curtain	17.0	16.1	13.7
2	4A	Two-Stage Confined Bubble Curtain	16.1	12.2	12.9
3	1B	Hard Bubble	16.0	15.7	12.2
4	1A	Unconfined Single-Tier Air Bubble Curtain	15.5	14.5	11.4
5	3A	Unconfined Multi-Tier Air Bubble Curtain	13.1	14.9	11.6
6	2A	Unconfined Multi-Tier Air Bubble Curtain	13.4	11.1	10.0
7	2B	Isolation Casing and Bubble	12.2	10.8	9.9

Figure 34 shows the mean 1/3-octave band attenuation of each of the NASs; measurements were taken 33 ft from the seven test piles. The data show that NAS performance was generally best in the 100-1000 Hz decade band and poorest at frequencies below 100 Hz. This corroborates the pre-program model assessment of NAS performance (see MacGillivray et al. 2010, Fig 11) and generally concurs with other measurements (see e.g., CALTRANS 2009).

The AMAR measurements showed the attenuation provided by the NASs was substantially reduced at longer distances (≥1000 ft) from the piles (see Table 14). The AMAR data showed propagation loss was greatest in the 100-1000 Hz frequency range (see Appendix G), where NAS performance was most effective. Therefore, the observed attenuation was reduced at longer distances because sound energy outside the mid-frequency band was less strongly attenuated by the NASs. This result corresponds with the pre-program model's prediction of a mid-frequency notch in the propagation loss at Tappan Zee Reach (see MacGillivray et al. 2010, §5.1), and an equivalent reduction in the attenuation performance at longer distances.

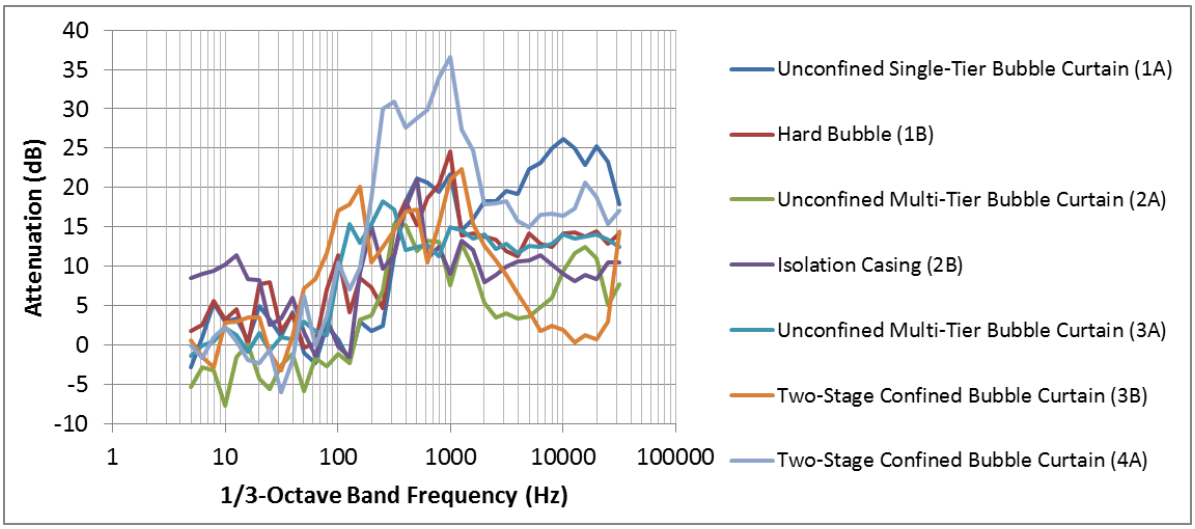

Figure 34. Mean 1/3-octave band NAS attenuation as measured at short-range (33 ft) from impact hammer pile driving. Attenuation levels are averaged over different airflow/pressure settings.

Literature Cited

CALTRANS. 2009. Technical guidance for assessment and mitigation of the hydroacoustic effects of pile driving on Fish. Technical report prepared by ICF Jones & Stokes and Illingworth and Rodkin, Inc., for California Department of Transportation, Sacramento CA.

Fisheries Hydroacoustic Working Group. 2008. Agreement in Principle for Interim Criteria for Injury to Fish From Pile Driving Activities. http://www.dot.ca.gov/hq/env/bio/files/fhwgcriteria_agree.pdf

MacGillivray, A., Warner, G., Racca, R., and O'Neill, C. 2011. Tappan Zee Bridge Construction Hydroacoustic Noise Modeling: Final report. Technical report prepared by JASCO Applied Sciences for AECOM. 71 pp.

Popper, A., Carlson, T., Hawkins, A., Southall, B., Gentry, R. 2006. Interim Criteria for Injury of Fish Exposed to Pile Driving Operations. White paper submitted to Fisheries Hydroacoustic Working Group. http://www.dot.ca.gov/hq/env/bio/files/piledrivinginterimcriteria_13may06.pdf

Appendix A. Glossary

1/3-octave band levels
: Frequency resolved SPLs in non-overlapping passbands that are 1/3 of an octave wide (where an octave is a doubling of frequency). Three adjacent 1/3-octave bands make up one octave. 1/3-octave bands become wider with increasing frequency.

90% energy window
: Time interval over which the cumulative energy rises from 5% to 95% of the total pulse energy, abbreviated with the symbol T_{90}. This interval contains 90% of the total pulse energy.

absorption
: Dissipation of sound energy through viscosity or chemical reactions.

ADCP
: Acoustic Doppler current profiler. Used to measure water current speeds. [Teledyne Workhorse Sentinel 1200 kHz]

ADAMS
: Acoustic Data Acquisition and Monitoring System. Used for short-range monitoring.

AMAR
: Autonomous Multichannel Acoustic Recorder. Used for long-range monitoring.

attenuation
: The acoustic energy loss due to absorption and scattering.

bottom segment
: The lower segment of each test pile. The bottom segment is driven first via vibratory pile driving.

broadband sound level
: The total sound pressure level measured over a specified frequency range. If the frequency range is unspecified, it is understood to be the entire measurement range.

CTD
: Conductivity-temperature-depth profiler. Used to derive salinity profile and sound speed profile of the water column.

decibel
: A logarithmic unit of the ratio of a quantity to a specific reference level (abbrev. dB).

ensonified
: Exposed to sound.

frequency
: Rate of oscillation measured in units of cycles-per-unit-time: e.g., 1 Hertz (abbrev. Hz) = 1 cycle/second.

impulsive sound
: Discrete sounds with very short durations (less than a few seconds). Sounds with longer durations are called continuous sounds.

intensity
: Sound energy flowing through a unit area perpendicular to the direction of propagation per unit time.

M8E

A spherical hydrophone manufactured by GeoSpectrum Technologies Inc, of Dartmouth NS, Canada. The M8E has a nominal sensitivity of −164 dBV/µPa ±3 dB from 5 Hz-180 kHz.

M8K

A spherical hydrophone manufactured by GeoSpectrum Technologies Inc, of Dartmouth NS, Canada. The M8K has a nominal sensitivity of −210 dBV/µPa ±3 dB from 5 Hz–180 kHz.

NMFS

National Marine Fisheries Service

NAS

Noise attenuation system

peak sound pressure level

Maximum instantaneous sound pressure, expressed in decibels, sometimes referred to as zero-to-peak level. Peak-to-peak level is the difference between the maximum and minimum instantaneous sound pressures, expressed in decibels.

percentile

Value below which an event occurs some percentage of the time. The n^{th} percentile level gives the level below which the signal is n% of the time.

PIDP

Pile installation demonstration project.

power spectrum density

The acoustic signal power per unit frequency as measured at a single frequency (units $\mu Pa^2/Hz$).

power spectrum density level

The dB level (10log10) of the power spectrum density, usually presented in 1 Hz bins (units dB re 1 $\mu Pa^2/Hz$).

pressure (hydrostatic)

The pressure at any given depth in a static liquid that is the result of the weight of the liquid acting on a unit area at that depth, plus any pressure acting on the surface of the liquid (SI unit Pa).

pressure (acoustic)

The deviation from the ambient hydrostatic pressure caused by a passing sound wave (SI unit Pa). Also referred to as overpressure.

rms sound pressure

The root-mean-square average of the instantaneous sound pressure (symbol L_p) as measured over some specified time interval (symbol T_{90}). The 90% energy time window (T_{90}) is typically used for pulse sounds. Consequently, the rms SPL for pulse sounds is often referred to as the 90% rms SPL (L_{p90}).

scfm/lf

standard cubic feet per minute per linear foot; measures flow rate.

sound

A time-varying pressure disturbance that is generated by mechanical vibration waves travelling through a fluid medium (e.g., air or water).

sound exposure level (SEL)

A measure of the total sound energy contained in one or more pulses. SEL is measured in units of dB re 1 µPas.

sound pressure level (SPL)

The decibel ratio of sound pressure to some reference pressure. Numerically, the dB level is equal to $20 \times \text{Log}_{10}(P/P_{ref})$, where P is the sound pressure and P_{ref} is the reference pressure. In underwater acoustics, the standard reference pressure is 1 µPa and the units of SPL are written: dB re 1 µPa. Unless otherwise stated, SPL refers to the root mean square (rms) sound pressure.

SpectroPlotter

An integral part of JASCO's Acoustic Analysis Suite of Java-based acoustic processing tools. Was used for short-range, real-time monitoring.

spectrum

The representation of an acoustic signal in terms of its power (or energy) distribution versus frequency (see Power Spectrum Density).

source level (SL)

The SPL that would be measured at 1 metre distance from a point-like source that radiates the same total amount of sound power as an actual source. Source levels are expressed in units of dB re 1 µPa at 1 m.

Tappan Zee Reach

The monitoring program study area. Reach of the Hudson River between Rockland and Westchester Counties, New York.

transmission loss (TL)

The dB reduction in sound level that results from the spreading of sound away from an acoustic source, subject to the influence of the surrounding environment. Also referred to as propagation loss.

wavelength

Distance over which a wave completes one cycle of oscillation, abbreviated with the symbol λ.

Appendix B. Hydroacoustic Computations and Metrics

B.1. Hydroacoustic Computations

Figure 35 shows the processing steps for the impact pile driving detection and analysis. Figure 36 shows the similarities between the processing steps for vibratory pile driving analysis and background noise.

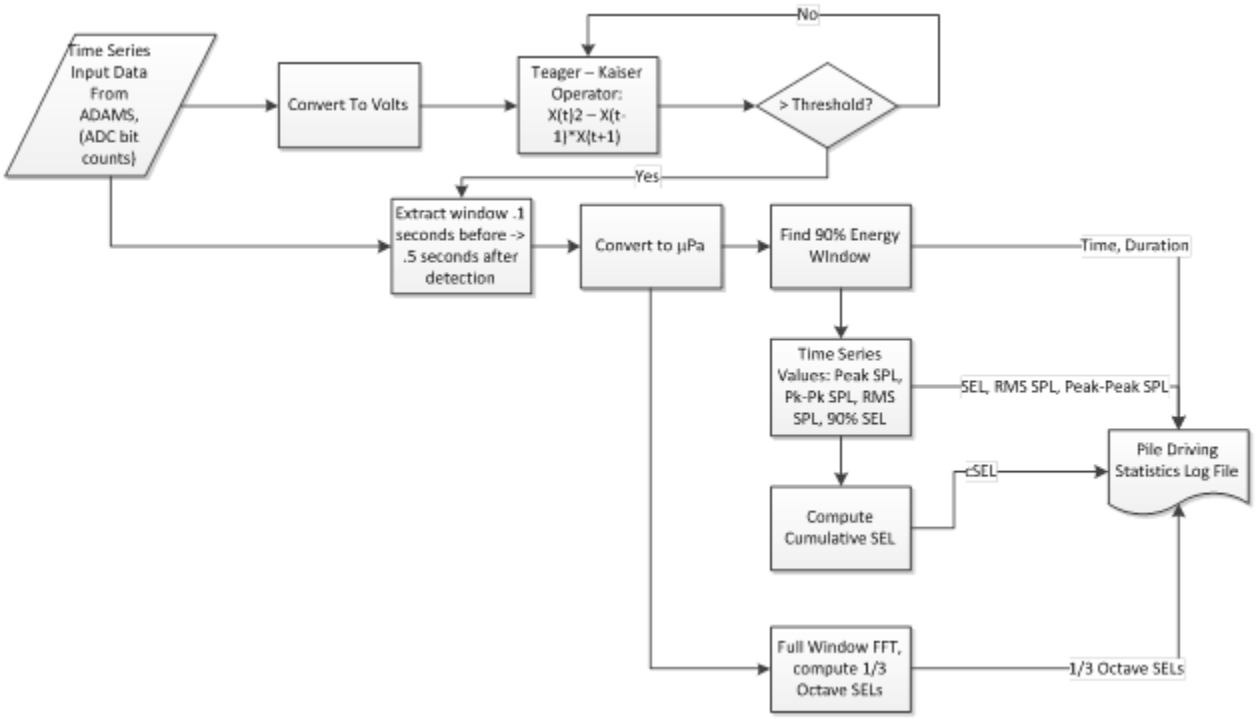

Figure 35. Processing steps for analyzing and detecting impact pile driving strikes.

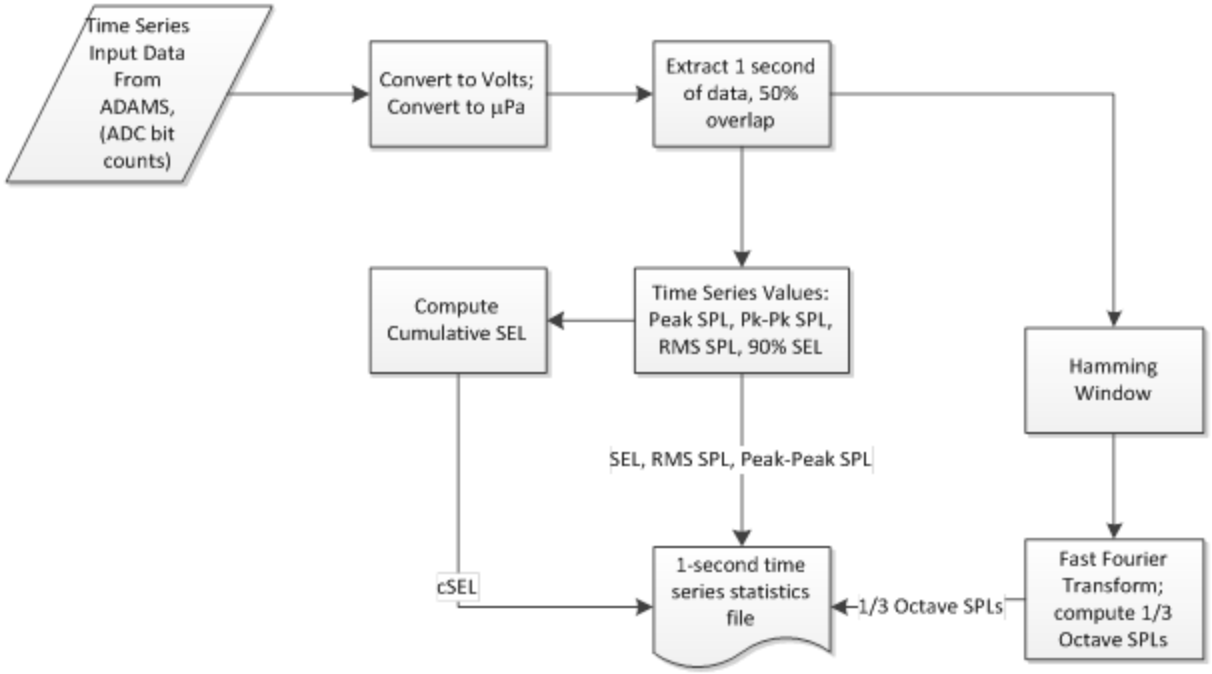

Figure 36. Processing steps for analyzing and detecting vibratory pile driving and background noise.

B.2. Hydroacoustic Metrics

Sound pressure and intensity are usually quantified on the decibel (dB) scale. The decibel scale is a logarithmic scale that expresses a quantity relative to a predefined reference quantity. Acoustic quantities expressed on the decibel scale are called levels. Sound pressure level in decibels (abbreviated as SPL; symbol, L_p) is calculated as follows:

$$L_p = 10\log_{10}\left(p^2 / p_o^2 \right) \quad \text{(B-1)}$$

where p is the pressure amplitude in Pascals (Pa) and p_o is the reference sound pressure. For underwater sound, the standard reference pressure is p_o = 1 µPa (equal to 10^{-6} Pa or 10^{-11} bar). In most cases, the sound intensity is directly proportional to the mean square of the sound pressure (i.e., $I \propto p^2$); therefore, the SPL is usually considered synonymous with the sound intensity level.

The decibel scale for quantifying underwater sound is different than that for quantifying airborne sound. Airborne decibel levels are relative to a standard reference pressure of p_o = 20 µPa, which is 20 times greater than the hydroacoustic reference pressure of 1 µPa. Furthermore, because of differences in compressibility and density between air and water, the impedance relationship between sound pressure and sound intensity is different between the two media. Accounting for the differences in reference pressure and acoustic impedance, for a sound wave with the same intensity in both media the hydroacoustic decibel level (in dB re 1 µPa) is approximately 63 dB greater than the standard airborne decibel level (in dB re 20 µPa).

Tones are sounds composed of single frequencies. Most sounds are *broadband* sounds—composed of a broad range of frequencies rather than pure tones. Sounds with very short durations (less than a few seconds) are said to be *impulsive*. Impulsive sounds typically have a

rapid onset and decay. *Continuous* sounds are steady and vary in intensity slowly with time, or not at all.

B.2.1. Continuous Sound

Continuous sound is characterized by gradual intensity variations over time. Noise from a transiting ship is an example. The intensity of continuous sound is generally given in terms of the root-mean-square (rms) SPL. Given a measurement of the time varying sound pressure, $p(t)$, from a given sound source, the rms SPL (symbol, L_p) is:

$$L_p = 10\log_{10}\left(\int_T p^2(t)dt \Big/ Tp_o^2\right) \quad \text{(B-2)}$$

where T is the duration of the measurement. Figure 37 shows an example of a continuous sound pressure waveform and the corresponding rms sound pressure.

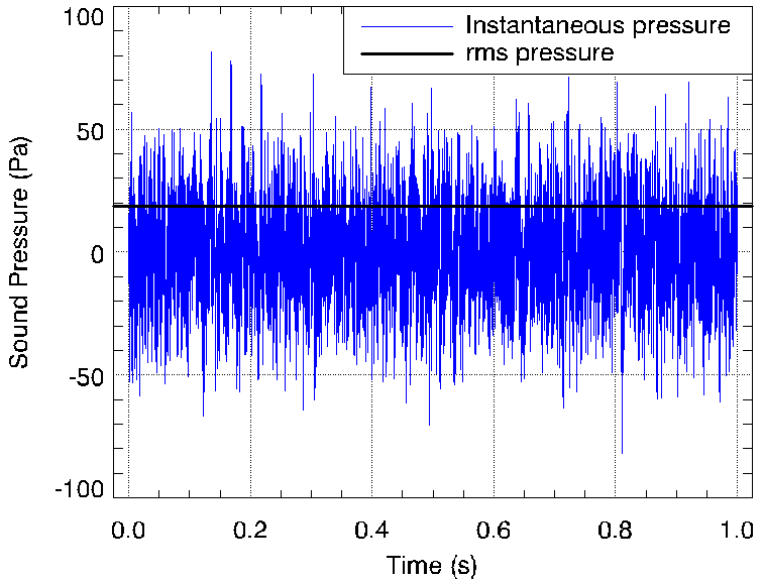

Figure 37. Pressure waveform of a continuous sound and the corresponding rms sound pressure.

B.2.2. Impulsive Sound

Impulsive or transient sounds are brief, intermittent acoustic events with rapid onset and rapid decay (within a few seconds) back to pre-existing levels. Noise from impact pile driving is an example. Impulse sound levels are commonly characterized using three acoustic metrics: peak SPL (also called zero-to-peak SPL), rms SPL, and sound exposure level (SEL). The peak SPL (symbol, L_{pk}) is the maximum instantaneous sound pressure level attained by an impulse:

$$L_{pk} = 10\log_{10}\left(\max\left|p(t)^2\right| \Big/ p_o^2\right) \quad \text{(B-3)}$$

where $p(t)$ is the instantaneous sound pressure as a function of time measured over the impulse duration $0 \le t \le T$. Peak SPL is commonly quoted for impulsive sounds, but it does not account for the duration or bandwidth of the sound.

The rms SPL in a stated frequency band can be computed over the impulse duration according to the following equation:

$$L_p = 10\log_{10}\left(\int_T p(t)^2\,dt \Big/ Tp_o^2\right) \quad \text{(B-4)}$$

The definition of the duration T is somewhat ambiguous because the beginning and end of a measured impulse can be difficult to precisely identify. In studies of impulsive sound, T is often T_{90}, the interval over which the cumulative energy curve rises from 5% to 95% of the total energy. The T_{90} interval contains 90% of the total energy. The rms SPL computed over the T_{90} interval is called the 90% rms SPL (symbol, L_{p90}). The relative energy, $E(t)$, of an impulse is computed from the time integral of the square pressure:

$$E(t) = \int_0^t p(t)^2\,dt \Big/ p_o^2 \quad \text{(B-5)}$$

According to this definition, denoting the time corresponding to n% of the total relative energy of the impulse as t_n, the 90% energy time interval is defined as $T_{90} = t_{95}–t_5$. Figure 38 shows an example of an impulsive sound pressure waveform with the corresponding peak pressure, rms pressure, and 90% energy time interval.

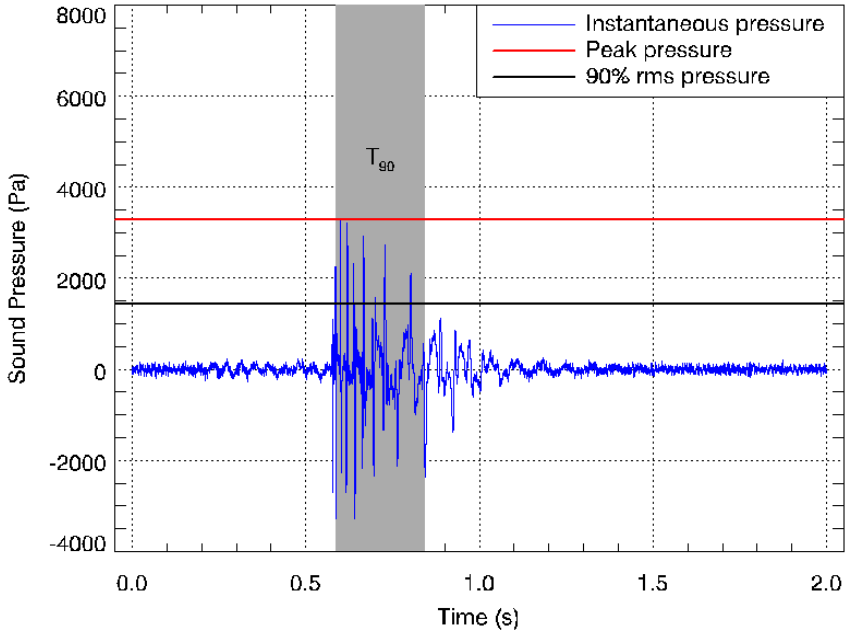

Figure 38. Waveform of an impulsive sound measurement. Horizontal lines indicate the peak pressure and 90% rms pressure of the impulse. The gray area is the 90% energy time interval (T_{90}) over which the 90% rms pressure was computed.

The sound exposure level (abbreviated SEL; symbol, L_E) is a measure of the total sound energy contained in one or more impulses. The SEL for a single impulse is computed from the time-integral of the squared pressure over the impulse duration:

$$L_E = 10\log_{10}\left(\int_{T_{100}} p(t)^2\,dt \Big/ p_o^2 \right) = 10\log_{10}\left(E(t_{100})\right) \quad \text{(B-6)}$$

Unlike SPL, SEL is generally applied as a dosage metric because its value increases with the number of exposure events. The cumulative SEL for multiple impulses (abbreviated cSEL; symbol, $L_E^{(\Sigma)}$) is computed from the linear sum of the SEL values:

$$L_E^{(\Sigma)} = 10\log_{10}\left(\sum_{n=1}^{N} 10^{L_E^{(n)}/10} \right) \quad \text{(B-7)}$$

In this formula, N is the total number of impulses, and $L_E^{(n)}$ is the SEL of the nth impulse event. Alternatively, given the mean (or expected) SEL for single impulse events, $\langle L_E \rangle$, the cumulative SEL from N impulses may be computed according the following formula:

$$L_E^{(\Sigma)} = \langle L_E \rangle + 10\log_{10}(N) \quad \text{(B-8)}$$

Sound exposure levels for impulsive sound sources (i.e., impact hammer pile driving) presented in this report refer to single pulse SELs as well as cumulative SELs (cSELs) where appropriate. Because the 90% rms SPL and SEL for a single impulse are both computed from the integral of square pressure, these metrics are related by a simple expression that depends only on the duration of the 90% energy time window T_{90}:

$$L_E = L_{P90} + 10\log_{10}(T_{90}) + 0.458 \quad \text{(B-9)}$$

In this formula, the 0.458 dB factor accounts for the remaining 10% of the impulse energy that is excluded from the 90% time window.

B.2.3. Source Level and Transmission Loss

Sources of underwater sound, such as ships and marine mammal calls, generate radiating sound waves of which the intensity generally decays with distance from the source. The dB reduction in sound level that results from propagation of sound away from an acoustic source is called *propagation loss* or *transmission loss* (TL). The loudness or intensity of a sound source is quantified in terms of the source level (SL), which is the sound level referenced to some fixed distance from a sound source. The standard reference distance for underwater sound is 1 m. By convention, TLs are specified in units of dB re 1 m and SLs, in units of dB re 1 µPa at 1 m.

In the source-path-receiver model of sound propagation, the received sound level RL at some receiver position is equal to the source level minus the transmission loss along the propagation path between the source and the receiver:

$$\text{RL} = \text{SL} - \text{TL} \quad \text{(B-10)}$$

B.2.4. Spectral Density and 1/3-Octave Band Analysis

The discussion of sound measurement presented thus far has not addressed frequency dependence. The sound power per unit frequency of an acoustic signal is described by the power spectral density (PSD) function. The PSD level of an acoustic signal is normally computed via the discrete Fourier transform (DFT) of the time-sampled pressure data. The units of power spectral density are 1 µPa^2/Hz, or dB re 1 µPa^2/Hz. For practical quantitative spectral analysis, a

coarser representation of the sound power distribution is often better. In 1/3-octave band analysis, the acoustic signal is filtered into multiple, non-overlapping passbands before computing the SPL. The 1/3-octave bands are defined such that three adjacent bands span approximately one octave (i.e., a doubling) of frequency. Figure 39 shows an example of power spectral density levels and the corresponding 1/3-octave band pressure levels for an ambient noise recording.

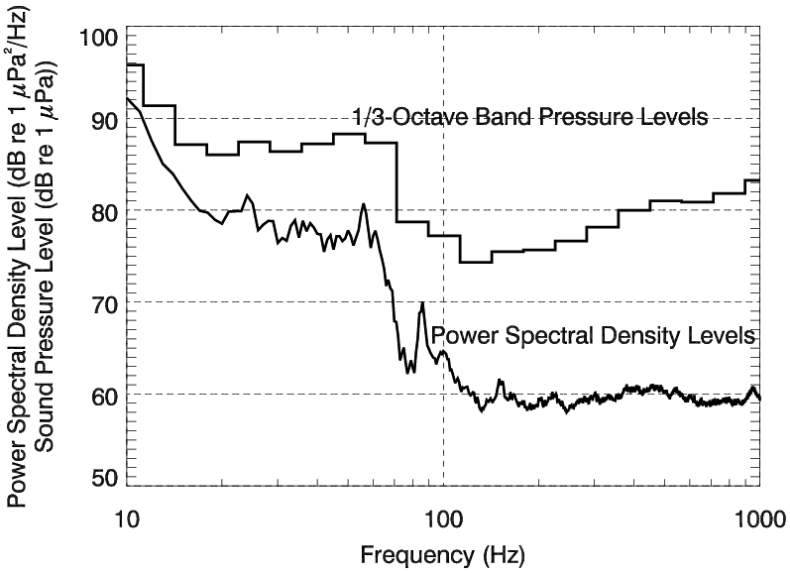

Figure 39. Power spectral density and corresponding 1/3-octave band levels of ambient noise. The frequency scale is logarithmic so the 1/3-octave bands are wider at higher frequencies.

The standard center frequencies for 1/3-octave bands (symbol, f_c; unit, Hz) are given by:

$$f_c(n) = 10^{n/10} \quad n = 1, 2, 3... \tag{B-11}$$

The ISO standards for nominal 1/3-octave band center frequencies for the range relevant to this study are listed in Table 26. The SPL of a 1/3-octave band, $L_{pb}(f_c)$, is related to the average PSD level inside that frequency band, $L_{ps}^{(avg)}(f_c)$, by the bandwidth, Δf:

$$L_{ps}^{(avg)}(f_c) = L_{pb}(f_c) - 10\log_{10}(\Delta f) \tag{B-12}$$

The bandwidth of a 1/3-octave band is equal to 23.1% of the band center frequency (i.e., $\Delta f = 0.231 f_c$). Power spectral density levels and band levels can apply not only to measurements of sound pressure; they can also apply, with appropriate selection of reference units, to measurements of SEL and particle velocity.

Table 26. The ISO standard nominal center frequencies of 1/3-octave bands from 10 Hz to 8 kHz.

n	Center frequency (Hz)	n	Center frequency (Hz)	n	Center frequency (Hz)
10	10	20	100	30	1000
11	12.5	21	125	31	1250
12	16	22	160	32	1600
13	20	23	200	33	2000
14	25	24	250	34	2500
15	31.5	25	315	35	3150
16	40	26	400	36	4000
17	50	27	500	37	5000
18	63	28	630	38	6300
19	80	29	800	39	8000

Appendix C. Environmental Data: CTD Measurements

C.1. Test Piles 1A and 1B

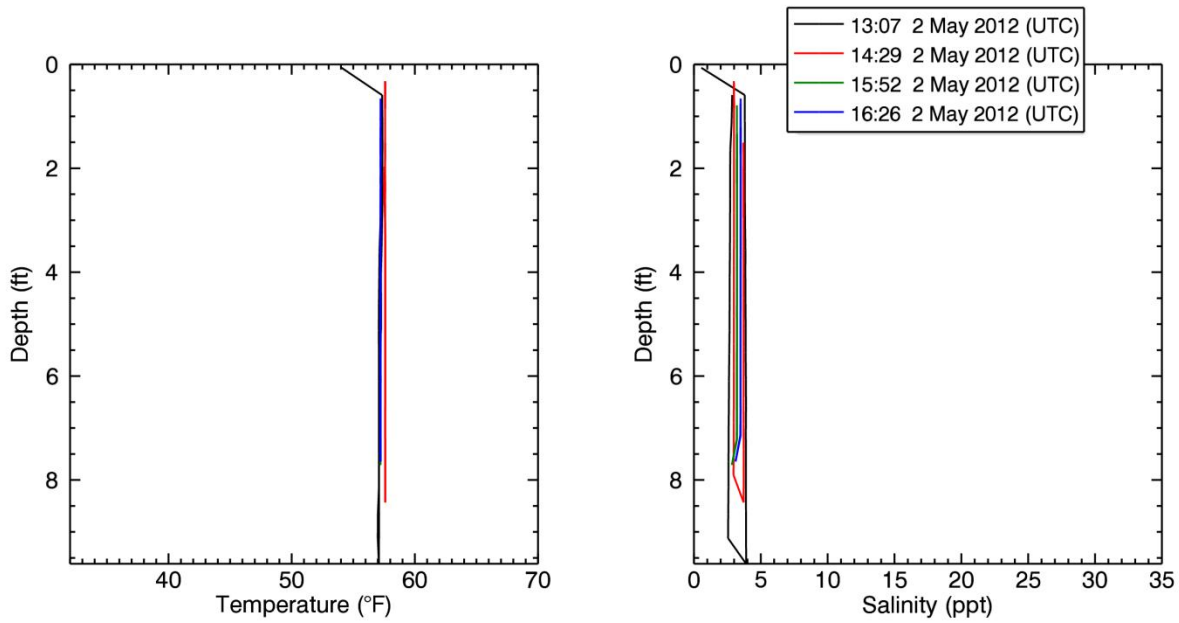

Figure 40. Water temperature and salinity profiles measured with each CTD cast during piling of the bottom segments. Times are in UTC.

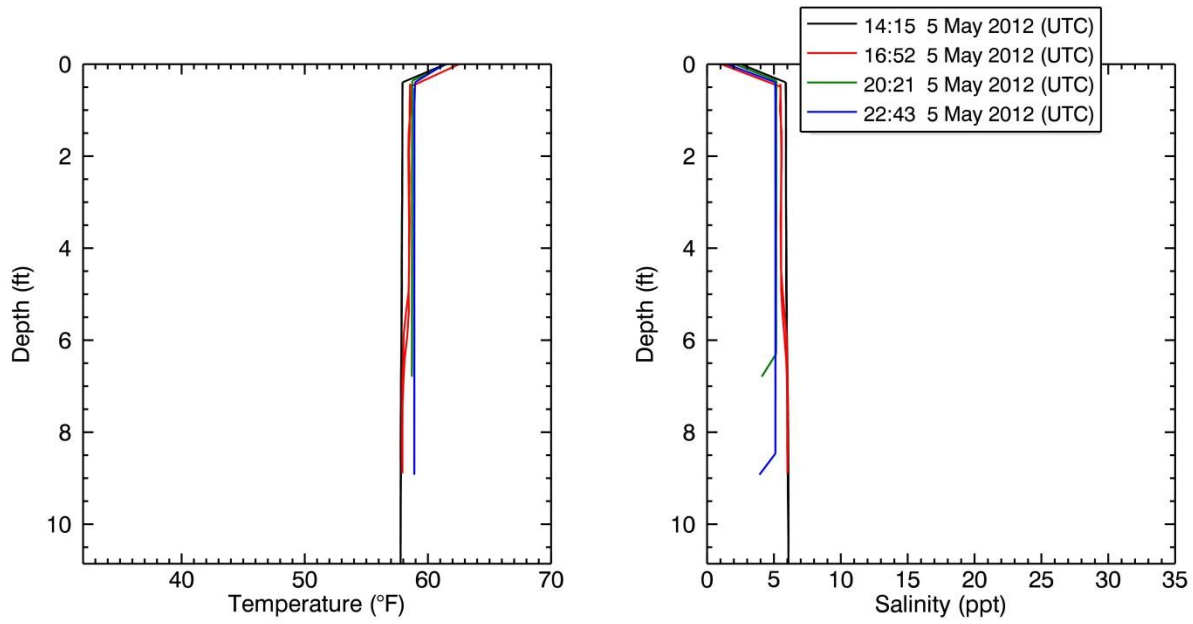

Figure 41. Water temperature and salinity profiles measured with each CTD cast during piling of the top segments of Test Piles 1A and 1B. Times are in UTC.

C.2. Test Piles 2A and 2B

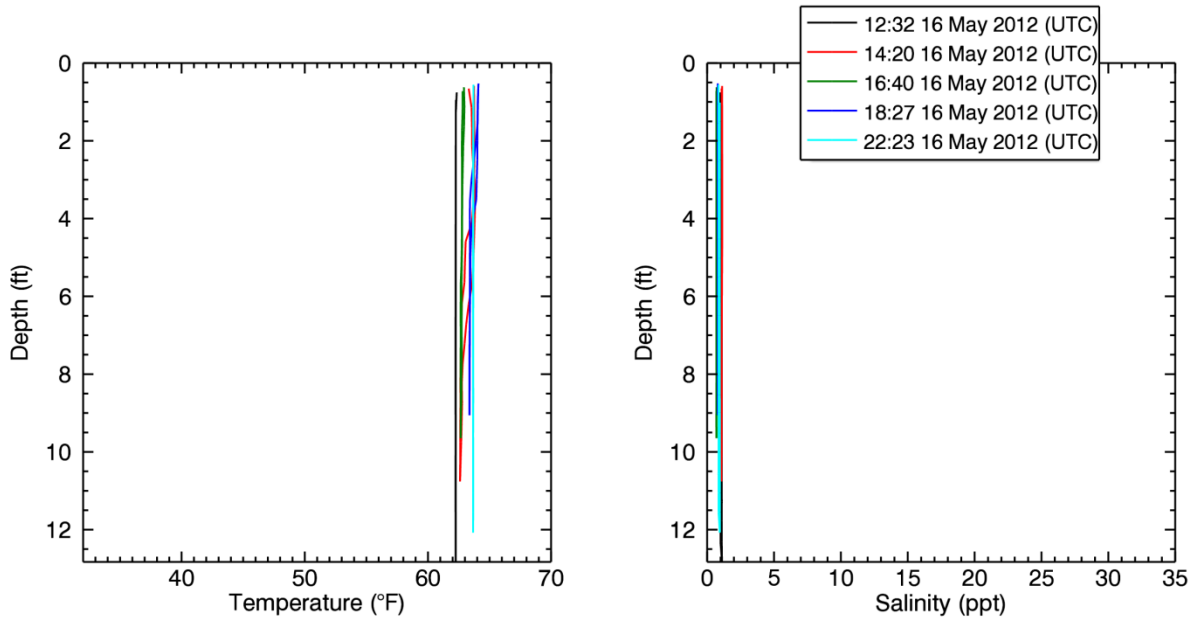

Figure 42. Water temperature and salinity profiles measured with each CTD cast during piling of the top segments of Test Piles 2A and 2B. Times are in UTC.

C.3. Test Pile 3A

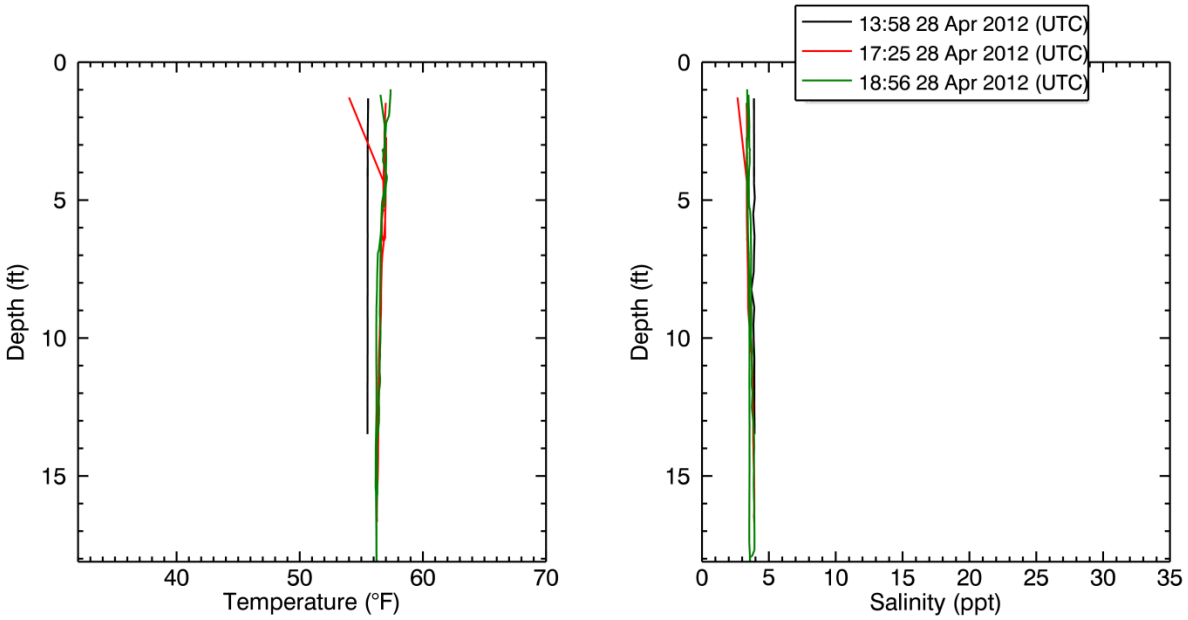

Figure 43. Water temperature and salinity profiles measured with each CTD cast during piling of the bottom segment of Test Pile 3A. Times are in UTC.

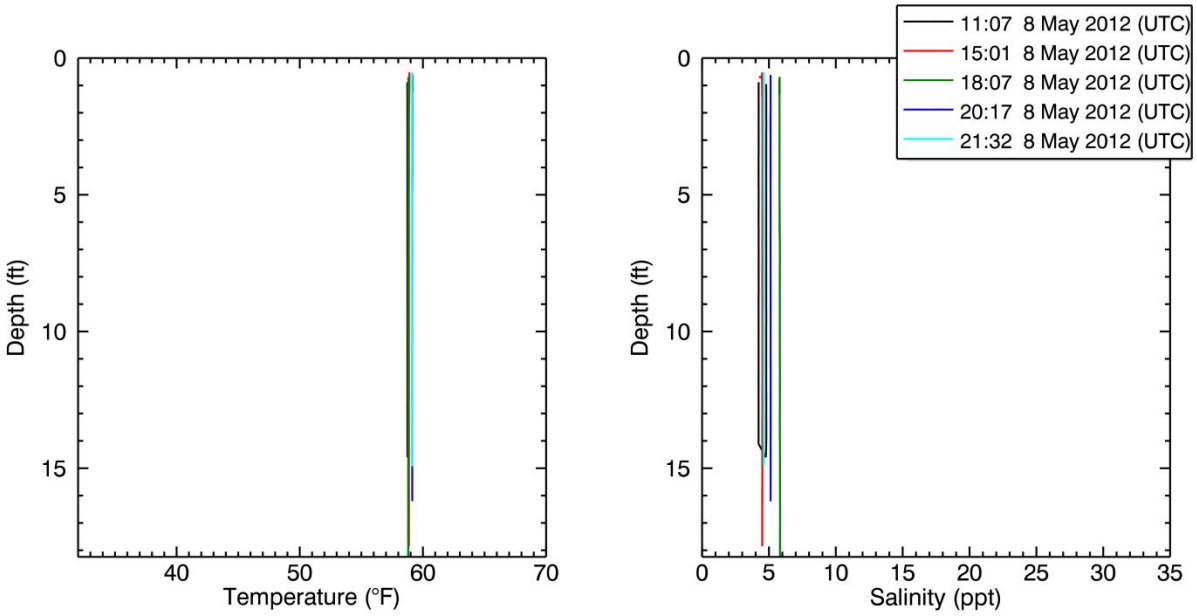

Figure 44. Water temperature and salinity profiles measured with each CTD cast during piling of the top segment of Test Pile 3A. Times are in UTC.

C.4. Test Pile 3B

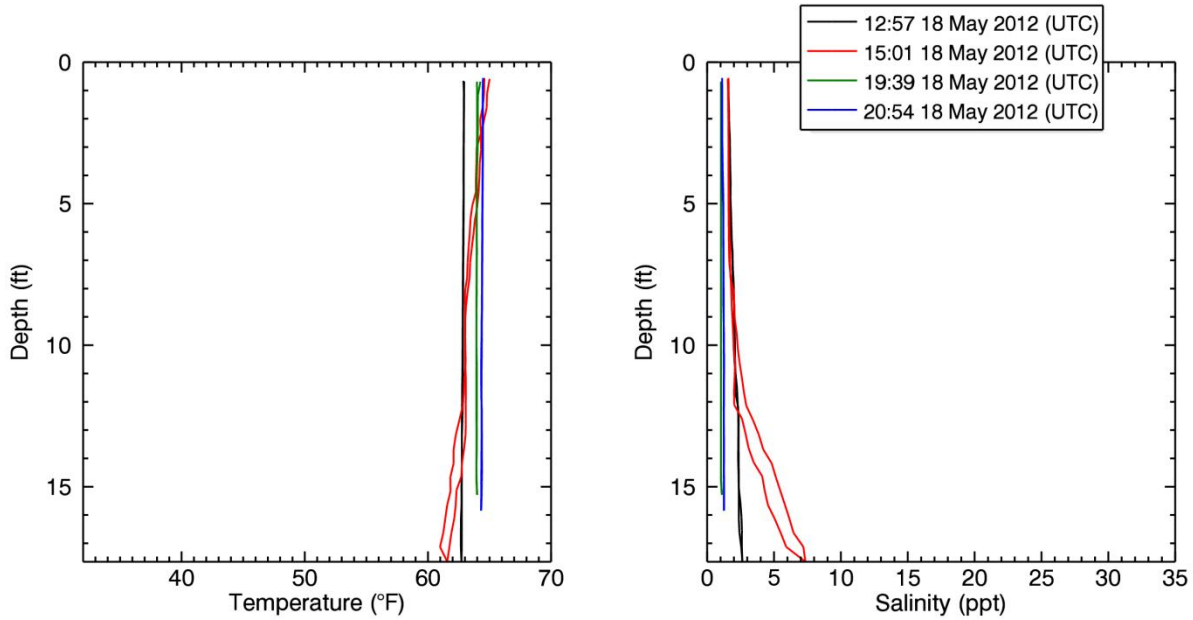

Figure 45. Water temperature and salinity profiles measured with each CTD cast during piling of the top segment of Test Pile 3B. Times are in UTC.

C.5. Test Pile 4A

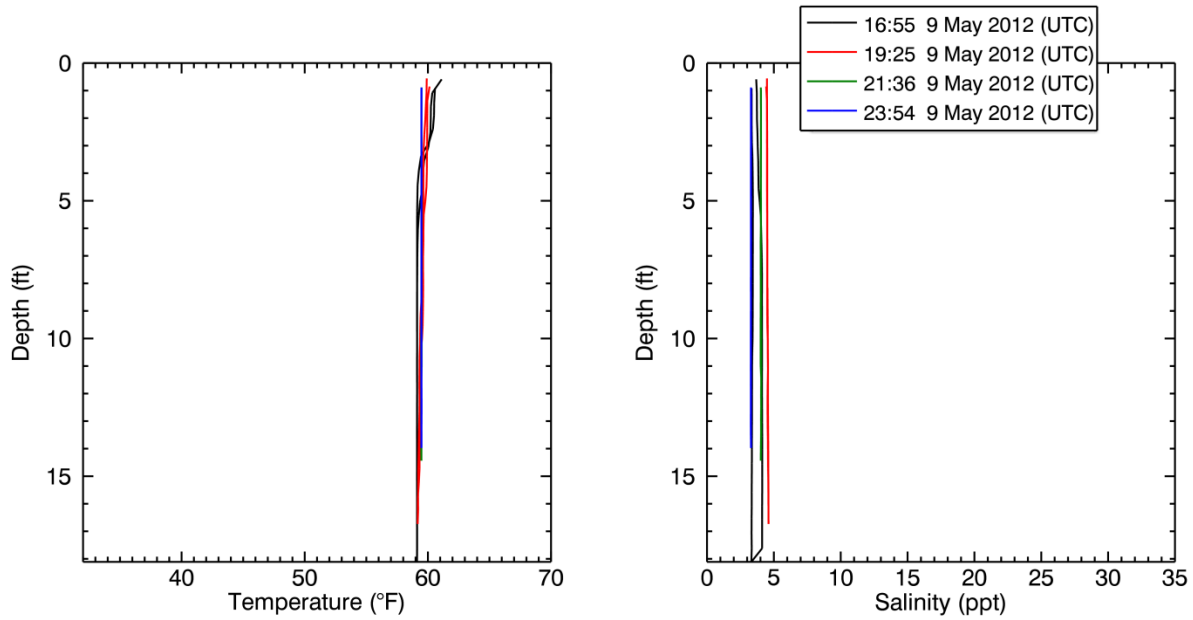

Figure 46. Water temperature and salinity profiles measured with each CTD cast during piling of the bottom segment of Test Pile 4A. Times are in UTC.

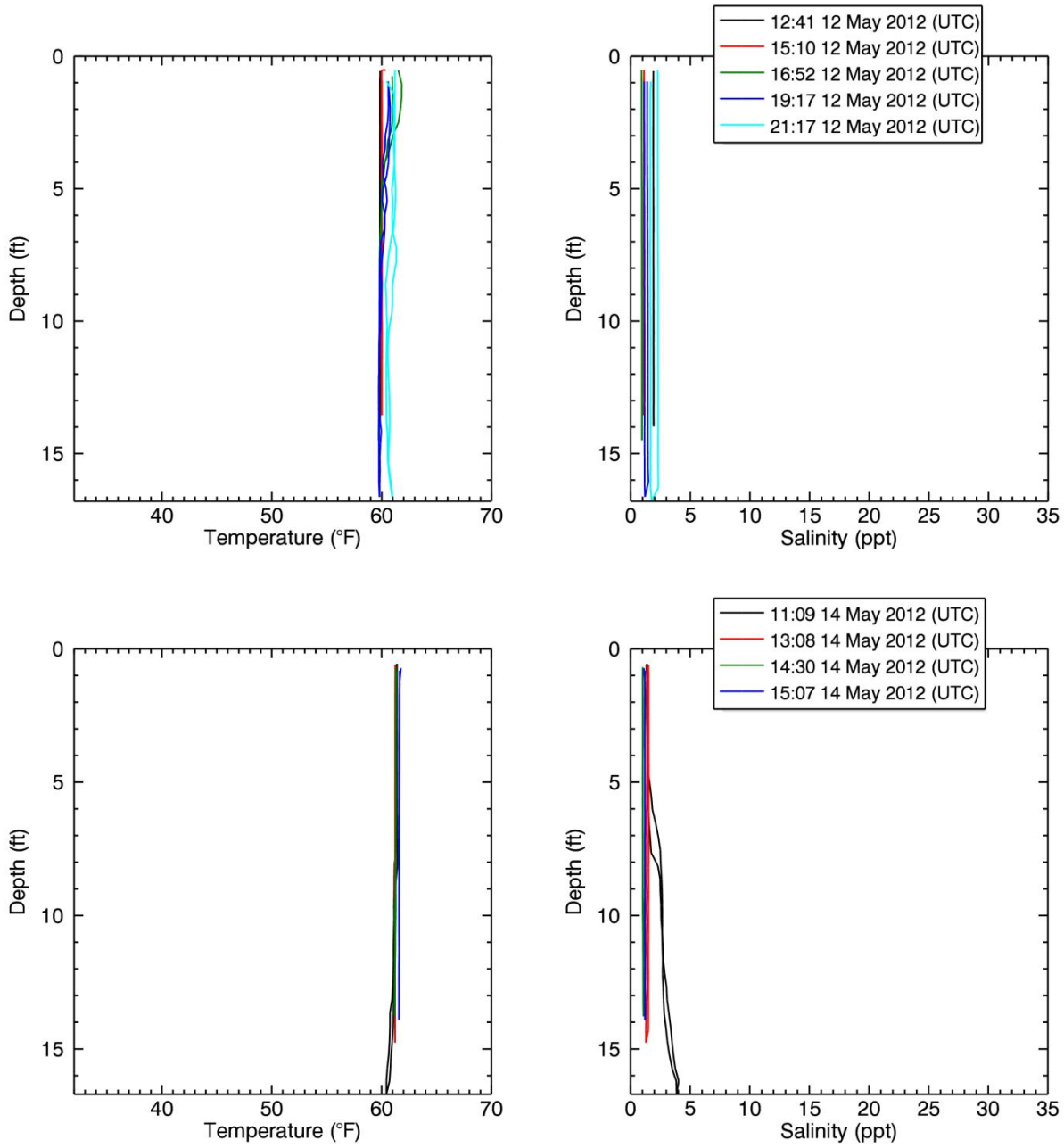

Figure 47. Water temperature and salinity profiles measured with each CTD cast during piling of the top segment of Test Pile 4A. Times are in UTC.

Appendix D. Environmental Data: ADCP Measurements

This appendix contains two sets of plots for each pile. The first set is the mean water speed and direction with overlays to show the times when impact pile driving occurred. The second set is the raw ensemble data from the ADCPs that show the measured current speeds as a function of depth and time.

D.1. Test Piles 1A and 1B

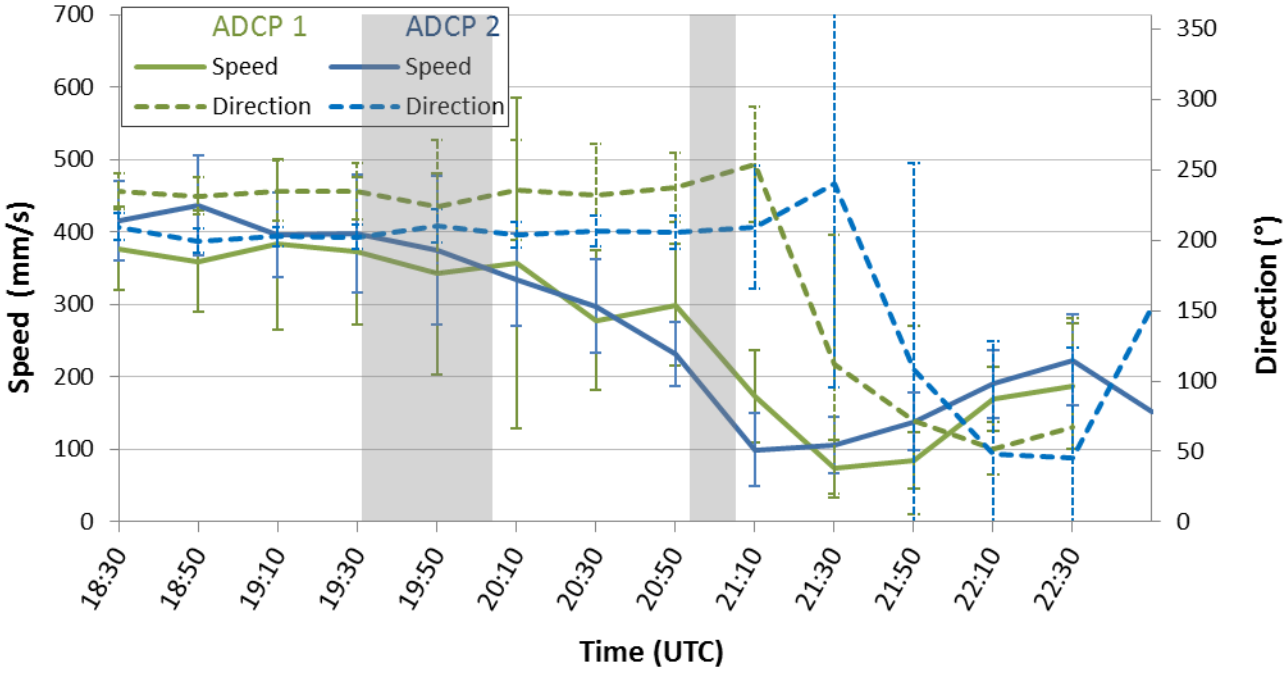

Figure 48. Mean water current speed and direction during driving of the top segment of Test Pile 1A, 5 May 2012. ADCP 1 was north (upstream), and ADCP 2 was south (downstream) of the pile.

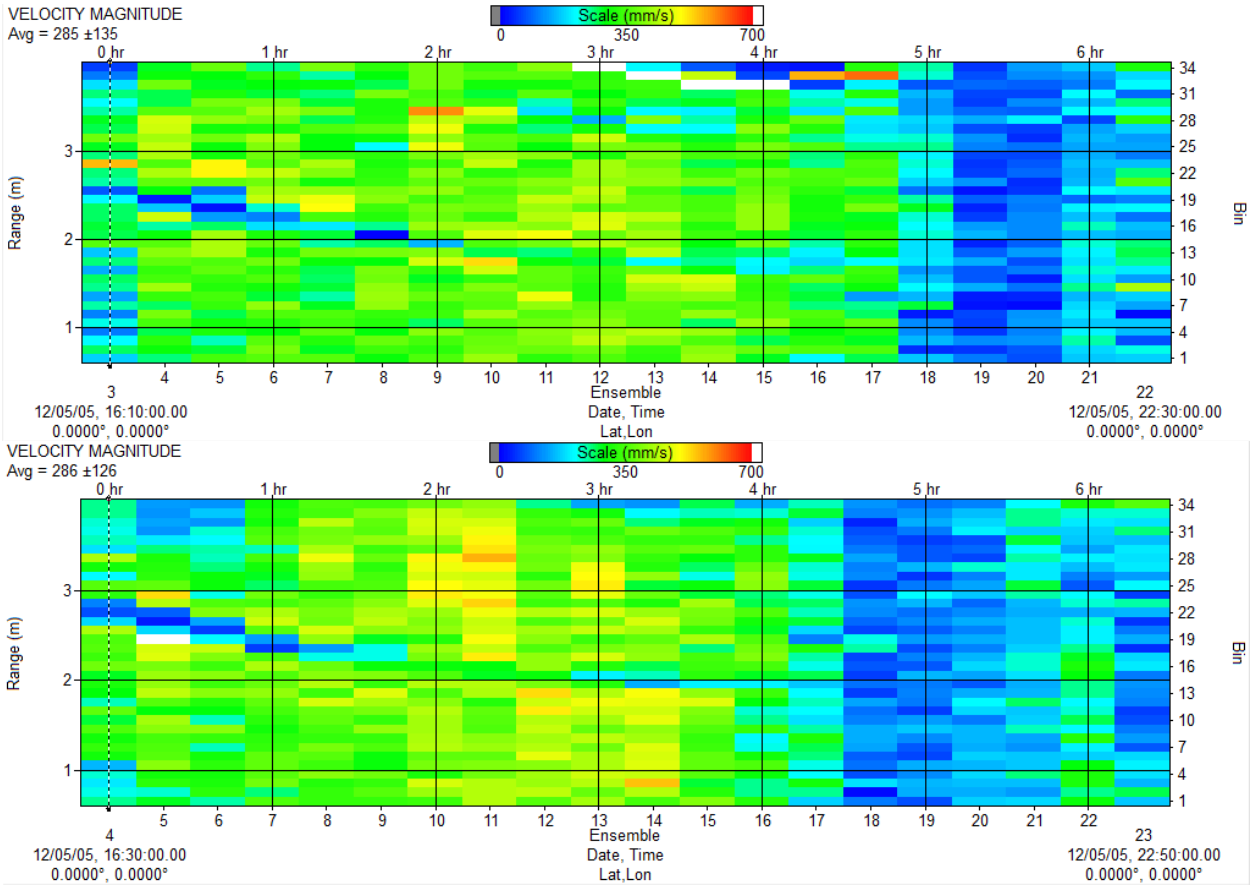

Figure 49. River current speed as a function of depth measured with the ADCP (top) upstream and (bottom) downstream of Test Pile 1A during impact pile driving of the top segment, 5 May 2012.

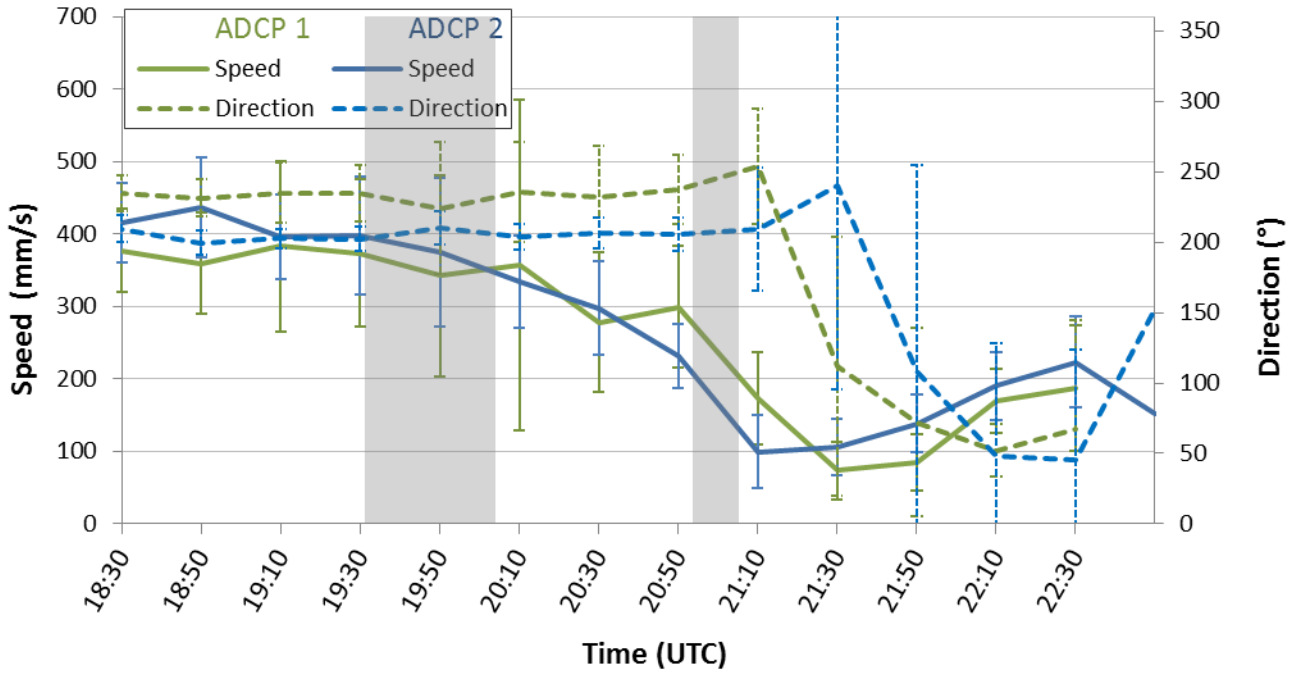

Figure 50. Average water current speed and direction during driving of the top segment of Test Pile 1B, 5 May 2012. ADCP 1 was north (upstream), and ADCP 2 was south (downstream) of the pile.

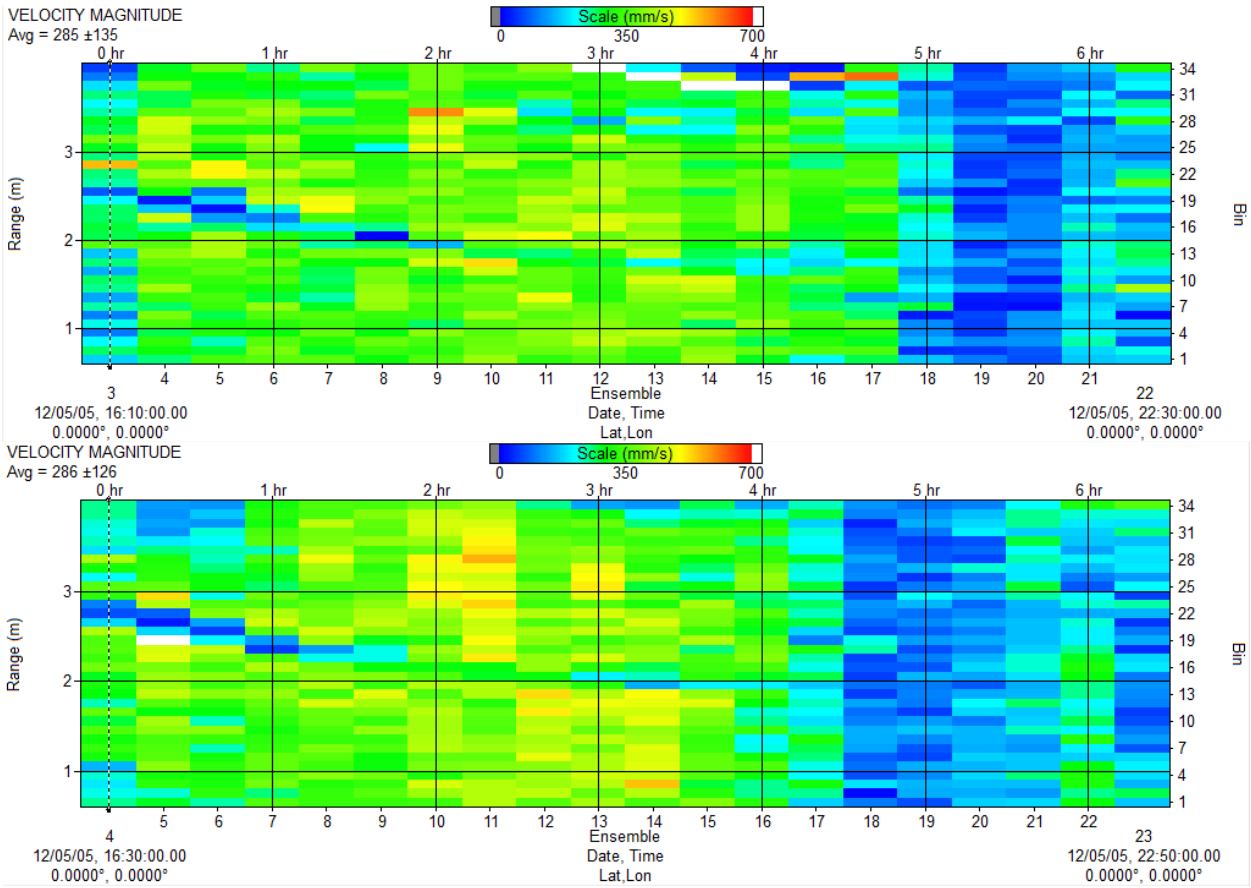

Figure 51. River current speed measured with the ADCPs upstream (top) and downstream (bottom) of during driving of the bottom segment of Test Pile1B.

D.2. Test Piles 2A and 2B

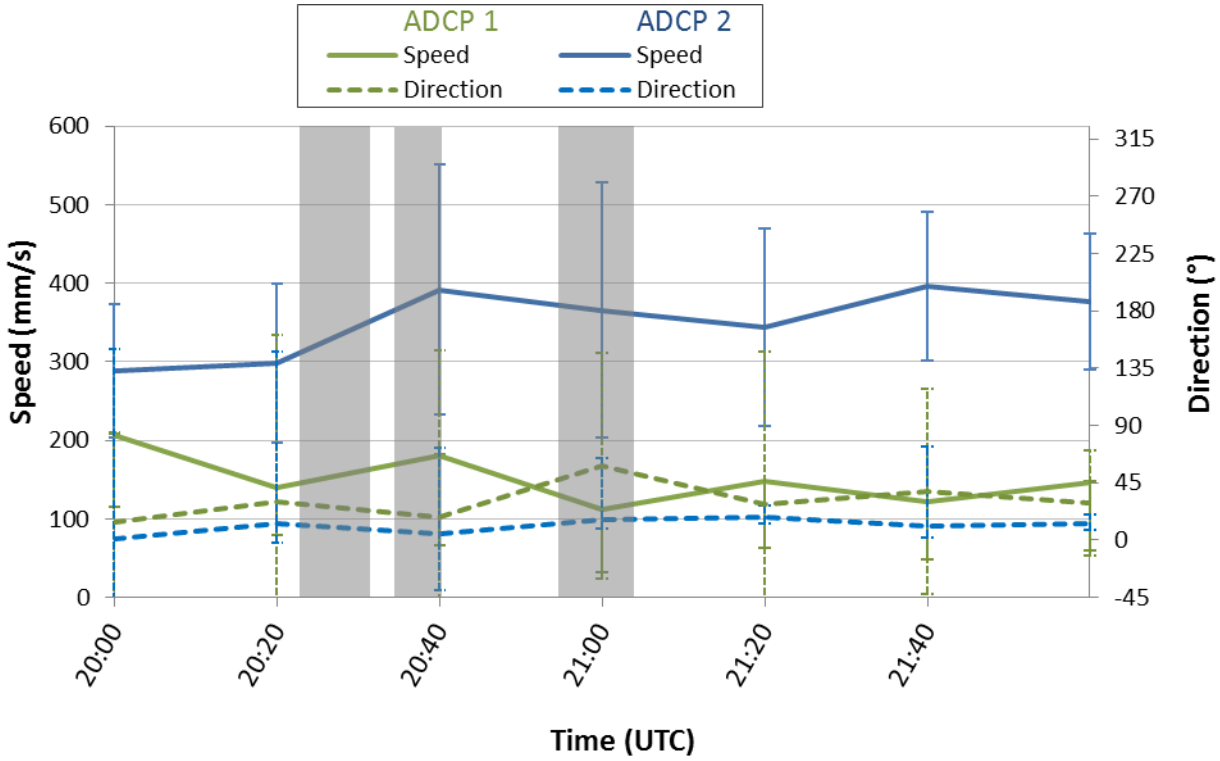

Figure 52. Average river current speed and direction during impact pile driving of the top segment of Test Pile 2A, 16 May 2012. ADCP 1 was north (upstream), and ADCP 2 was south (downstream) of the pile. Gray areas indicate impact piling.

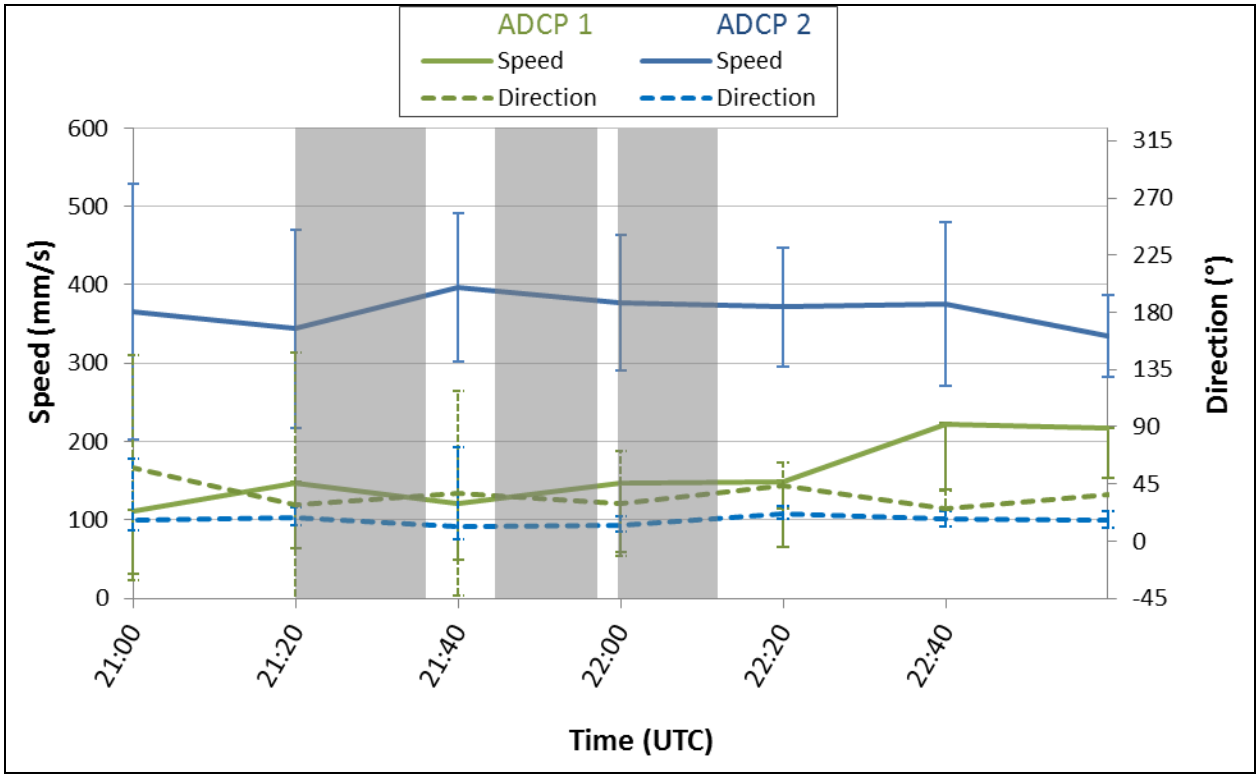

Figure 53. Average river current speed and direction during impact pile driving of the top segment of Test Pile 2B, 16 May 2012. ADCP 1 was north (upstream), and ADCP 2 was south (downstream) of the pile. Gray areas indicate impact piling.

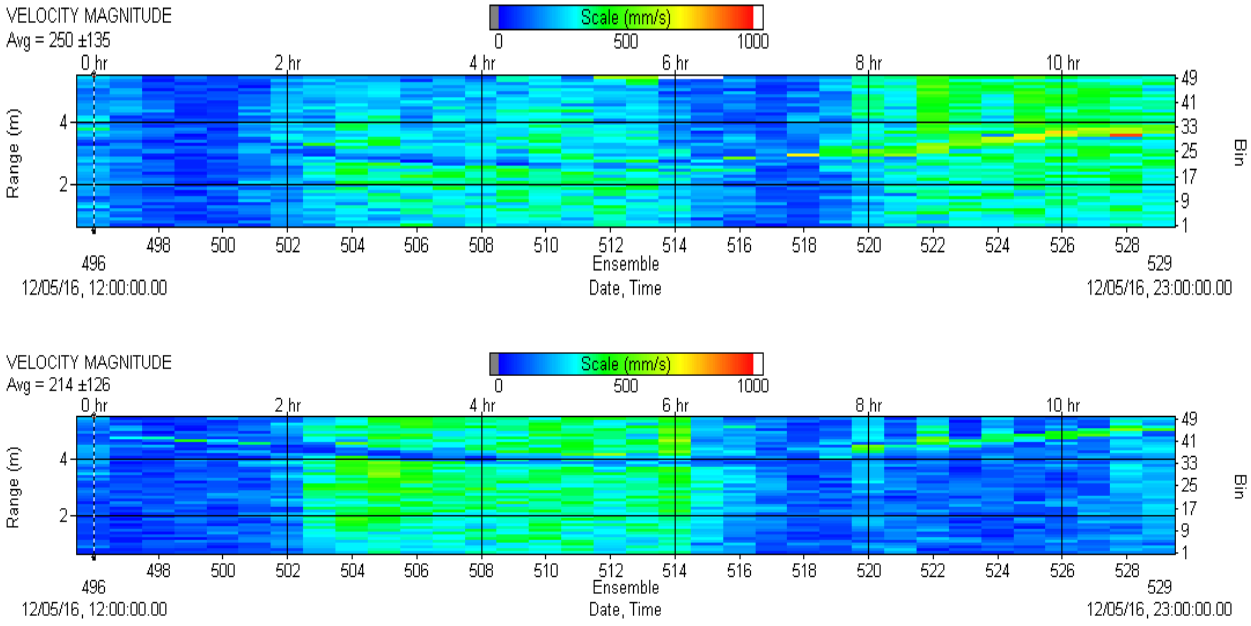

Figure 54. River current speed as a function of depth during piling at Test Pile 2A and 2B, 16 May 2012. (Top) ADCP 150 m south of Test Pile 2B. (Bottom) ADCP 100 m north of Test Pile 3A.

D.3. Test Pile 3A

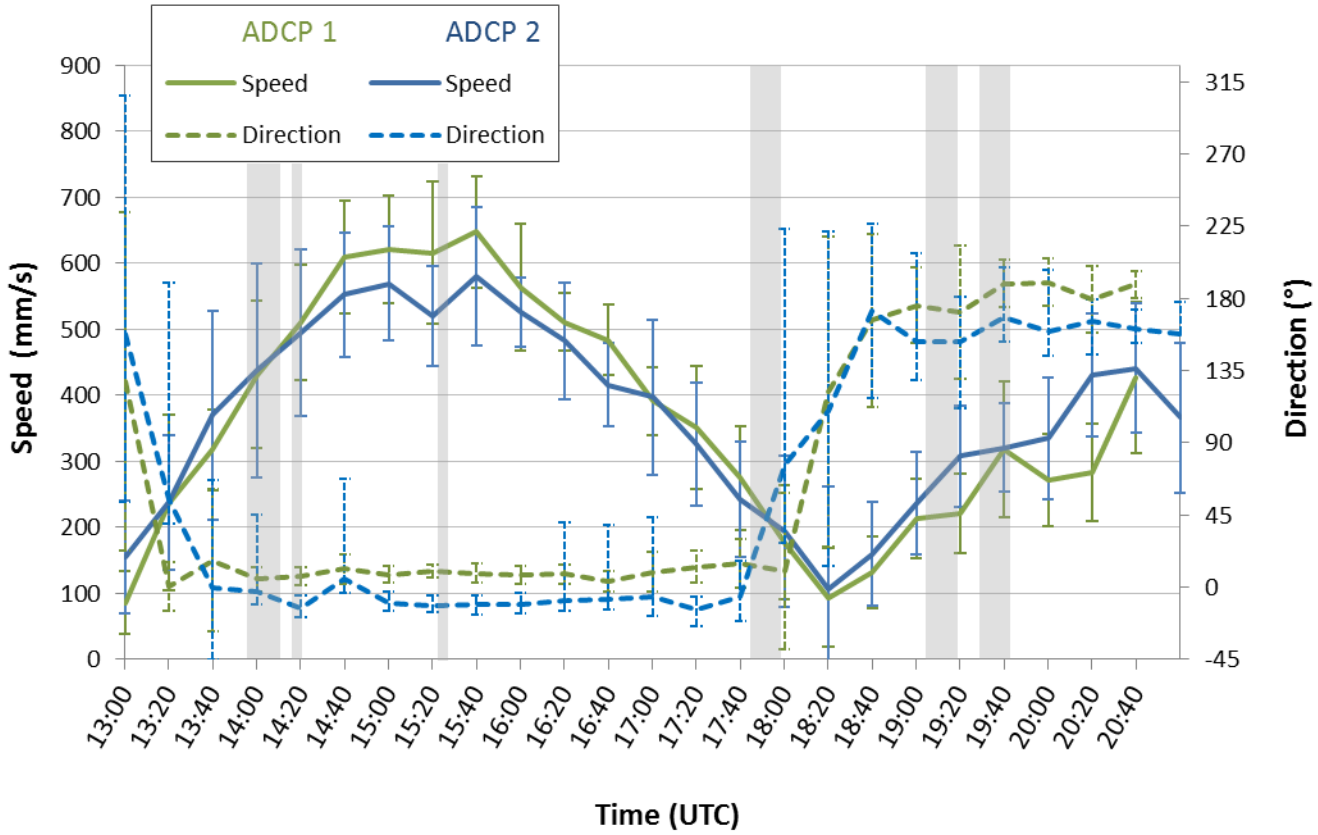

Figure 55. Mean water current speed and direction during driving of the top segment of Test Pile 3A, 8 May 2012. ADCP 1 was north (upstream), and ADCP 2 was south (downstream) of the pile. Gray areas represent occurrence of impact pile driving.

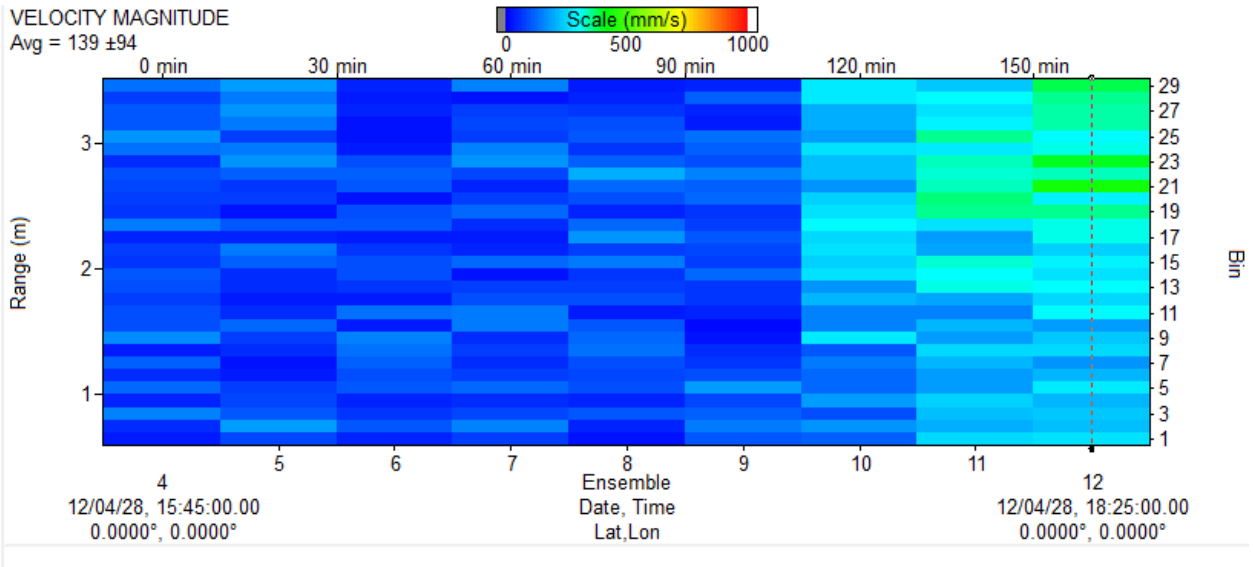

Figure 56. River current speed measured with the ADCP during vibratory pile driving of the bottom segment of Test Pile 3A, 28 April 2012.

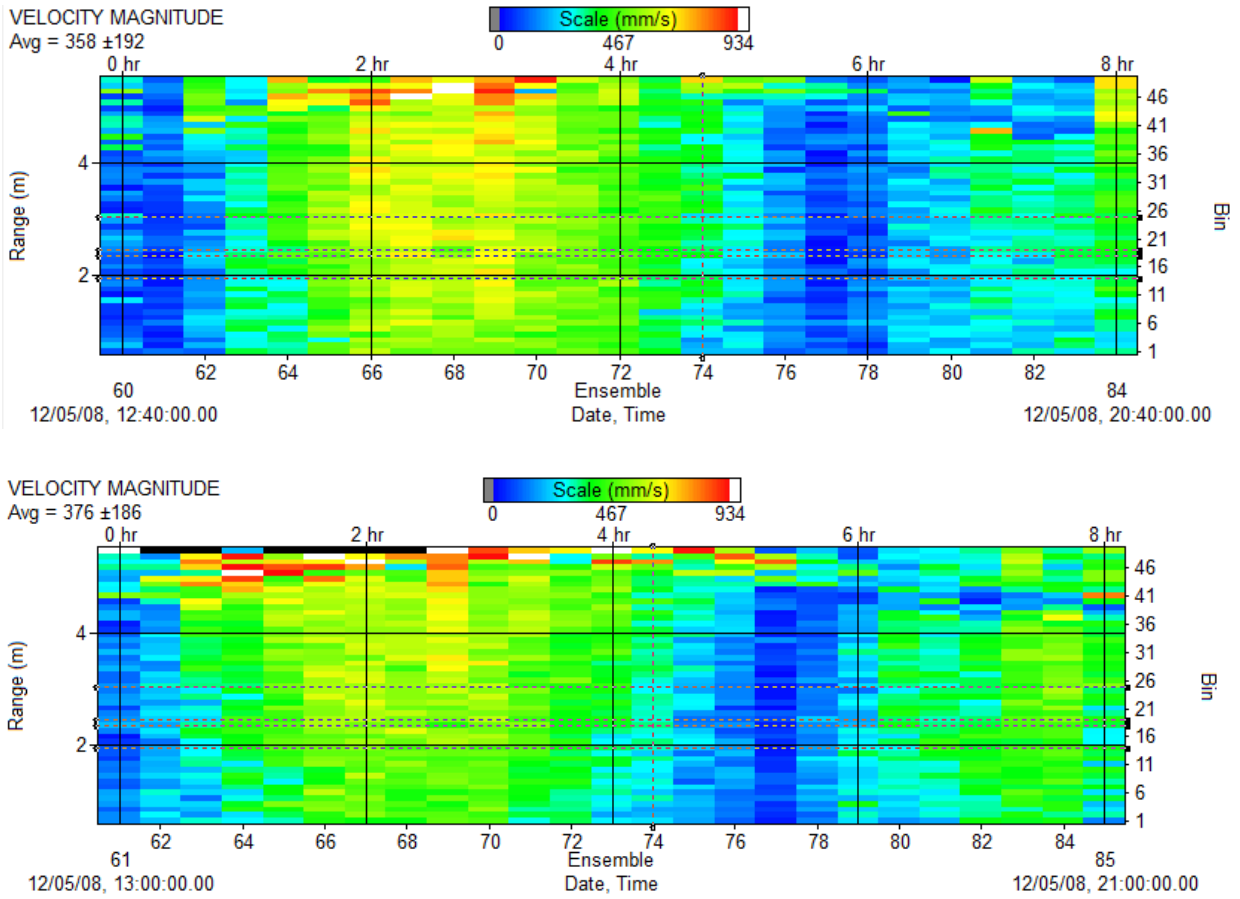

Figure 57. River current speed measured with the ADCP (top) upstream and (bottom) downstream of Test Pile 3A during impact pile driving of the top segment, 8 May 2012.

D.4. Test Pile 3B

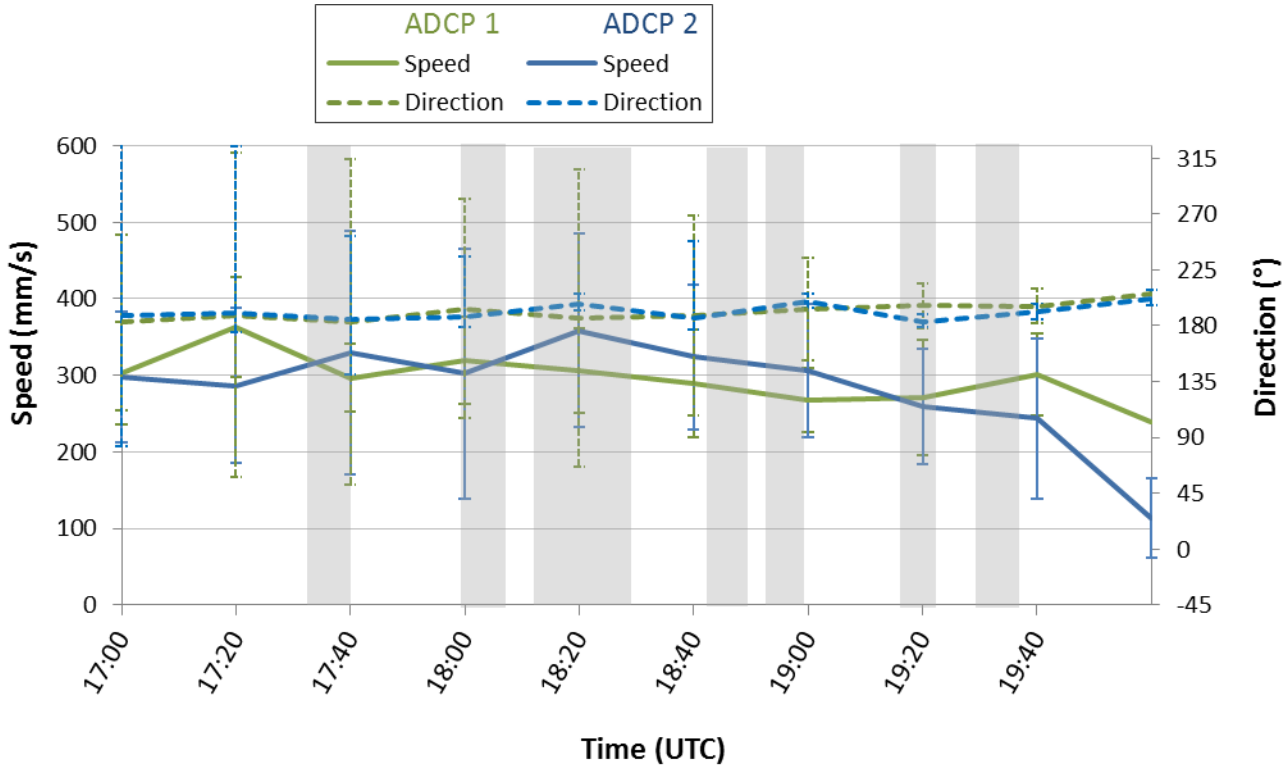

Figure 58. Mean water current speed and direction during impact driving of the top segment of Test Pile 3B, 18 May 2012. ADCP 1 was north (upstream), and ADCP 2 was south (downstream) of the pile. Gray areas represent occurrence of impact pile driving.

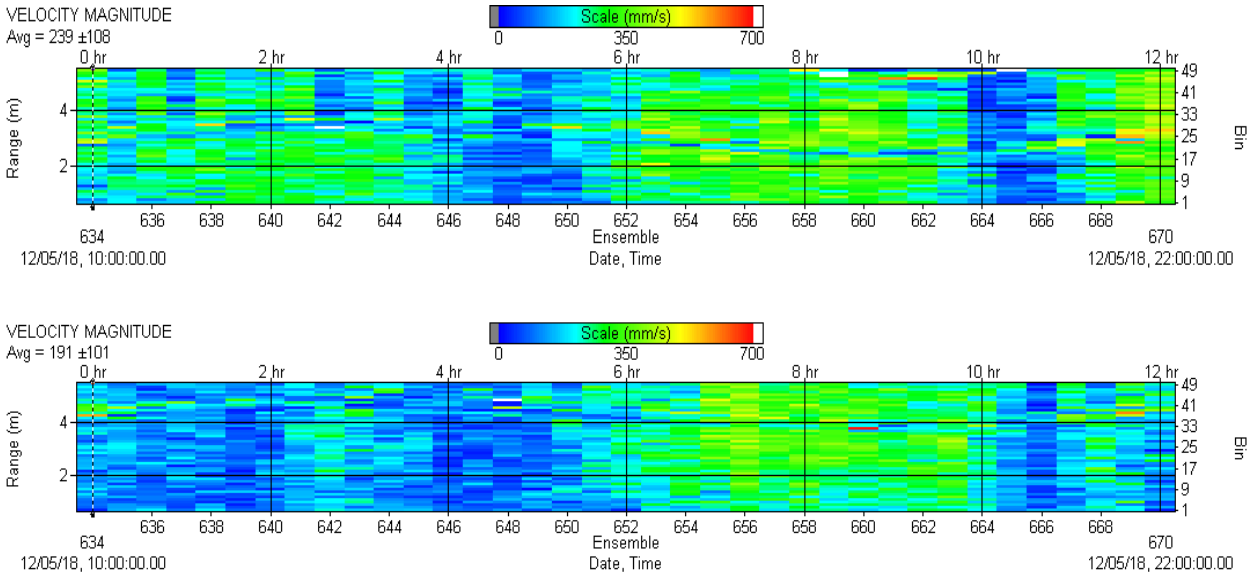

Figure 59. River current speed as a function of depth during piling at Test Pile 3B, 18 May 2012. (Top) ADCP 150 m south of Test Pile 2B. (Bottom) ADCP 100 m north of Test Pile 3A.

D.5. Test Pile 4A

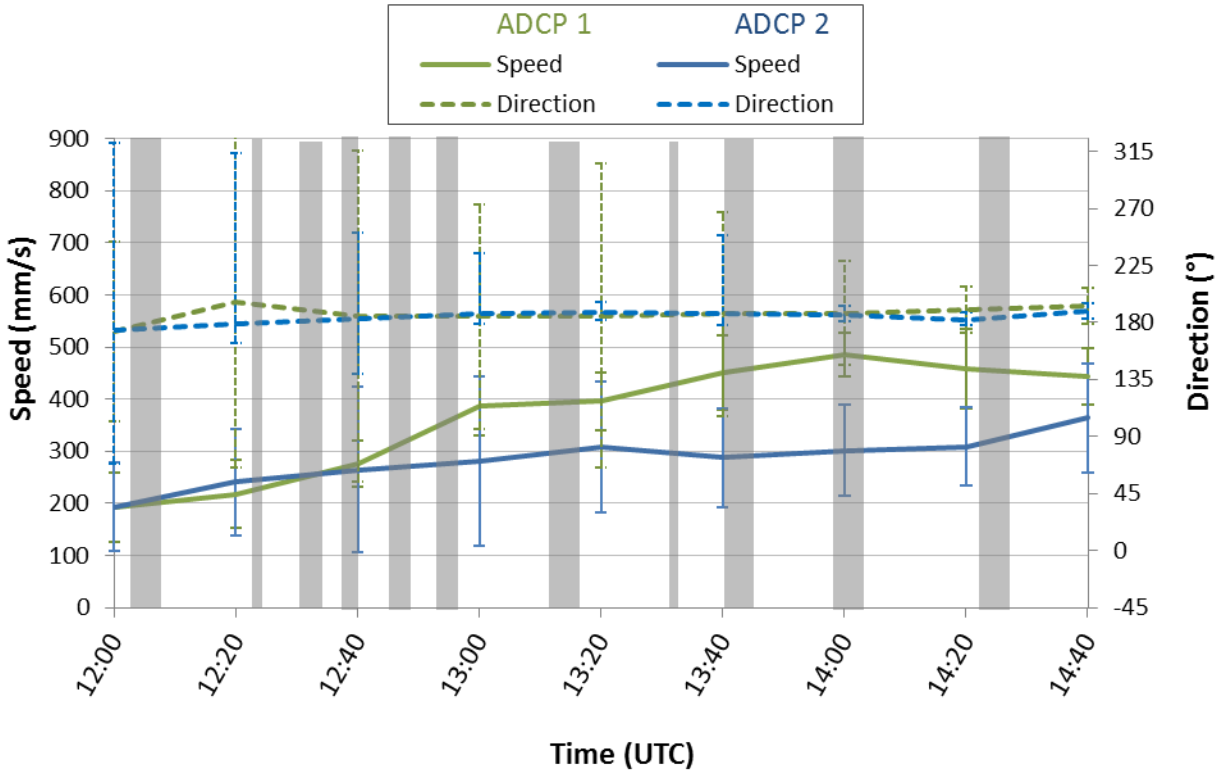

Figure 60. Mean water current speed and direction during impact driving of the top segment of Test Pile 4A on 14 May 2012. ADCP 1 was north (upstream), and ADCP 2 was south (downstream) of the pile. Gray areas represent occurrence of impact pile driving.

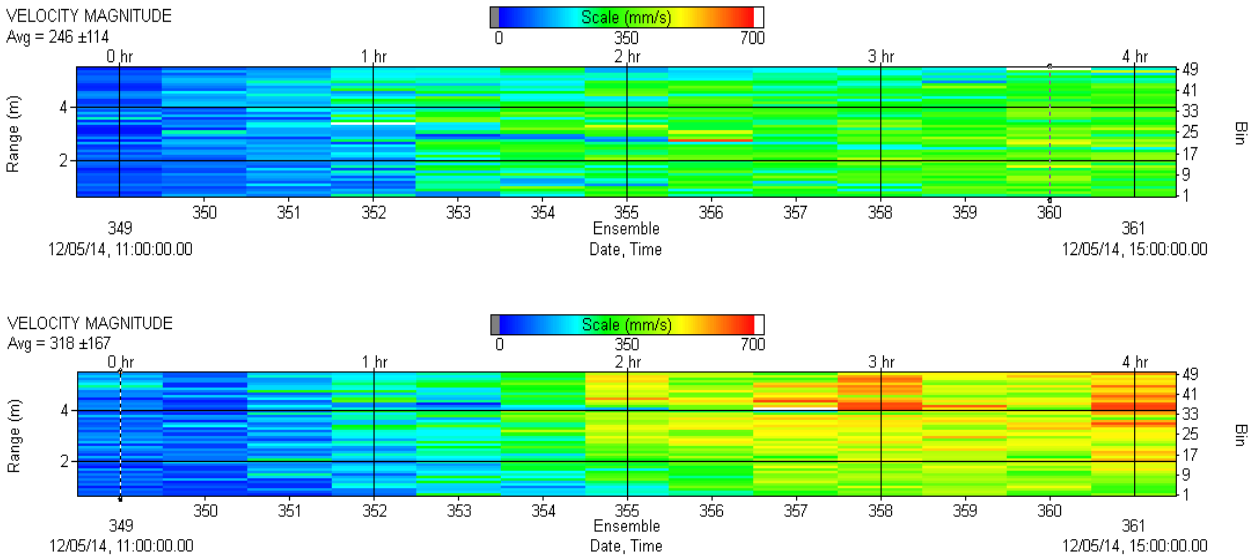

Figure 61. River current speed as a function of depth during piling at Test Pile 4A, 14 May 2012. (Top) ADCP 150 m south of Test Pile 2B. (Bottom) ADCP 100 m north of Test Pile 3A.

Appendix E. Pile Driving Logs

This appendix contains plots of the impact pile driving blow energy as a function of time for each impact pile driving event and describes vibratory pile driving. NYSDOT provided all data.

E.1. Test Pile 1A

Vibratory pile driving was performed using an ICE 66 vibratory driver on May 2 and 5, 2012. On both days the hammer ran at its maximum rate of 1800 vibrations per minute. The hammer has an eccentric moment of 6600 in-lb and weighs 26,170 lb.

Impact pile driving was performed on May 5 using the MENCK MHU 270T hydraulic impact hammer, which struck 1658 blows with energies ranging between 90 and 135 kJ/blow after the ramp-up (Figure 62). The total hammer energy transferred was 159.79 MJ.

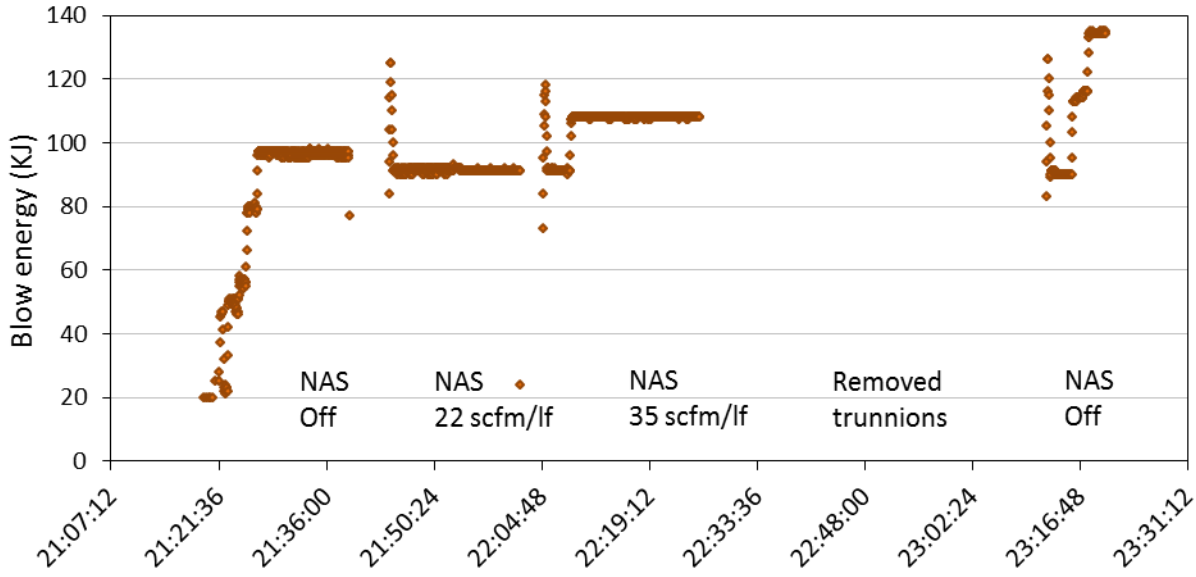

Figure 62. Blow energy for Test Pile 1A impact piling on 5 May 2012 using a MENCK MHU 270T hydraulic impact hammer. The airflow rate of the Unconfined Single-Tier Air Bubble Curtain is shown for reference.

E.2. Test Pile 1B

Vibratory pile driving was performed using an ICE 66 Vvibratory driver on 2 and 5 May. On both days the hammer ran at its maximum rate of 1800 vibrations per minute. The hammer has an eccentric moment of 6600 in-lb and weighs 26,170 lb.

Impact pile driving was performed on May 5 with the MENCK MHU 270T hammer, which struck 1695 blows with energies ranging between 70–110 kJ/blow after the ramp-up (Figure 63). The total hammer energy transferred was 127.4 MJ.

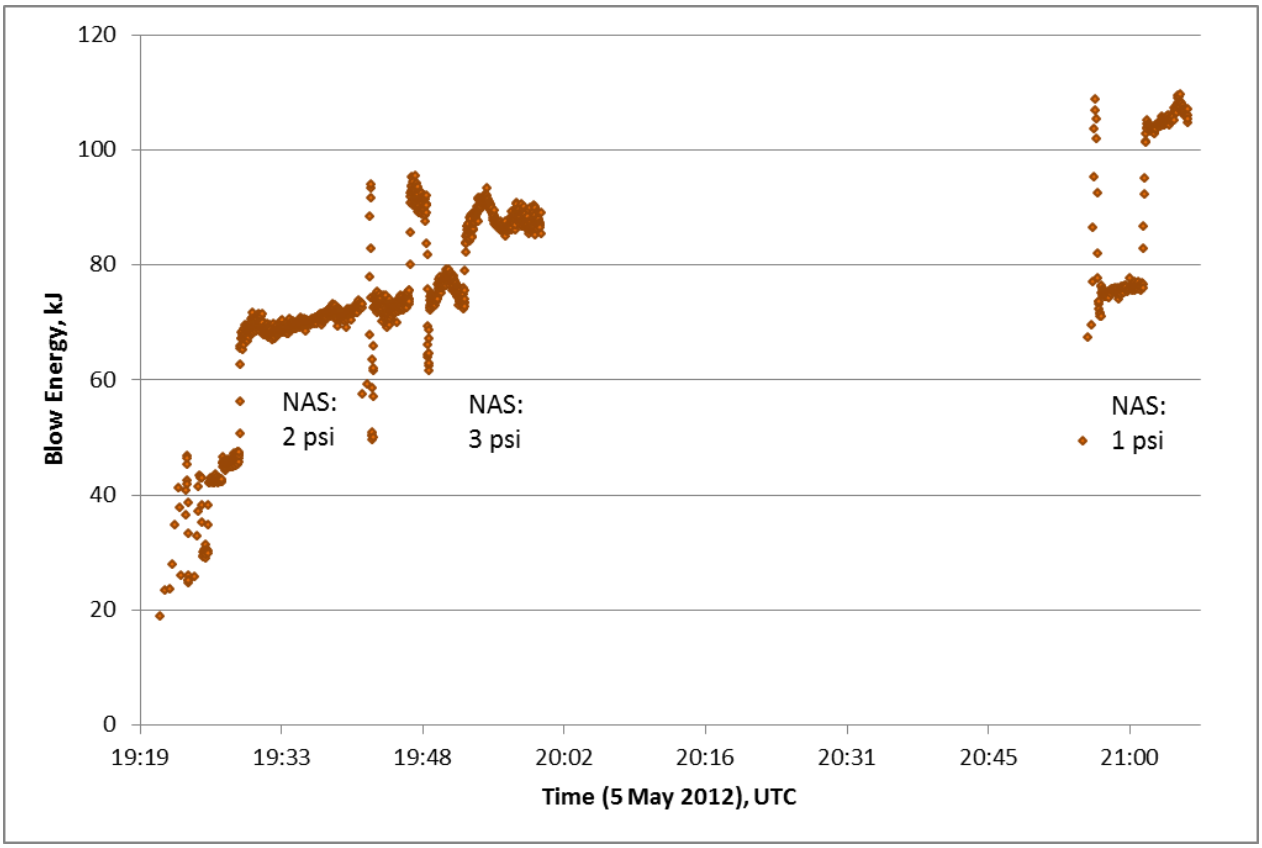

Figure 63. Blow energy for Test Pile 1B impact piling on 5 May 2012 using a MENCK MHU 270T hammer. Data supplied by NYSDOT, from file *96702-PDA and CAPWAP Result 5-10-12.pdf*. Strike times interpolated from JASCO's logs of start and stop times for impact piling.

E.3. Test Pile 2A

An ICE 66 vibratory driver and a Super Kong 600 vibratory hammer drove Test Pile 2A on 16 May. The ICE 66 vibratory driver ran at its maximum rate of 1800 vibrations per minute. The hammer has an eccentric moment of 6600 in-lb and weighs 26,170 lb. The Super Kong 600 ran at its maximum rate of 1400 vibrations per minute. The hammer has an eccentric moment of 20,000 in-lb and weighs 68,000 lb (34 tons).

Impact pile driving was performed on 16 May using the MENCK MHU 270T hydraulic impact hammer, which struck 406 blows with energies ranging between 210 and 253 kJ/blow after the ramp-up (Figure 64). The total hammer energy transferred was 96.6 MJ.

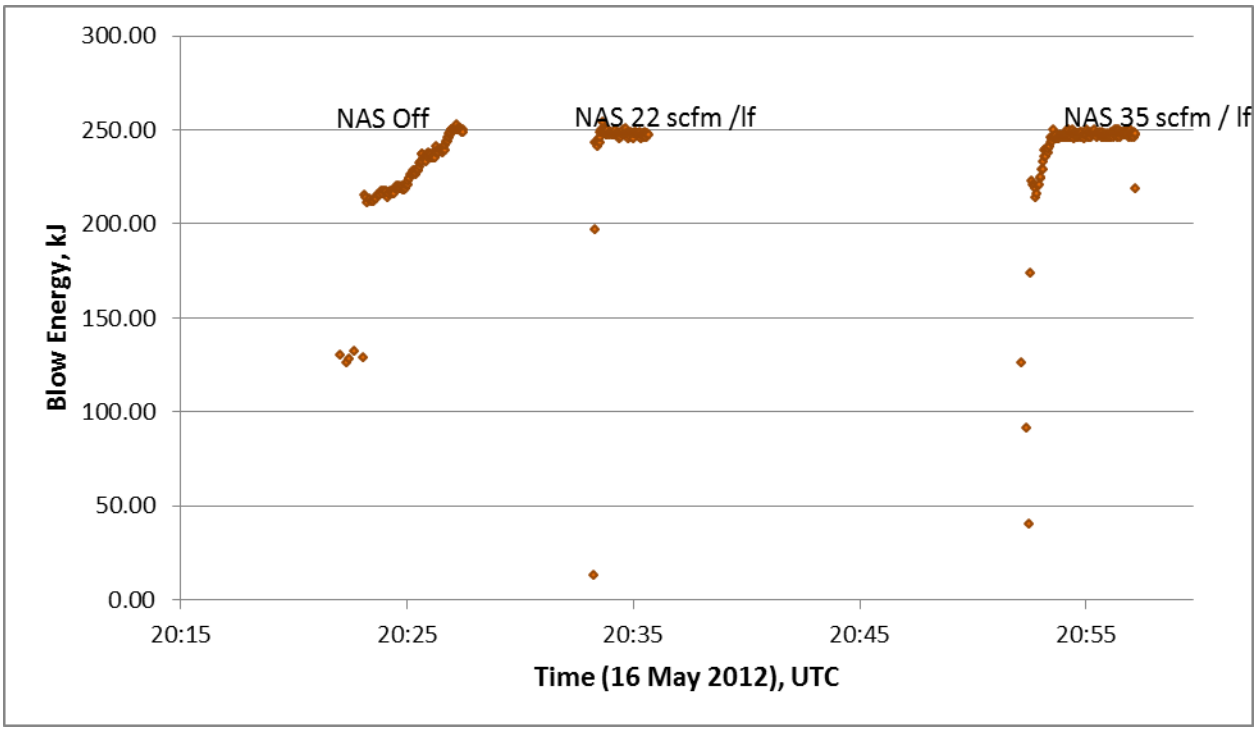

Figure 64. Blow energy for Test Pile 2A impact piling on 16 May 2012 using a MENCK MHU 270T hammer. Data supplied by NYSDOT.

E.4. Test Pile 2B

An ICE 66 vibratory driver and a Super Kong 600 vibratory hammer drove Test Pile 2B on 16 May. The ICE 66 vibratory driver ran at its maximum rate of 1800 vibrations per minute. The hammer has an eccentric moment of 6600 in-lb and weighs 26,170 lb. The Super Kong 600 vibratory hammer ran at its maximum rate of 1400 vibrations per minute. The hammer has an eccentric moment of 20,000 in-lb and weighs 68,000 lb (34 tons).

Impact pile driving was performed on 16 May using the MENCK MHU 270T impact hammer, which struck 1393 blows with energies ranging between 200 and 261 kJ/blow after the ramp-up (Figure 65). The total hammer energy transferred was 340.1 MJ.

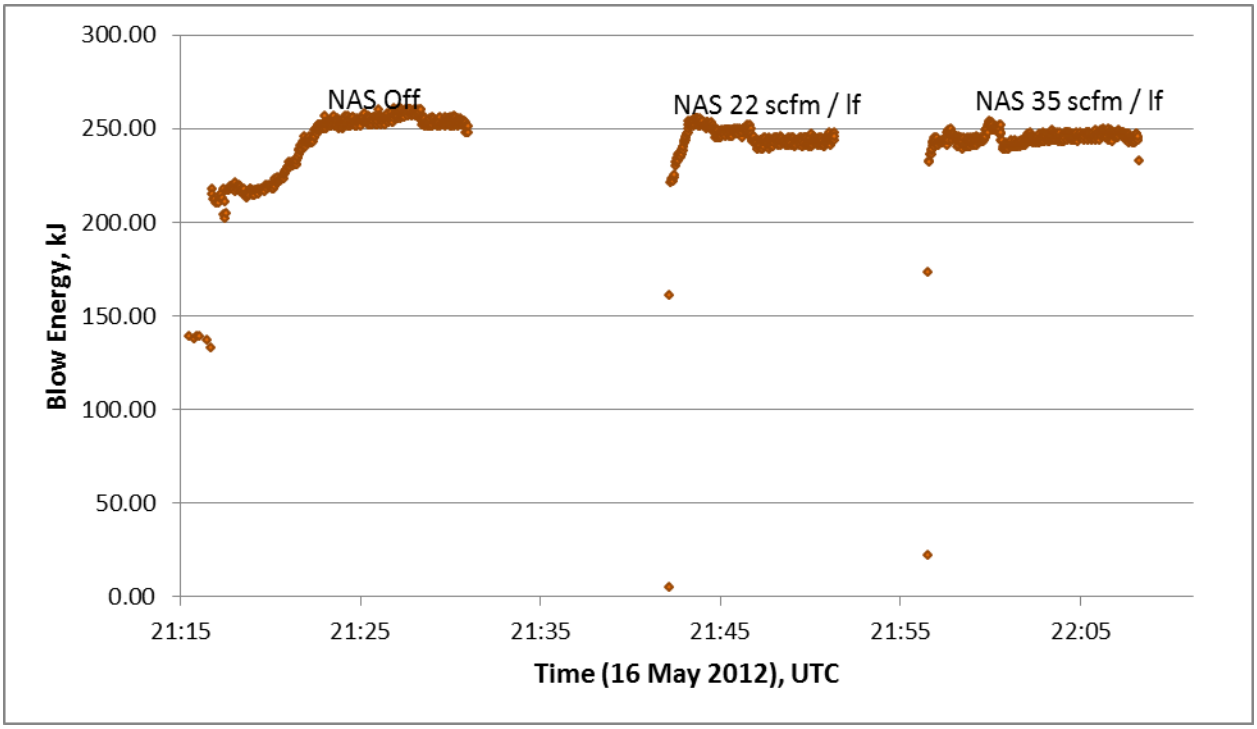

Figure 65. Blow energy for Test Pile 2B impact piling on 16 May 2012 using a MENCK MHU 270T hammer. Data supplied by NYSDOT.

E.5. Test Pile 3A

Vibratory pile driving was performed using an ICE 66 vibratory driver on 28 April, 2012. The driver ran at its maximum rate of 1800 vibrations per minute. The driver has an eccentric moment of 6600 in-lb and weighs 26,170 lb.

Impact pile driving was performed on 8 May using the MENCK MHU 800S hydraulic impact hammer, which struck 1231 blows with energies ranging between 109 and 942 kJ/blow after the ramp-up (Figure 66). The total hammer energy transferred was 501.18 MJ.

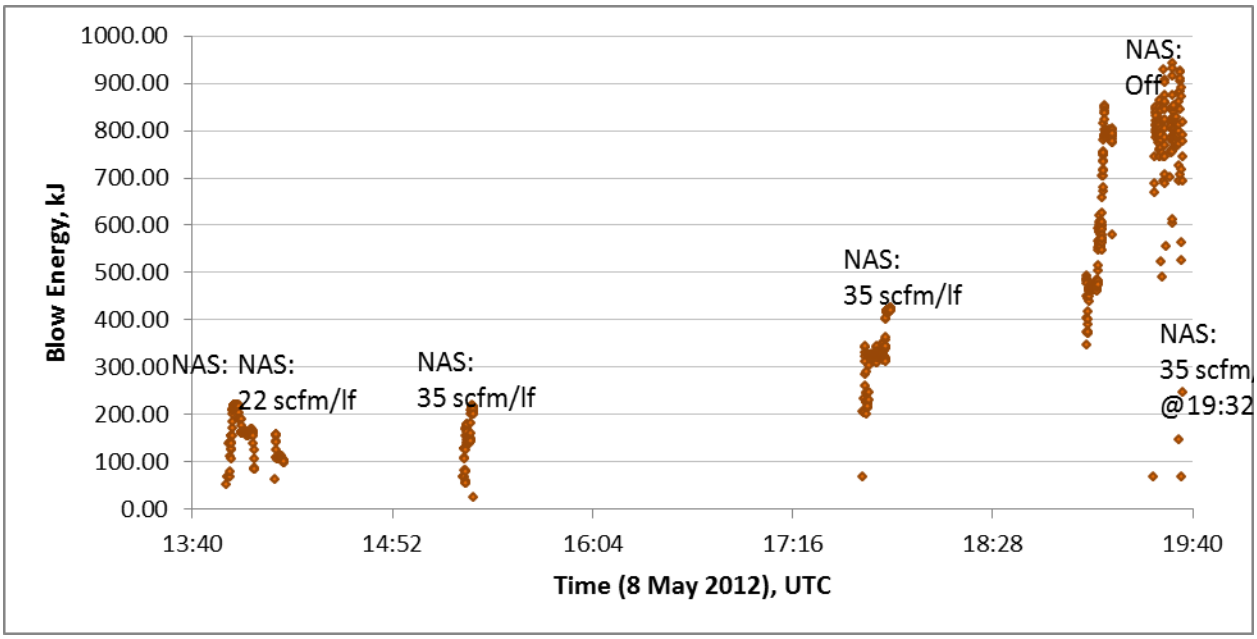

Figure 66. Blow energy for Test Pile 3A impact piling on 8 May 2012 using a MENCK MHU 800S hydraulic impact hammer. The airflow rate of the Unconfined Multi-Tier Air Bubble Curtain is shown for reference.

E.6. Test Pile 3B

Vibratory pile driving was performed using a Super Kong 600 vibratory hammer on 18 May. The hammer ran at 1400 vibrations per minute, with an eccentric moment of 20,000 in-lb, and weighs 34 tons.

Impact pile driving was performed on 18 May using the MENCK MHU 800S hydraulic impact hammer, which struck 2181 blows with energies ranging between 195 and 907 kJ/blow after the ramp-up (Figure 67). The total hammer energy transferred was 1.43 GJ.

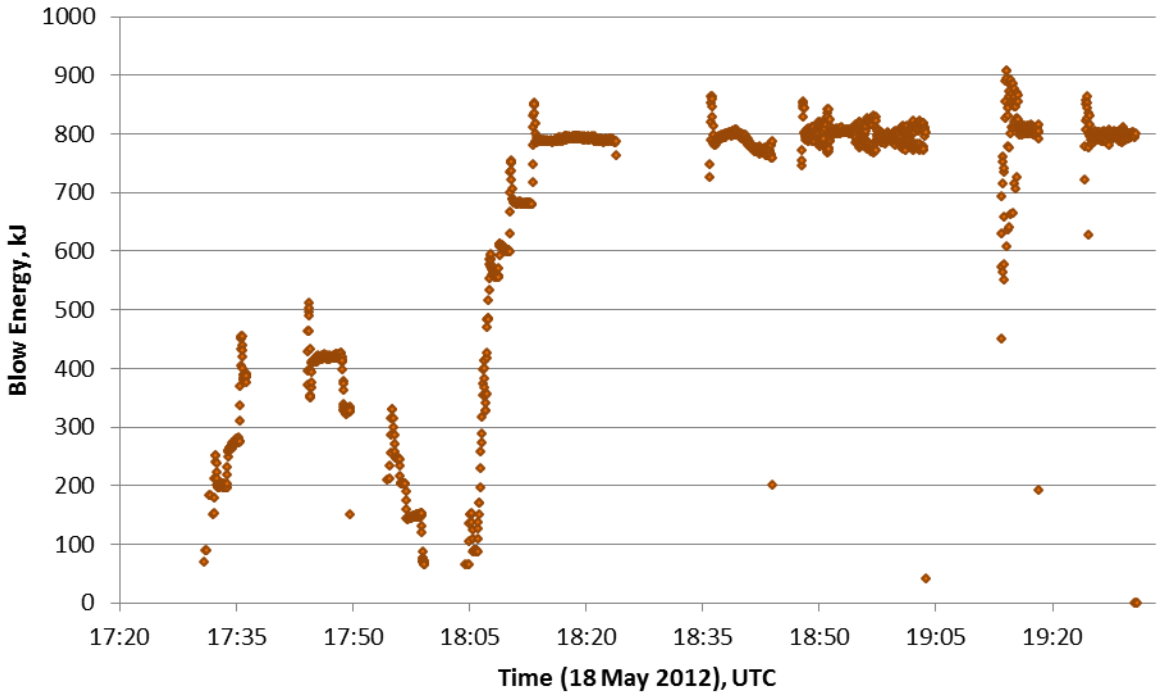

Figure 67. Blow energy for Test Pile 3B impact piling on 18 May 2012 using a MENCK MHU 800S hydraulic impact hammer.

E.7. Test Pile 4A

Vibratory pile driving was performed using an ICE 66 vibratory driver on May 2 and 5, 2012. On both days the hammer ran at its maximum rate of 1800 vibrations per minute. The hammer has an eccentric moment of 6600 in-lb and weight of 26,170 lb.

Impact pile driving was performed on 5 May using the MENCK MHU 270T hydraulic impact hammer ,which struck 1658 blows with energies ranging between 90 and 135 kJ/blow after the ramp-up (Figure 68). The total hammer energy transferred was 159.79 MJ.

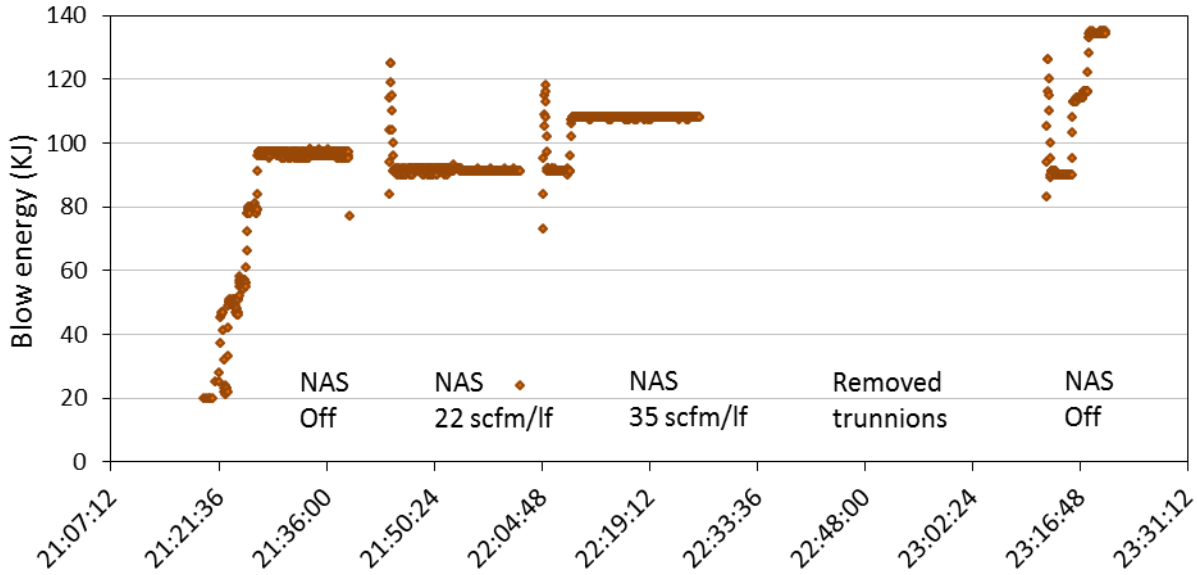

Figure 68. Blow energy for Test Pile 1A impact piling on 5 May 2012 using a MENCK MHU 270T hydraulic impact hammer. The airflow rate of the Unconfined Single-Tier Air Bubble Curtain is shown for reference.

Appendix F. Noise Attenuation System Logs

This appendix contains plots of the noise attenuation system airflow settings as a function of time for the impact piling events. All data were provided by NYSDOT.

F.1. Test Pile 1A

During impact piling, Test Pile 1A used an Unconfined Single-Tier Air Bubble Curtain with two airflow settings: 22 and 35 scfm/lf (standard cubic feet per minute per linear foot, Figure 69).

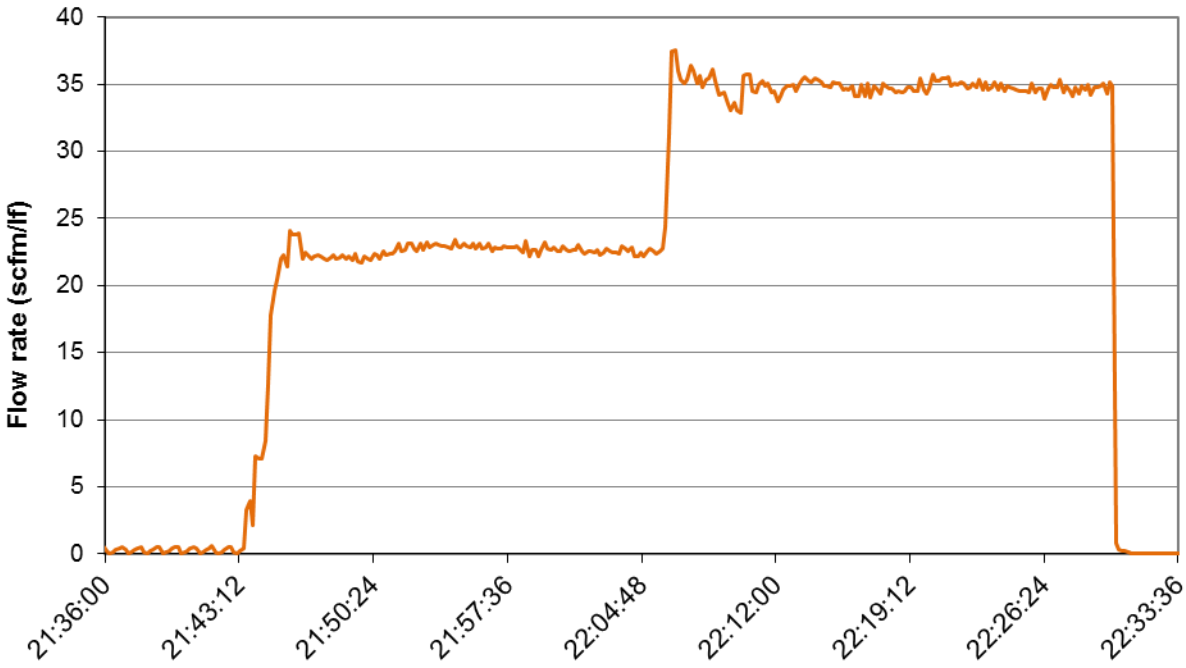

Figure 69. Airflow rate into the Unconfined Single-Tier Air Bubble Curtain at Test Pile 1A, 5 May 2012.

F.2. Test Pile 1B

During impact piling, Test Pile 1B used a Hard Bubble Noise Attenuation System. Table 27 shows the different air pressure settings used for this test pile.

Table 27. Hard Bubble NAS pressure settings logged by JASCO, 5 May 2012.

Time (UTC)	Pressure setting (PSI)*
5 May 19:21	2
5 May 19:42	3
5 May 19:55	1

*Pounds per square inch.

F.3. Test Pile 2A

During impact piling, Test Pile 2A used an Unconfined Multi-Tier Air Bubble Curtain with two different airflow settings: 22 and 35 scfm/lf (standard cubic feet per minute per linear foot, Figure 70).

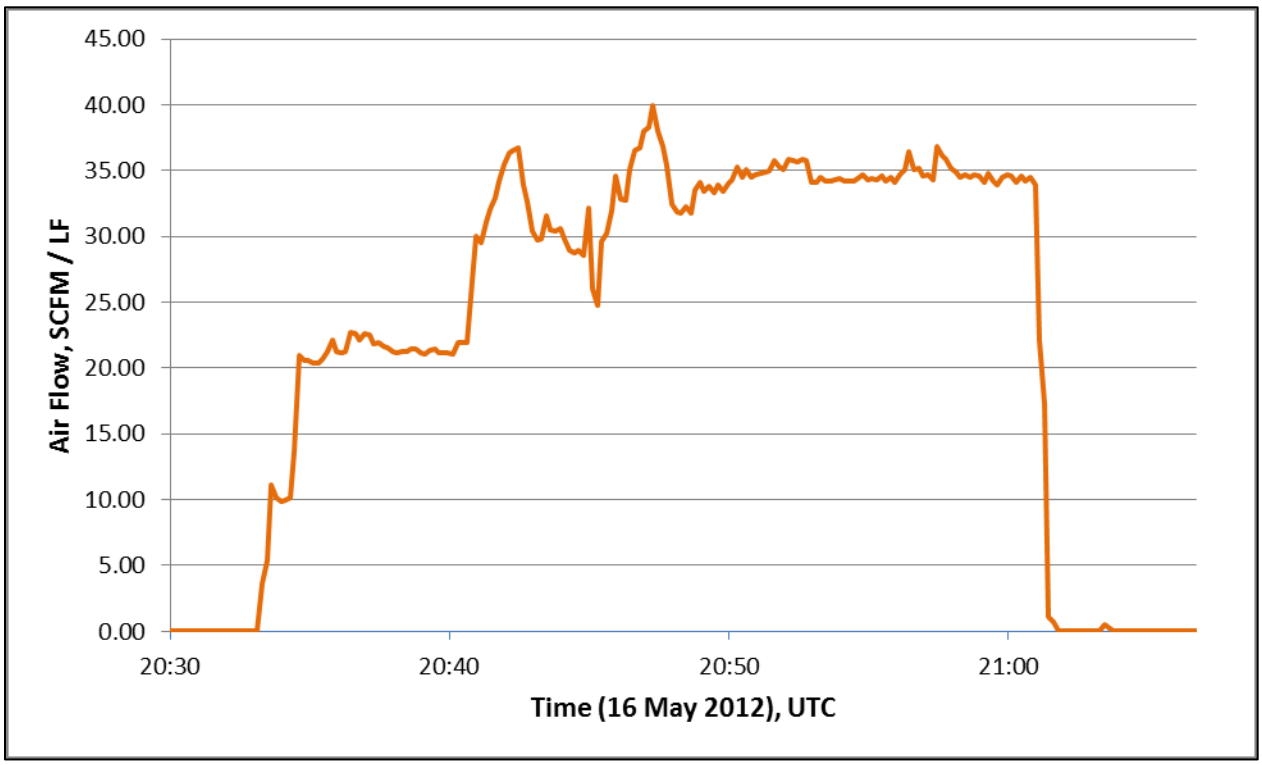

Figure 70. Airflow data for Unconfined Multi-Tier Air Bubble Curtain, 16 May 2012, data supplied by NYSDOT.

F.4. Test Pile 2B

During impact piling, Test Pile 2B used an Isolation Casing and Bubble NAS with two different airflow settings: 22 and 35 scfm/lf (standard cubic feet per minute per linear foot, Figure 71).

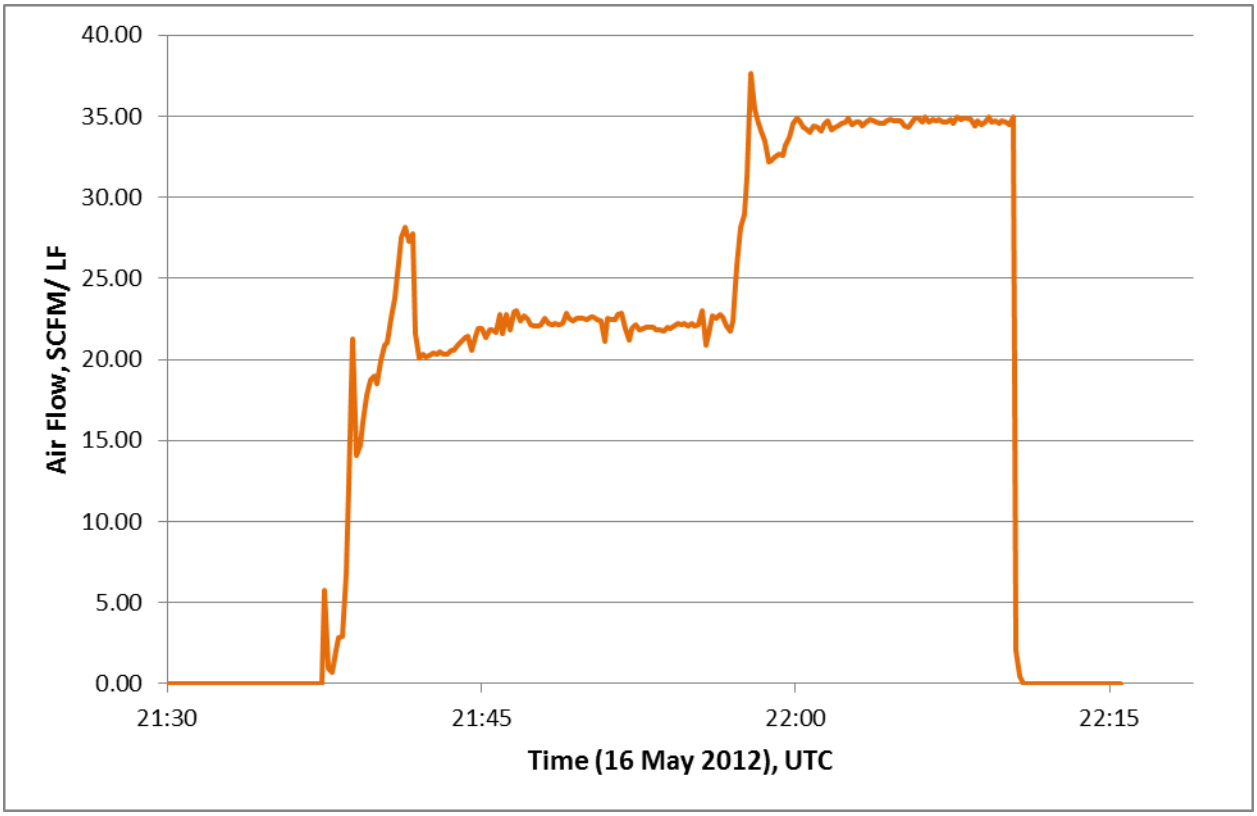

Figure 71. Airflow data for Isolation Casing and Bubble NAS, 16 May 2012, data supplied by NYSDOT.

F.5. Test Pile 3A

During impact piling, Test Pile 3A used an Unconfined Multi-Tier Air Bubble Curtain with two different airflow settings: 22 and 35 scfm/lf (standard cubic feet per minute per linear foot, Figure 72).

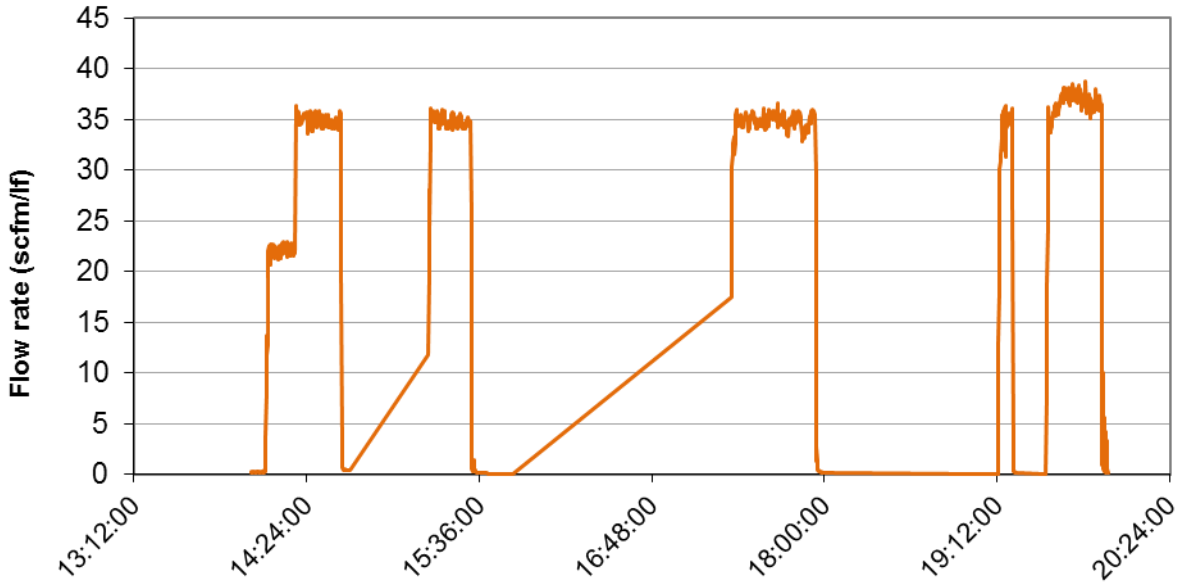

Figure 72. Airflow rate into the Unconfined Multi-Tier Air Bubble Curtain at Test Pile 3A, 8 May 2012.

F.6. Test Pile 3B

During impact piling, Test Pile 3B used a Two-Stage Confined Bubble Curtain with two different airflow settings: 22 and 35 scfm/lf (standard cubic feet per minute per linear foot, below).

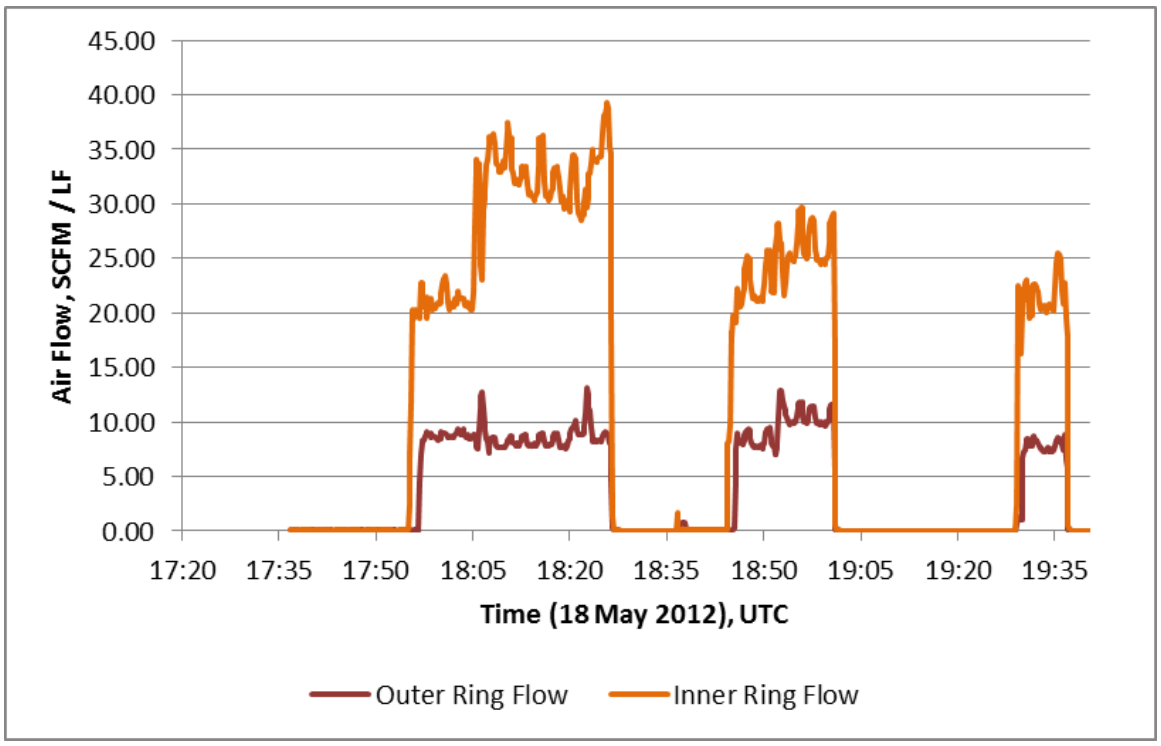

Figure 73. Airflow rate into the Two-Stage Confined Bubble Curtain at Test Pile 3B, 18 May 2012.

F.7. Test Pile 4A

During impact piling, Test Pile 1A used an Unconfined Single-Tier Air Bubble Curtain with two different airflow settings: 22 and 35 scfm/lf (standard cubic feet per minute per linear foot, Figure 74).

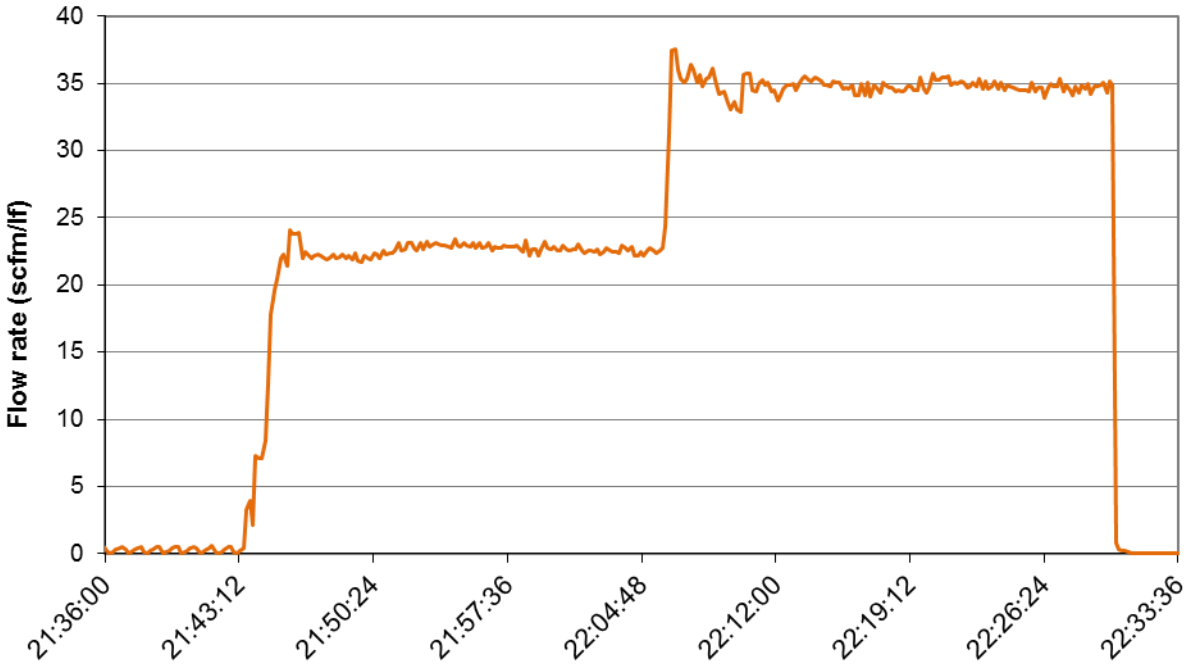

Figure 74. Airflow rate into the Unconfined Single-Tier Air Bubble Curtain at Test Pile 1A, 5 May 2012.

Appendix G. Impact Pile Driving Received Levels

This appendix contains plots of the received levels for each impact pile driving event. One set of plots shows the peak SPL, rms SPL, SEL, and cumulative SEL for the event. There are plots for short-range measurements and each long-range recorder that detected pile driving. The second set of plots contains the 1/3-octave band SEL statistics without the NAS. The final set of plots contains the 1/3-octave band SEL statistics with the NAS on.

G.1. Test Pile 1A

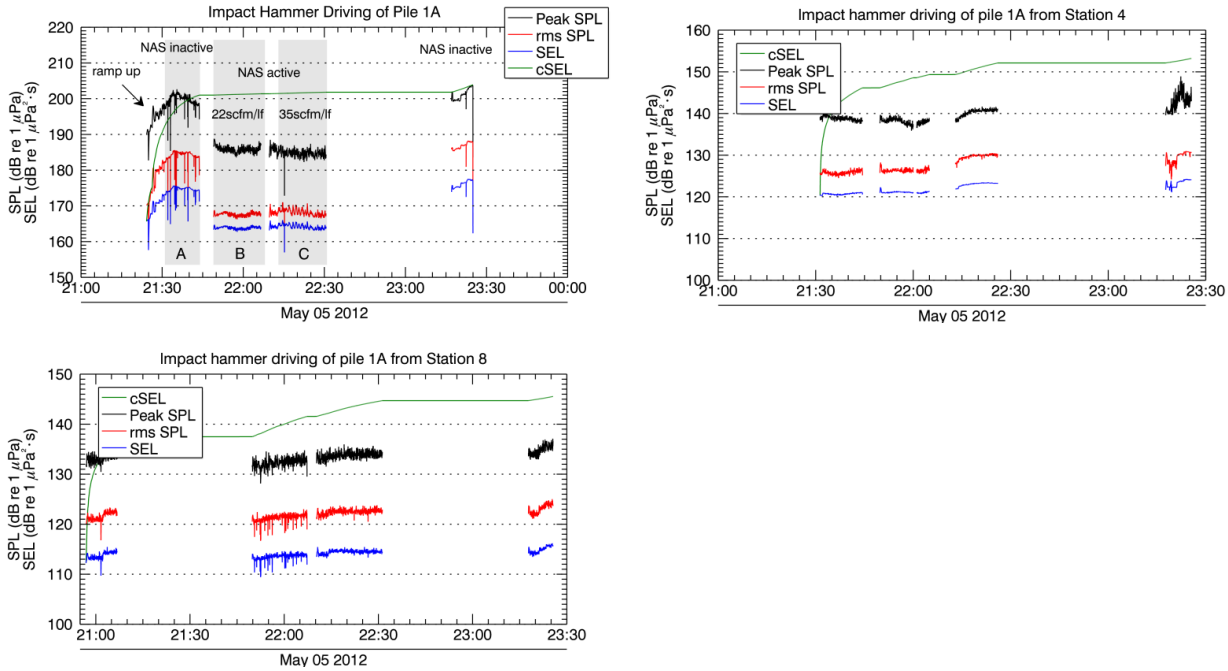

Figure 75. Plots of received sound levels for impact pile driving at Test Pile 1A, 5 May 2012, with MENCK MHU 270T hydraulic impact hammer and an Unconfined Single-Tier Air Bubble Curtain. (Top Left) Short-range monitoring at 35.1 ft horizontal distance. (Top Right) Long-range monitoring at Station 4. (Bottom Left) Long-range monitoring at Station 8.

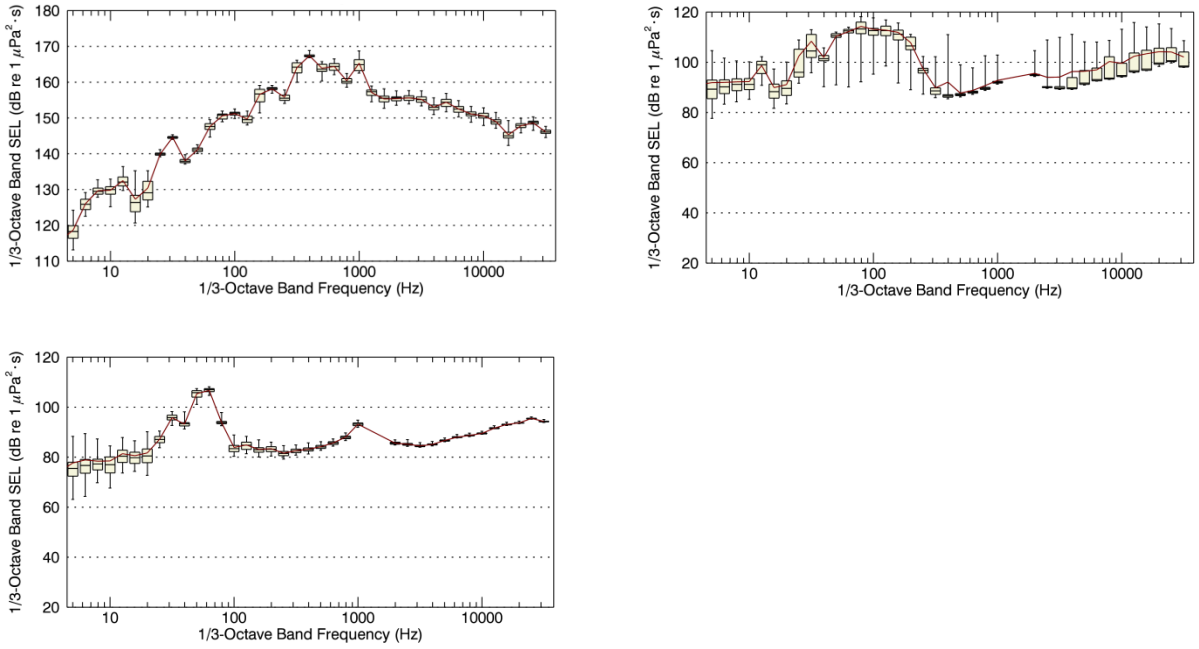

Figure 76. 1/3-octave band SEL statistics for impact driving of Test Pile 1A, 5 May 2012, with the MENCK MHU 270T hydraulic impact hammer and the Unconfined Single-Tier Air Bubble Curtain off. Beige bars indicate the first, second, and third quartiles (L_{25}, L_{50}, and L_{75}). Upper error-bars indicate the maximum levels (L_{max}). Lower error bars indicate the 95% exceedance percentiles (L_{95}). The maroon line indicates the arithmetic mean (L_{mean}). (Top Left) Short-range monitoring at 35.1 ft horizontal distance. (Top Right) Long-range monitoring at Station 4. (Bottom Left) Long-range monitoring at Station 8.

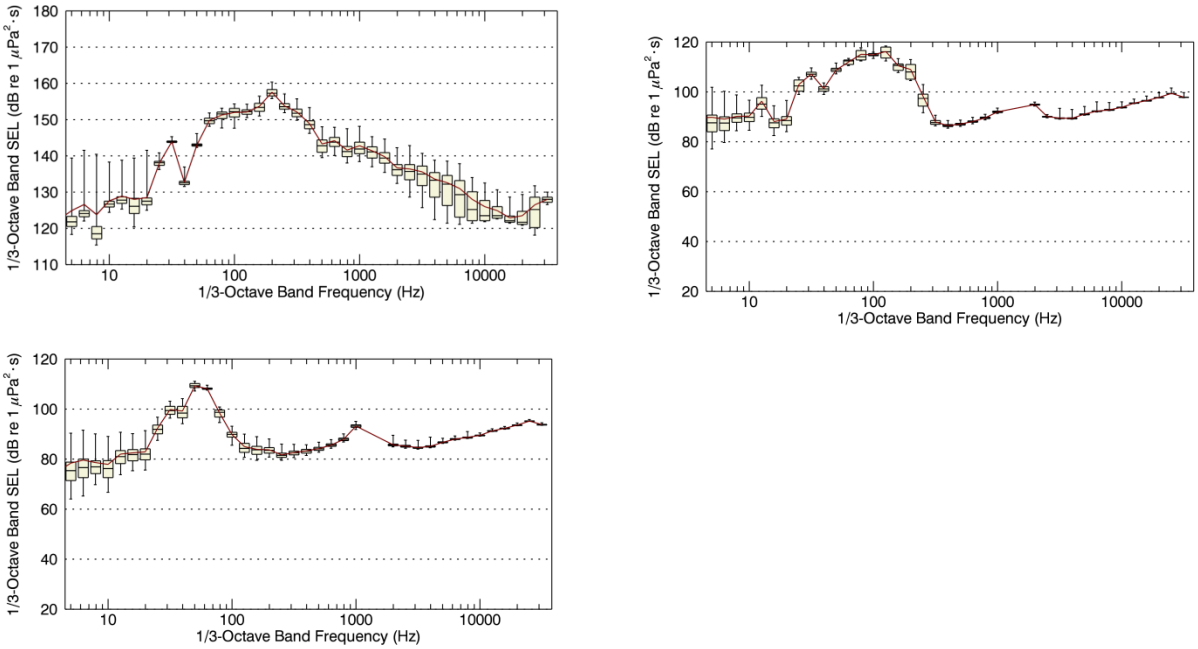

Figure 77. 1/3-octave band SEL statistics for impact driving of Test Pile 1A, 5 May 2012, with the MENCK MHU 270T hydraulic impact hammer and the Unconfined Single-Tier Air Bubble Curtain on. Beige bars indicate the first, second, and third quartiles (L_{25}, L_{50}, and L_{75}). Upper error-bars indicate the maximum levels (L_{max}). Lower error bars indicate the 95% exceedance percentiles (L_{95}). The maroon line indicates the arithmetic mean (L_{mean}). (Top Left) Short-range monitoring at 35.1 ft horizontal distance, airflow at 35 scfm/lf. (Top Right) Long-range monitoring at Station 4. (Bottom Left) Long-range monitoring at Station 8.

G.2. Test Pile 1B

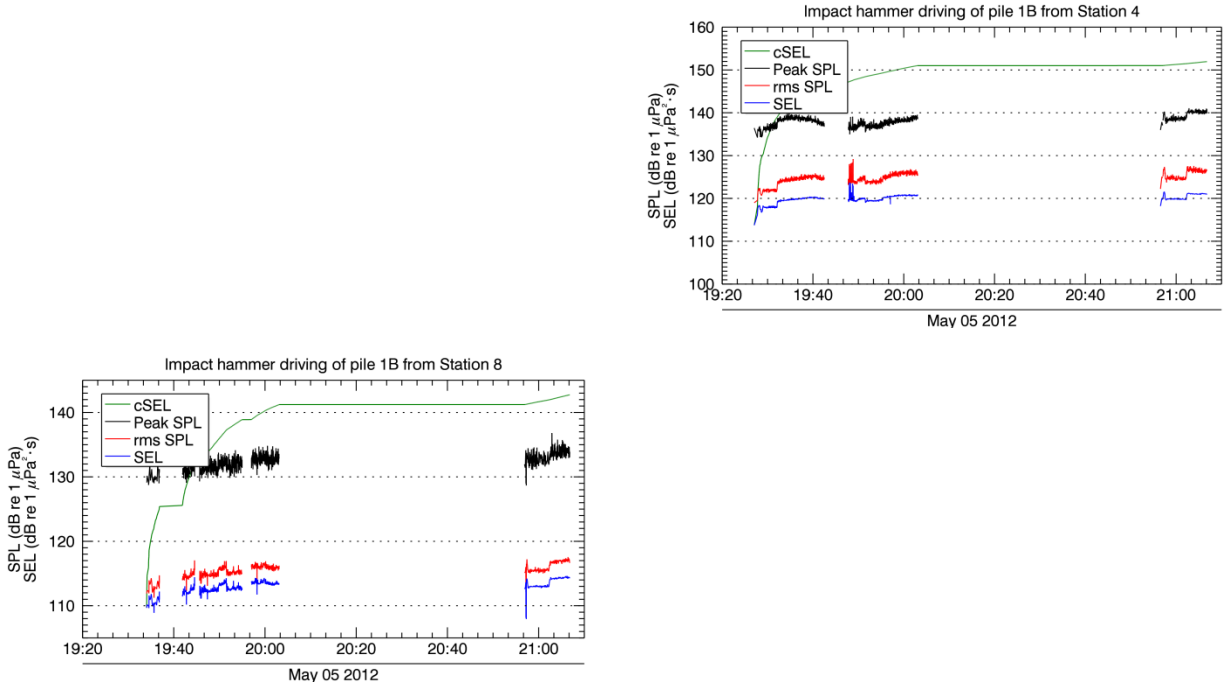

Figure 78. Plots of received sound levels for impact pile driving at Test Pile 1B, 5 May 2012, with MENCK MHU 270T hydraulic impact hammer and Hard Bubble NAS. (Top Left) Short-range monitoring at 31.8 ft horizontal distance. (Top Right) Long-range monitoring at Station 4. (Bottom Left) Long-range monitoring at Station 8.

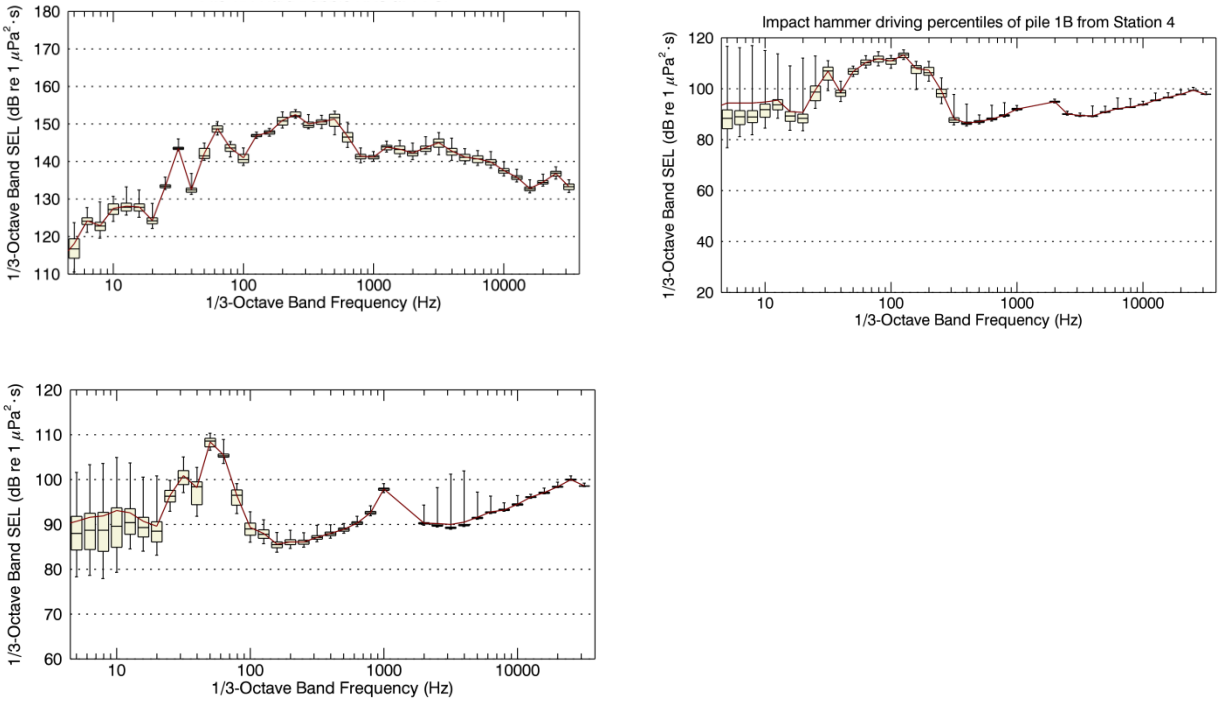

Figure 79. 1/3-octave band SEL statistics for impact driving of Test Pile 1B, 5 May 2012, with the MENCK MHU 270T hydraulic impact hammer and the Hard Bubble NAS. Beige bars indicate the first, second, and third quartiles (L_{25}, L_{50}, and L_{75}). Upper error-bars indicate the maximum levels (L_{max}). Lower error bars indicate the 95% exceedance percentiles (L_{95}). The maroon line indicates the arithmetic mean (L_{mean}). (Top Left) Short-range monitoring at 31.8 ft horizontal distance, Hard Bubble NAS at 1 psi. (Top Right) Long-range monitoring at Station 4. (Bottom Left) Long-range monitoring at Station 8.

G.3. Test Pile 2A

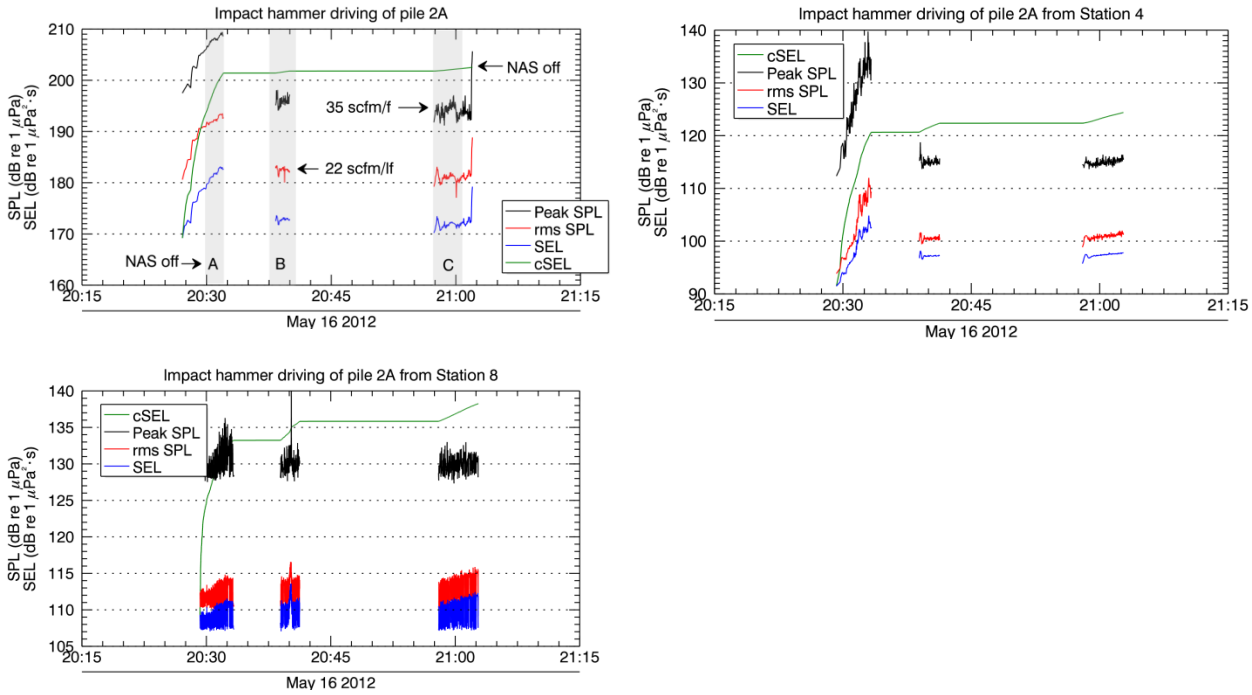

Figure 80. Plots of received sound levels for impact pile driving at Test Pile 2A, 16 May 2012, with MENCK MHU 270T hydraulic impact hammer and an Unconfined Multi-Tier Air Bubble Curtain. (Top Left) Short-range monitoring at 34.1 ft horizontal distance. (Top Right) Long-range monitoring at Station 4. (Bottom Left) Long-range monitoring at Station 8.

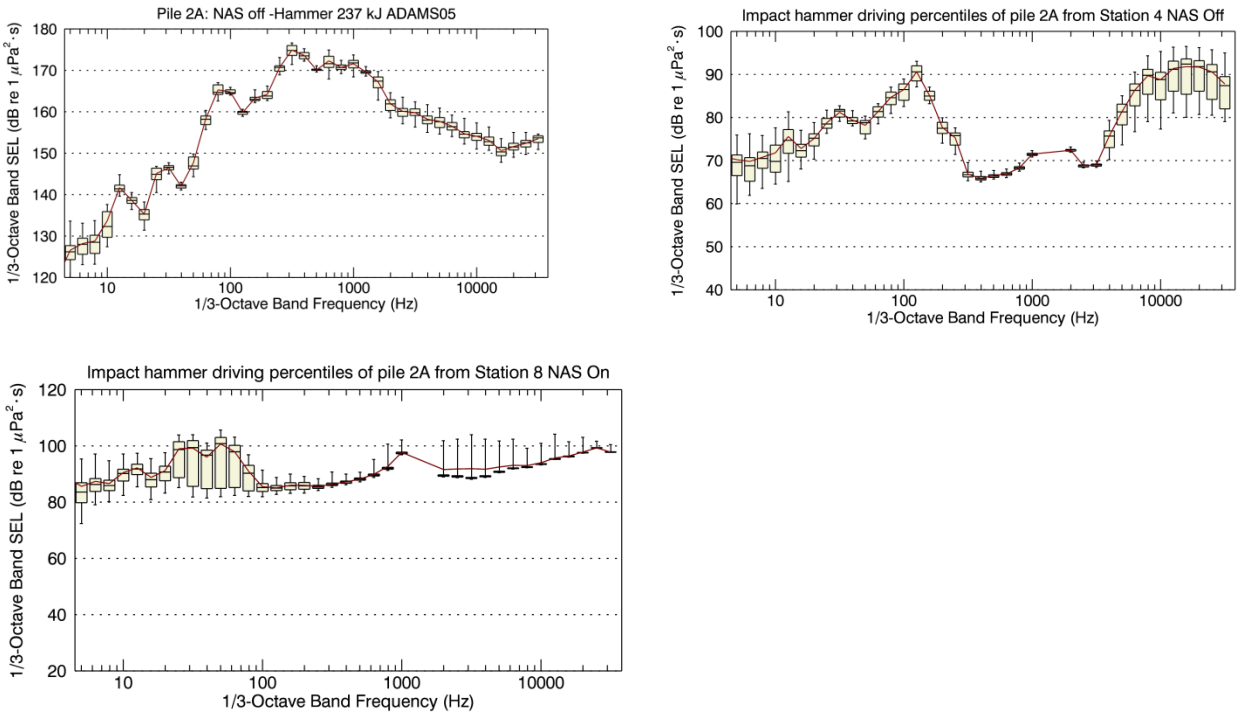

Figure 81. 1/3-octave band SEL statistics for impact driving of Test Pile 2A, 16 May 2012, with the MENCK MHU 270T hydraulic impact hammer and the Unconfined Multi-Tier Air Bubble Curtain off. Beige bars indicate the first, second, and third quartiles (L_{25}, L_{50}, and L_{75}). Upper error-bars indicate the maximum levels (L_{max}). Lower error bars indicate the 95% exceedance percentiles (L_{95}). The maroon line indicates the arithmetic mean (L_{mean}). (Top Left) Short-range monitoring at 34.1 ft horizontal distance. (Top Right) Long-range monitoring at Station 4. (Bottom Left) Long-range monitoring at Station 8.

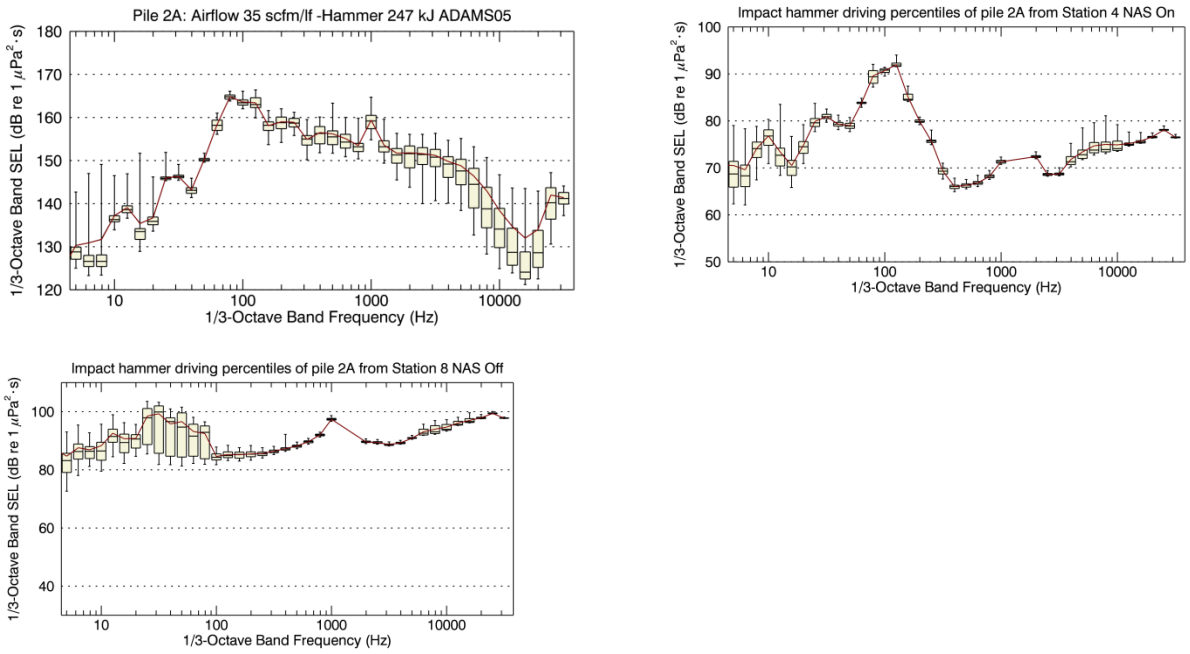

Figure 82. 1/3-octave band SEL statistics for impact driving of Test Pile 2A, 16 May 2012, with the MENCK MHU 270T hydraulic impact hammer and the Unconfined Multi-Tier Air Bubble Curtain on. Beige bars indicate the first, second, and third quartiles (L_{25}, L_{50}, and L_{75}). Upper error-bars indicate the maximum levels (L_{max}). Lower error bars indicate the 95% exceedance percentiles (L_{95}). The maroon line indicates the arithmetic mean (L_{mean}). (Top Left) Short-range monitoring at 34.1 ft horizontal distance, airflow at 35 scfm/lf. (Top Right) Long-range monitoring at Station 4. (Bottom Left) Long-range monitoring at Station 8.

G.4. Test Pile 2B

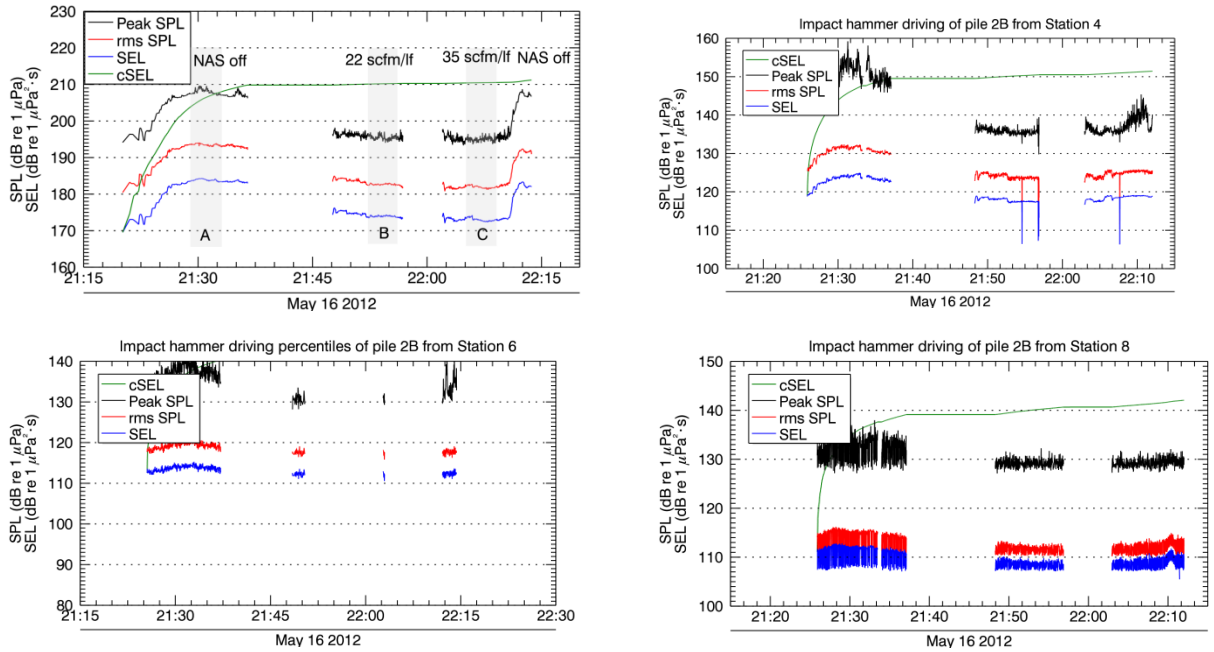

Figure 83. Plots of received sound levels for impact pile driving at Test Pile 2B, 16 May 2012, with MENCK MHU 270T hydraulic impact hammer and an Isolation Casing and Bubble System. (Top Left) Short-range monitoring at 35.4 ft horizontal distance. (Top Right) Long-range monitoring at Station 4. (Bottom Left) Long-range monitoring at Station 6. (Bottom Right) Long-range monitoring at Station 8.

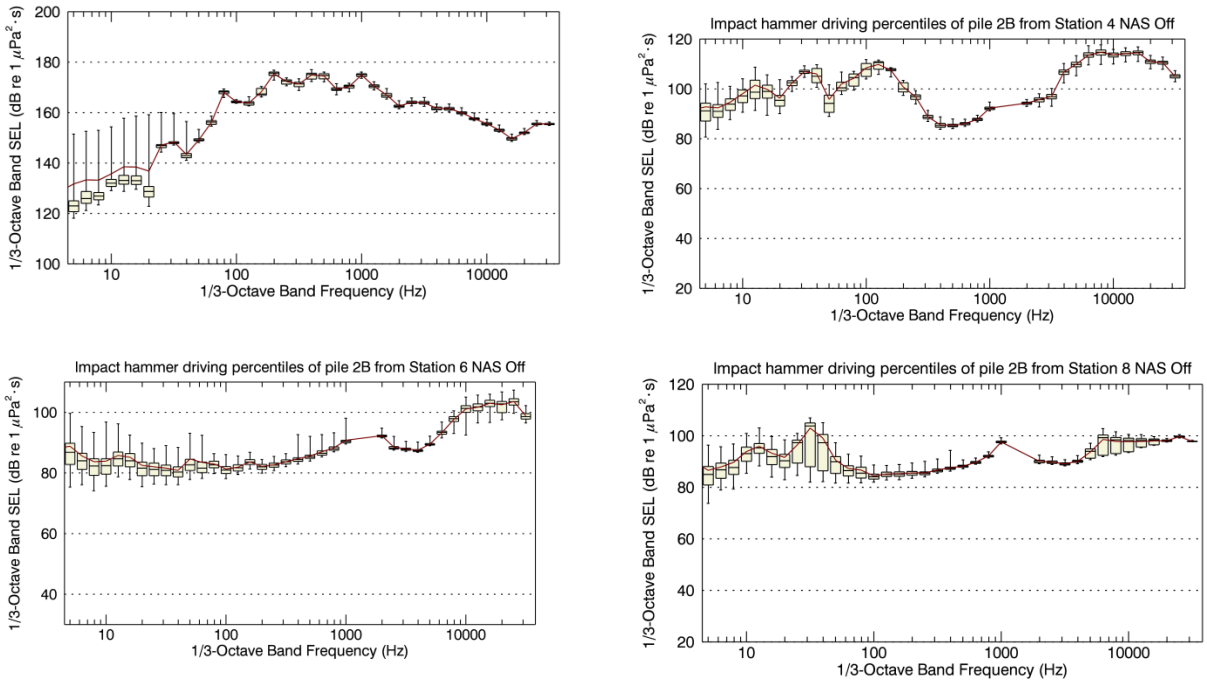

Figure 84. 1/3-octave band SEL statistics for impact driving of Test Pile 2B, 16 May 2012, with the MENCK MHU 270T hydraulic impact hammer and the Isolation Casing and Bubble System off. Beige bars indicate the first, second, and third quartiles (L_{25}, L_{50}, and L_{75}). Upper error-bars indicate the maximum levels (L_{max}). Lower error bars indicate the 95% exceedance percentiles (L_{95}). The maroon line indicates the arithmetic mean (L_{mean}). (Top Left) Short-range monitoring at 35.4 ft horizontal distance. (Top Right) Long-range monitoring at Station 4. (Bottom Left) Long-range monitoring at Station 6. (Bottom Right) Long-range monitoring at Station 8.

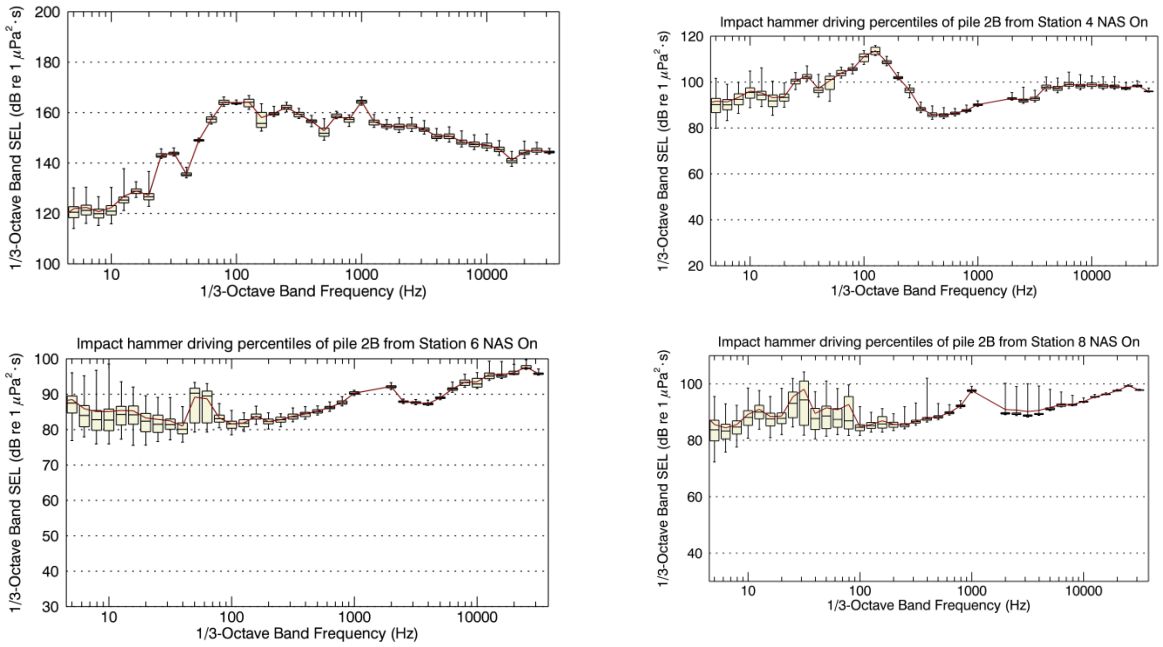

Figure 85. 1/3-octave band SEL statistics for impact driving of Test Pile 2B, 16 May 2012, with the MENCK MHU 270T hydraulic impact hammer and the Isolation Casing and Bubble System on. Beige bars indicate the first, second, and third quartiles (L_{25}, L_{50}, and L_{75}). Upper error-bars indicate the maximum levels (L_{max}). Lower error bars indicate the 95% exceedance percentiles (L_{95}). The maroon line indicates the arithmetic mean (L_{mean}). (Top Left) Short-range monitoring at 35.4 ft horizontal distance, airflow at 35 scfm/lf. (Top Right) Long-range monitoring at Station 4. (Bottom Left) Long-range monitoring at Station 6. (Bottom Right) Long-range monitoring at Station 8.

G.5. Test Pile 3A

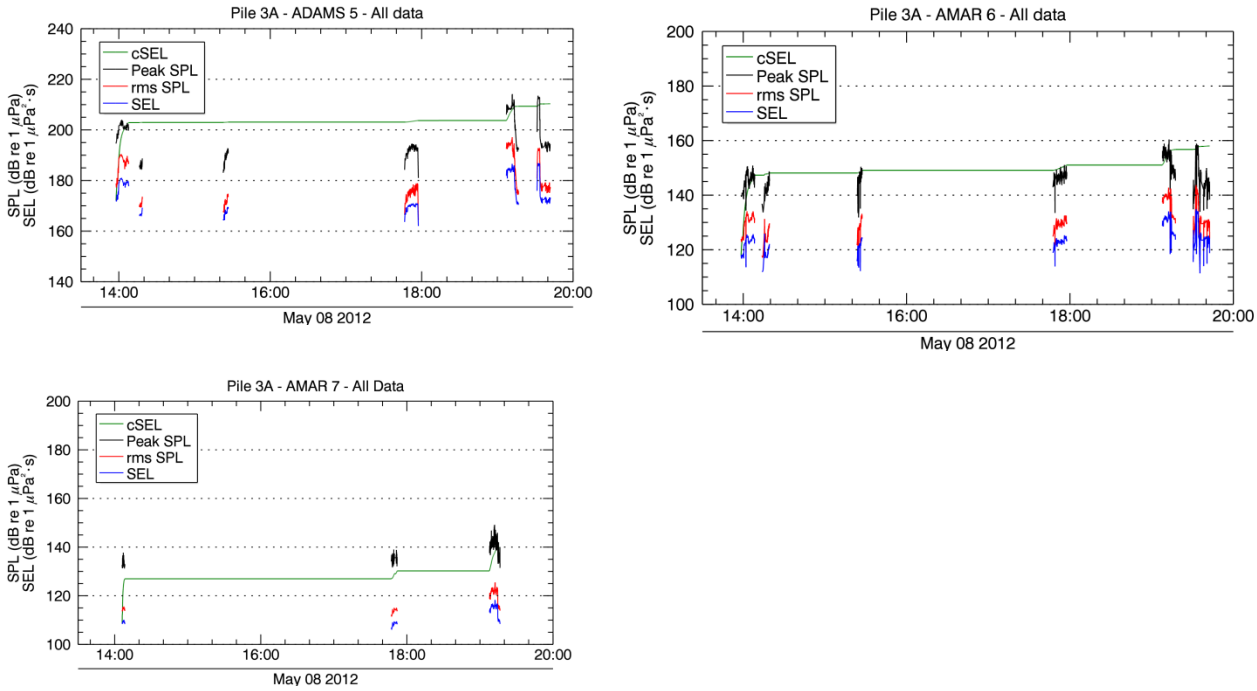

Figure 86. Plots of received sound levels for impact pile driving at Test Pile 3A, 8 May 2012, with MENCK MHU 800S hydraulic impact hammer and an Unconfined Multi-Tier Air Bubble Curtain. (Top Left) Short-range monitoring at 39.7 ft horizontal distance. (Top Right) Long-range monitoring data from Station 6. (Bottom Left) Long-range monitoring data from Station 7.

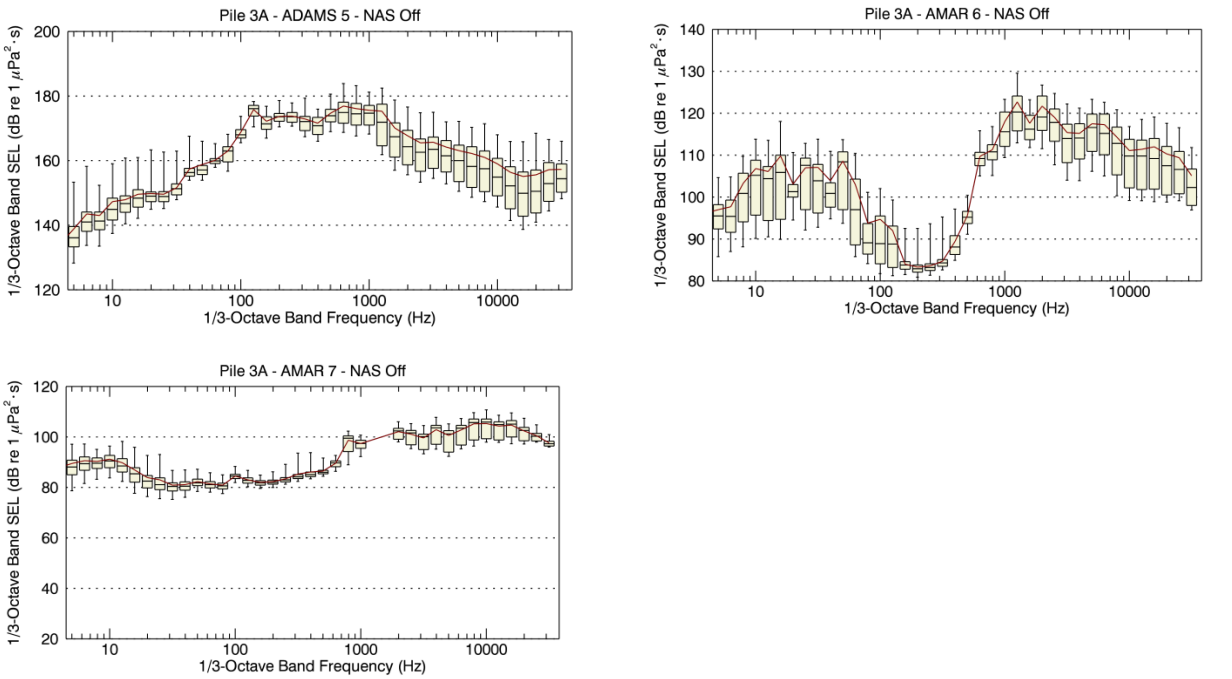

Figure 87. 1/3-octave band SEL statistics for impact driving of Test Pile 3A, 8 May 2012, with the MENCK MHU 800S hydraulic impact hammer and the Unconfined Multi-Tier Air Bubble Curtain off. Beige bars indicate the first, second, and third quartiles (L_{25}, L_{50}, and L_{75}). Upper error-bars indicate the maximum levels (L_{max}). Lower error bars indicate the 95% exceedance percentiles (L_{95}). The maroon line indicates the arithmetic mean (L_{mean}). (Top Left) Short-range monitoring at 39.7 ft horizontal distance. (Top Right) Long-range monitoring data from Station 6. (Bottom Left) Long-range monitoring data from Station 7.

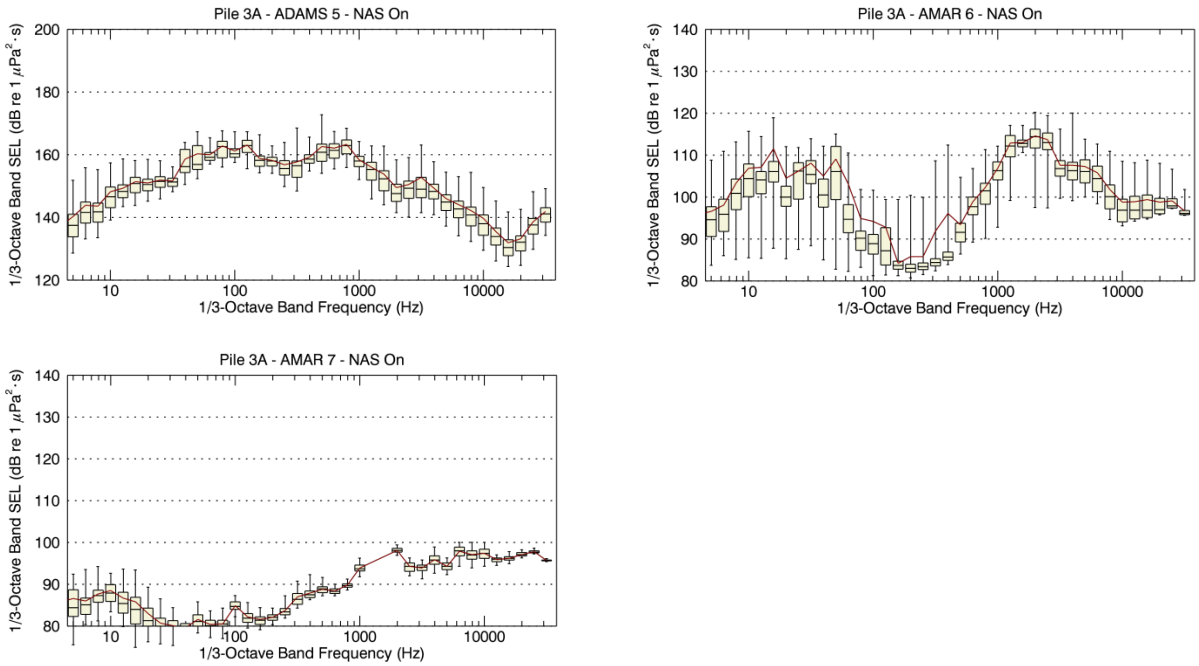

Figure 88. 1/3-octave band SEL statistics for impact driving of Test Pile 3A, 8 May 2012, with the MENCK MHU 800S hydraulic impact hammer and the Unconfined Multi-Tier Air Bubble Curtain on. Beige bars indicate the first, second, and third quartiles (L_{25}, L_{50}, and L_{75}). Upper error-bars indicate the maximum levels (L_{max}). Lower error bars indicate the 95% exceedance percentiles (L_{95}). The maroon line indicates the arithmetic mean (L_{mean}). (Top Left) Short-range monitoring at 39.7 ft horizontal distance. (Top Right) Long-range monitoring data from Station 6. (Bottom Left) Long-range monitoring data from Station 7.

G.6. Test Pile 3B

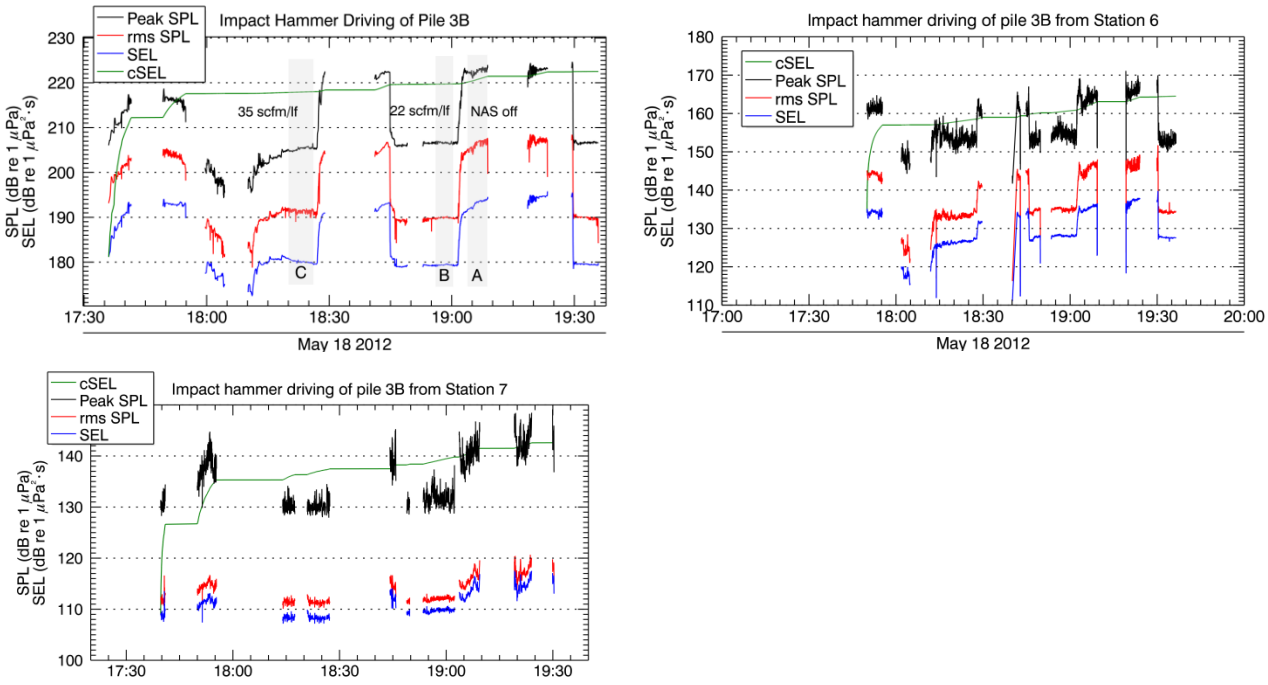

Figure 89. Plots of received sound levels for impact pile driving at Test Pile 3B, 18 May 2012, with MENCK MHU 800S hydraulic impact hammer and a Two-Stage Confined Bubble Curtain NAS. (Top Left) Short-range monitoring at 33.7 ft horizontal distance. (Top Right) Long-range monitoring data from Station 6. (Bottom Left) Long-range monitoring data from Station 7.

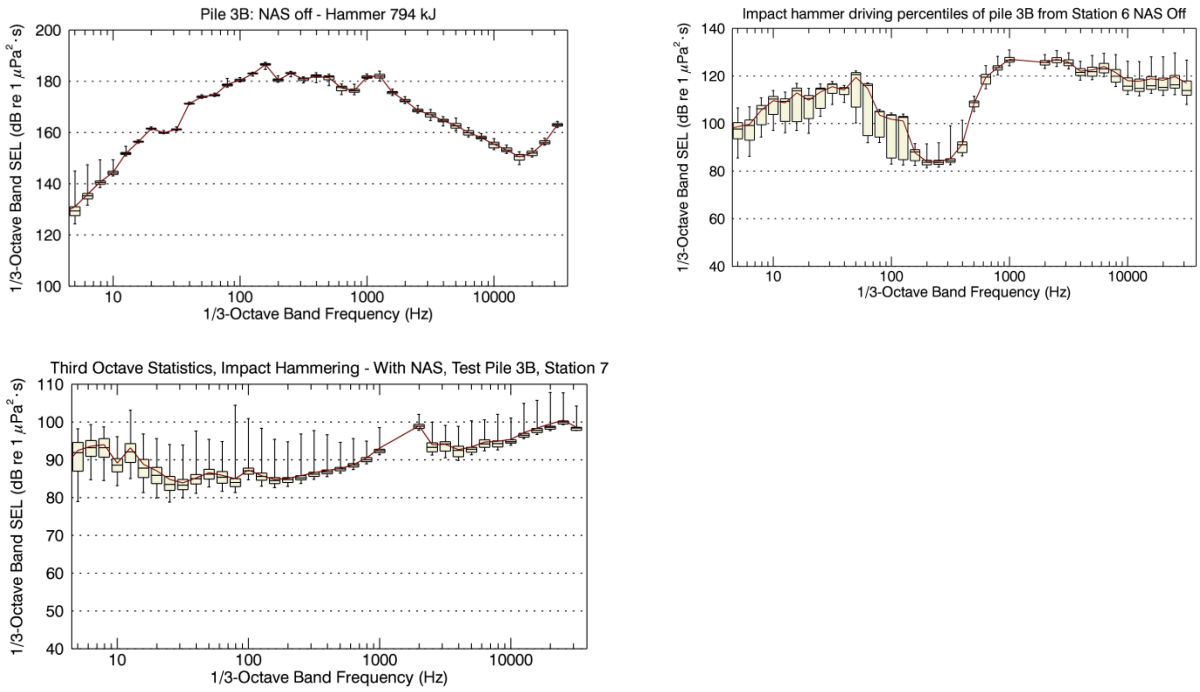

Figure 90. 1/3-octave band SEL statistics for impact driving of Test Pile 3B, 18 May 2012, with the MENCK MHU 800S hydraulic impact hammer and the Two-Stage Confined Bubble Curtain NAS off. Beige bars indicate the first, second, and third quartiles (L_{25}, L_{50}, and L_{75}). Upper error-bars indicate the maximum levels (L_{max}). Lower error bars indicate the 95% exceedance percentiles (L_{95}). The maroon line indicates the arithmetic mean (L_{mean}). (Top Left) Short-range monitoring at 33.7 ft horizontal distance. (Top Right) Long-range monitoring data from Station 6. (Bottom Left) Long-range monitoring data from Station 7.

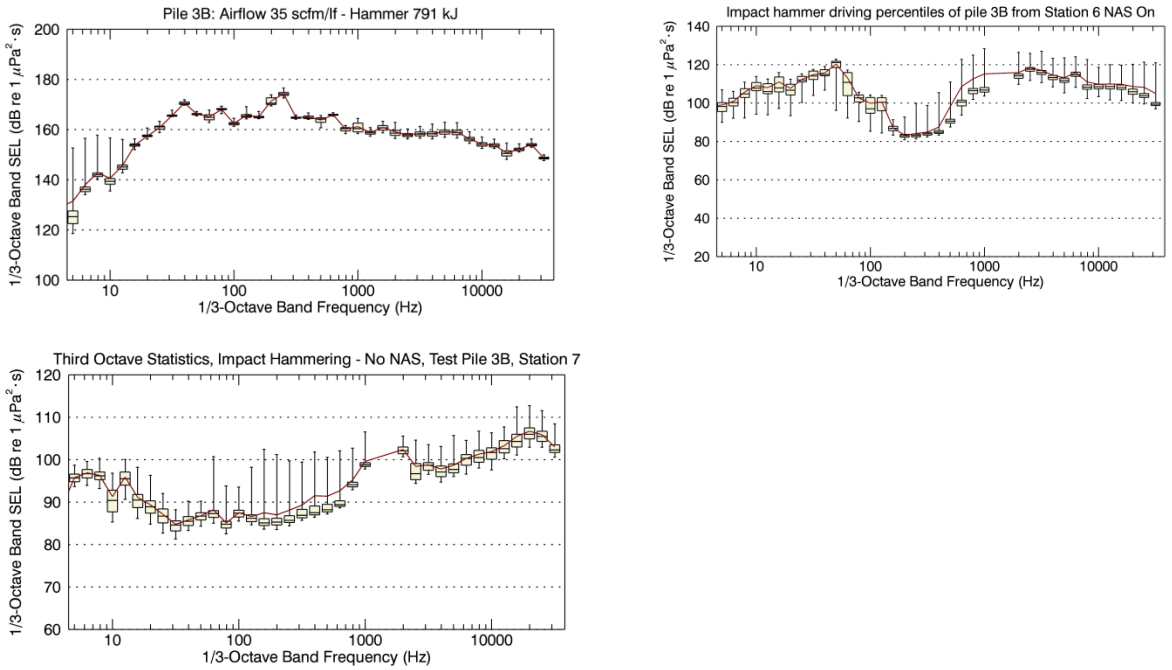

Figure 91. 1/3-octave band SEL statistics for impact driving of Test Pile 3B, 18 May 2012, with the MENCK MHU 800S hydraulic impact hammer and the Two-Stage Confined Bubble NAS on. Beige bars indicate the first, second, and third quartiles (L_{25}, L_{50}, and L_{75}). Upper error-bars indicate the maximum levels (L_{max}). Lower error bars indicate the 95% exceedance percentiles (L_{95}). The maroon line indicates the arithmetic mean (L_{mean}). (Top Left) short-range monitoring at 33.7 ft horizontal distance. (Top Right) Long-range monitoring data from Station 6. (Bottom Left) Long-range monitoring data from Station 7.

G.7. Test Pile 4A

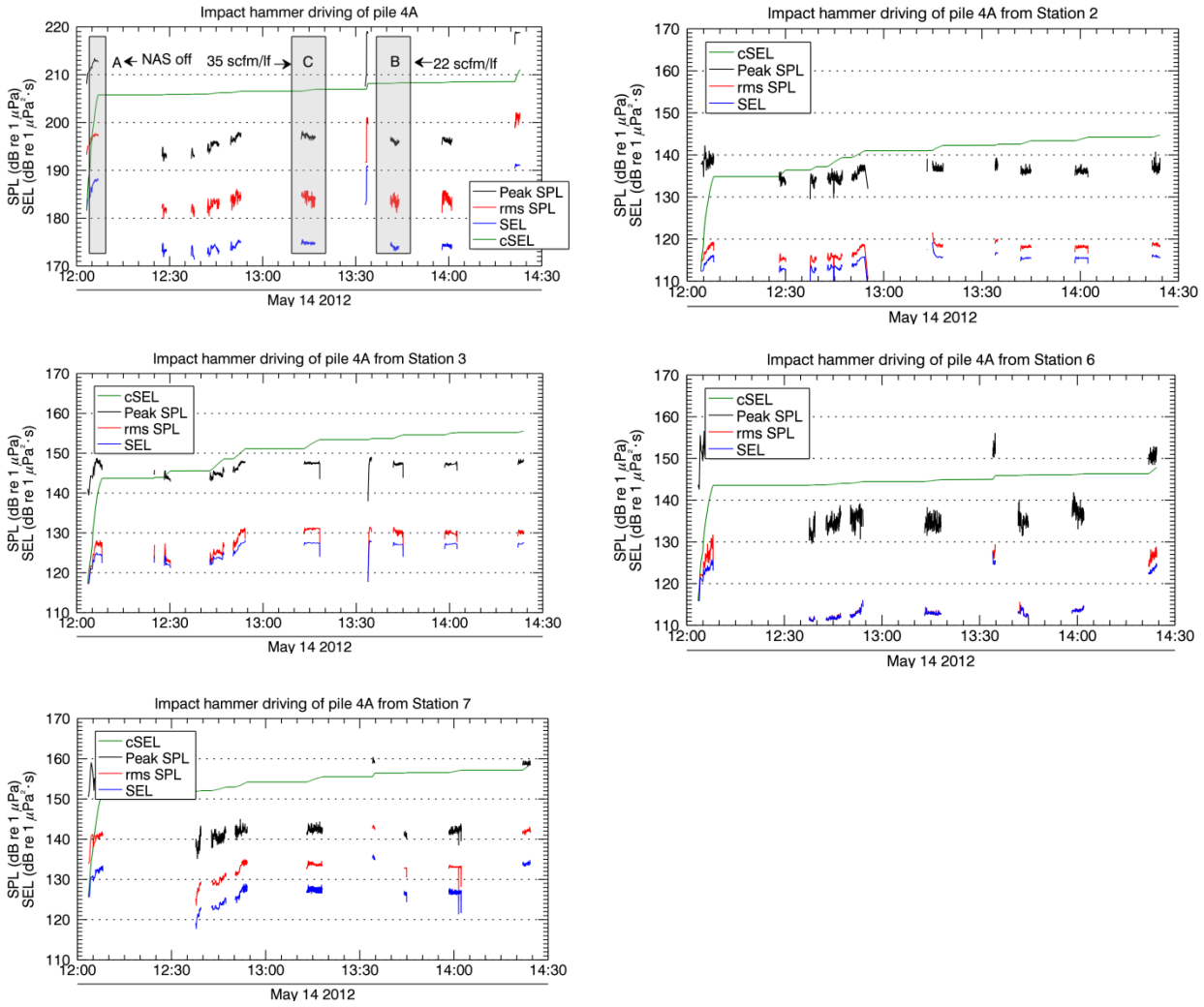

Figure 92. Plots of received sound levels for impact pile driving at Test Pile 4A, 14 May 2012, with MENCK MHU 800S hydraulic impact hammer and a Two-Stage Confined Bubble Curtain NAS. (Top Left) Short-range monitoring at 33.5 ft horizontal distance. (Top Right) Long-range monitoring at Station 2. (Middle Left) Long-range monitoring at Station 3. (Middle Right) Long-range monitoring at Station 6. (Bottom Left) Long-range monitoring at Station 7.

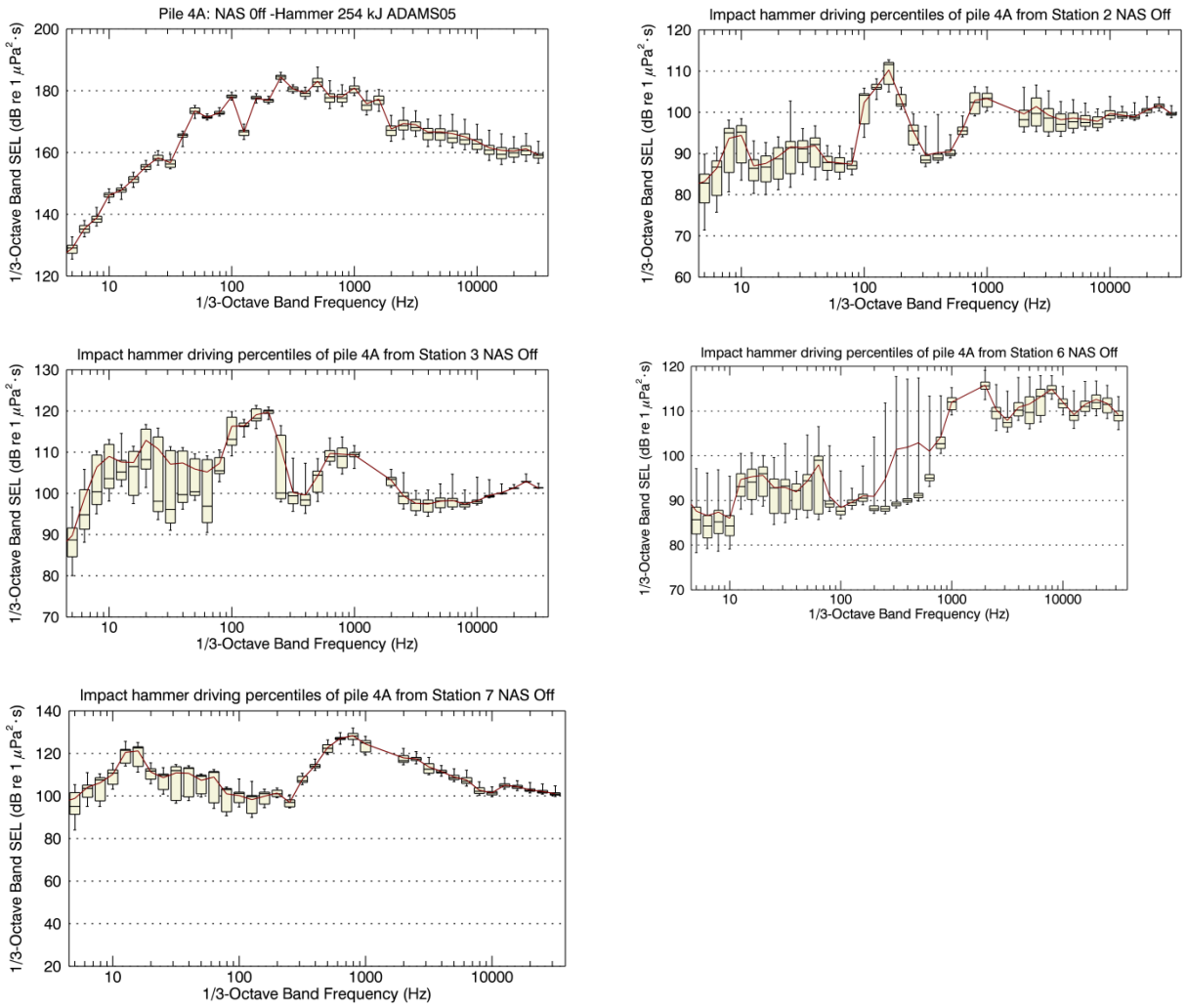

Figure 93. 1/3-octave band SEL statistics for impact driving of Test Pile 4A, 14 May 2012, with the MENCK MHU 800S hydraulic impact hammer and the Two-Stage Confined Bubble Curtain NAS off. Beige bars indicate the first, second, and third quartiles (L25, L50, and L75). Upper error-bars indicate the maximum levels (Lmax). Lower error bars indicate the 95% exceedance percentiles (L95). The maroon line indicates the arithmetic mean (Lmean). (Top Left) Short-range monitoring at 33.5 ft horizontal distance. (Top Right) Long-range monitoring at Station 2. (Middle Left) Long-range monitoring at Station 3. (Middle Right) Long-range monitoring at Station 6. (Bottom Left) Long-range monitoring at Station 7.

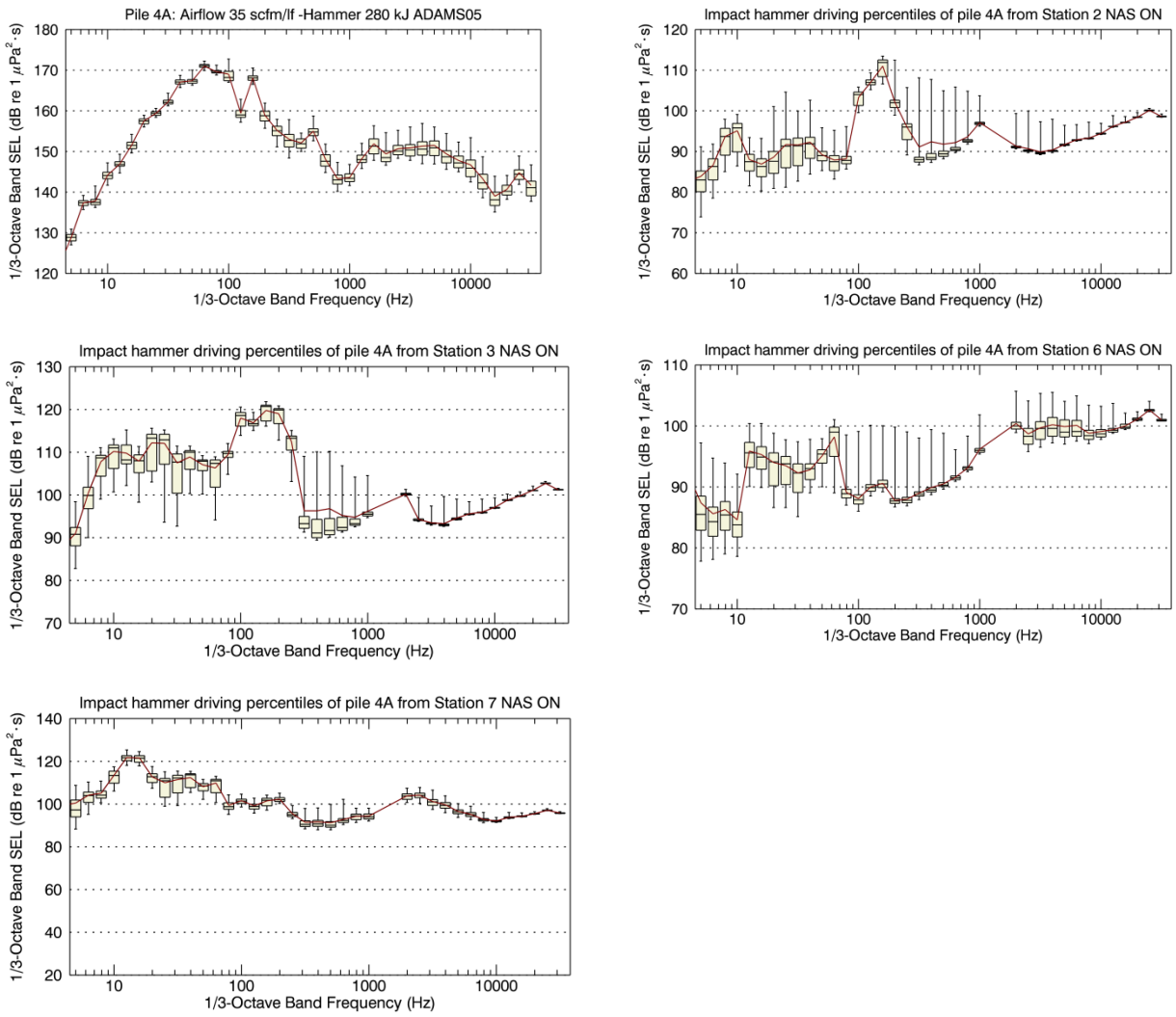

Figure 94. 1/3-octave band SEL statistics for impact driving of Test Pile 4A, 14 May 2012, with the MENCK MHU 800S hydraulic impact hammer and the Two-Stage Confined Bubble Curtain NAS on with airflow at 35 scfm/lf. Beige bars indicate the first, second, and third quartiles (L25, L50, and L75). Upper error-bars indicate the maximum levels (Lmax). Lower error bars indicate the 95% exceedance percentiles (L95). The maroon line indicates the arithmetic mean (Lmean). (Top Left) Short-range monitoring at 33.5 ft horizontal distance. (Top Right) Long-range monitoring at Station 2. (Middle Left) Long-range monitoring at Station 3. (Middle Right) Long-range monitoring at Station 6. (Bottom Left) Long-range monitoring at Station 7.

Appendix H. Threshold Range Calculations

An important outcome of the PIDP is determining the range at which sound levels from impact pile driving exceed the physiological and behavioral thresholds contained in the DEIS and the Biological Opinion. JASCO determined the ranges by performing a linear regression of the sound levels from the short-range monitoring and each long-range recorder where impact piling was measured. The figures and tables in this section present the results.

H.1. Test Pile 1A

At Test Pile 1A, impact piling was detected at Stations 4 and 8. Figures 95 and 96 plot the linear regression. Table 28 lists estimates of the threshold ranges and spreading law coefficients.

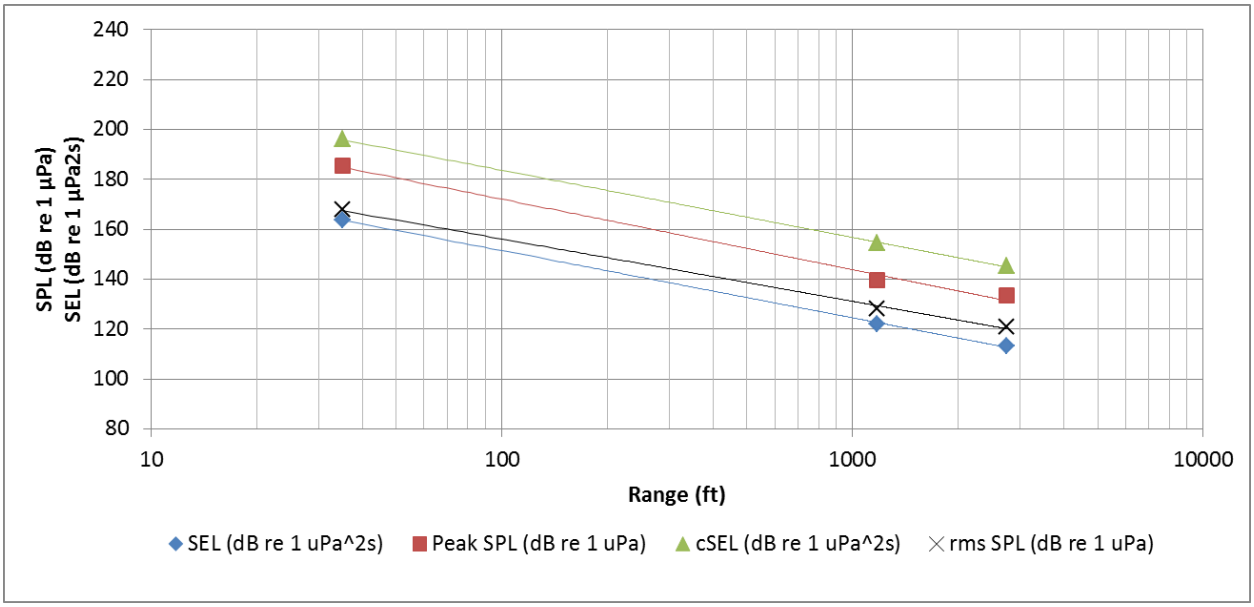

Figure 95. Measured acoustic quantities versus range for Test Pile 1A with NAS on. Lines show the best fit to the data, which was derived with linear regression.

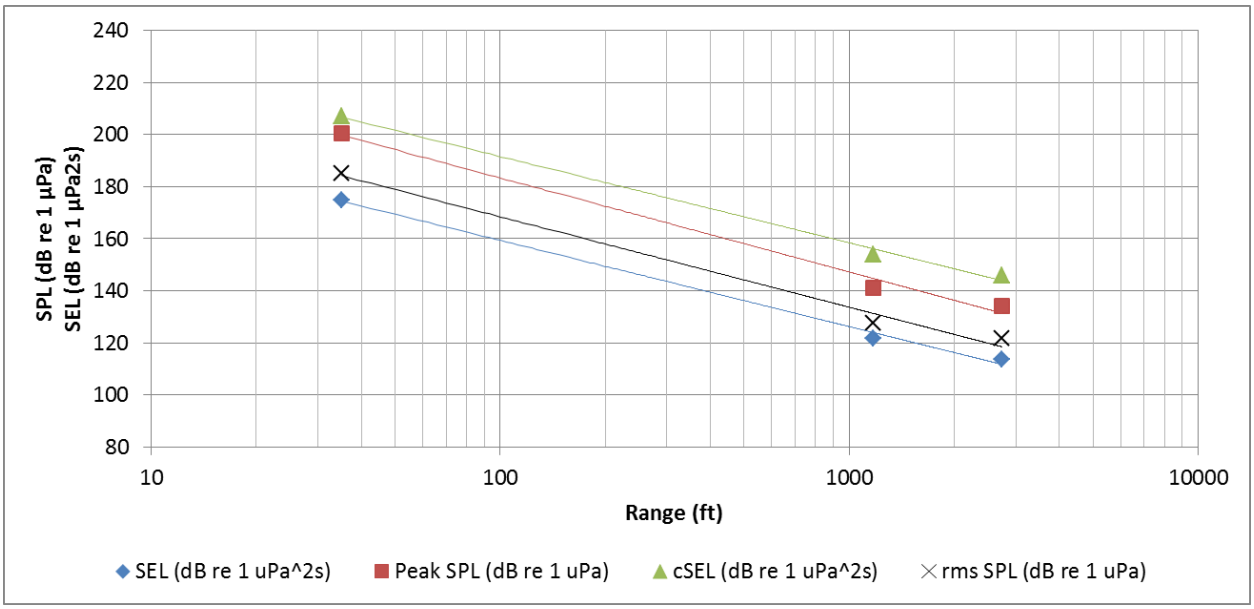

Figure 96. Measured acoustic quantities versus range for Test Pile 1A with NAS off. Lines show the best fit to the data, which was derived with linear regression.

Table 28. Estimates of the threshold ranges and spreading law coefficients for Test Pile 1A.

Threshold	Value	Mean Distance, ft	Minimum Distance, ft	Maximum distance, ft	Spreading Law Coefficient
NAS On					
cSEL	187 dB re 1 µPa^2·s	75.0	n/a	n/a	27.0
Peak SPL	206 dB re 1 µPa	6.3	5.4	8.3	28.3
rms SPL	150 dB re 1 µPa	175.6	158.7	294.1	25.0
NAS Off					
cSEL	187 dB re 1 µPa^2·s	137.3	n/a	n/a	33.2
Peak SPL	206 dB re 1 µPa	23.7	20.1	29.2	36.2
rms SPL	150 dB re 1 µPa	338.9	287.2	405.3	34.8

H.2. Test Pile 1B

At Test Pile 1B, impact piling was detected at Stations 4 and 8. Figures 97 and 98 plot the linear regression. Table 29 lists estimates the threshold ranges and spreading law coefficients.

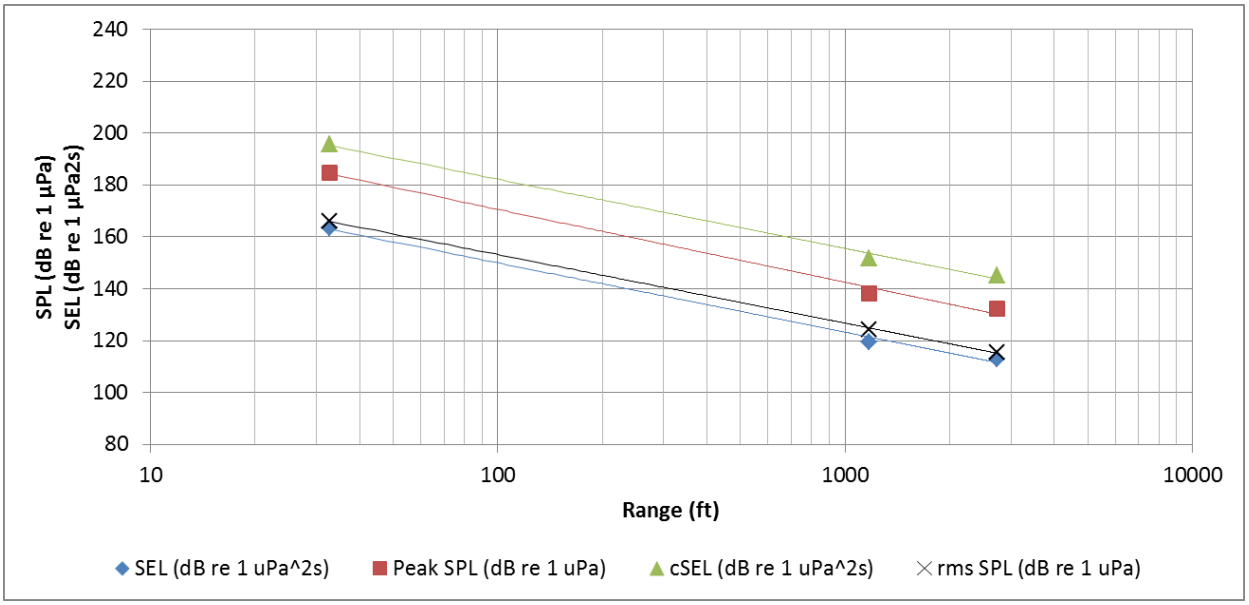

Figure 97. Measured acoustic quantities versus range for Test Pile 1B with NAS on. Lines show the best fit to the data, which was derived with linear regression.

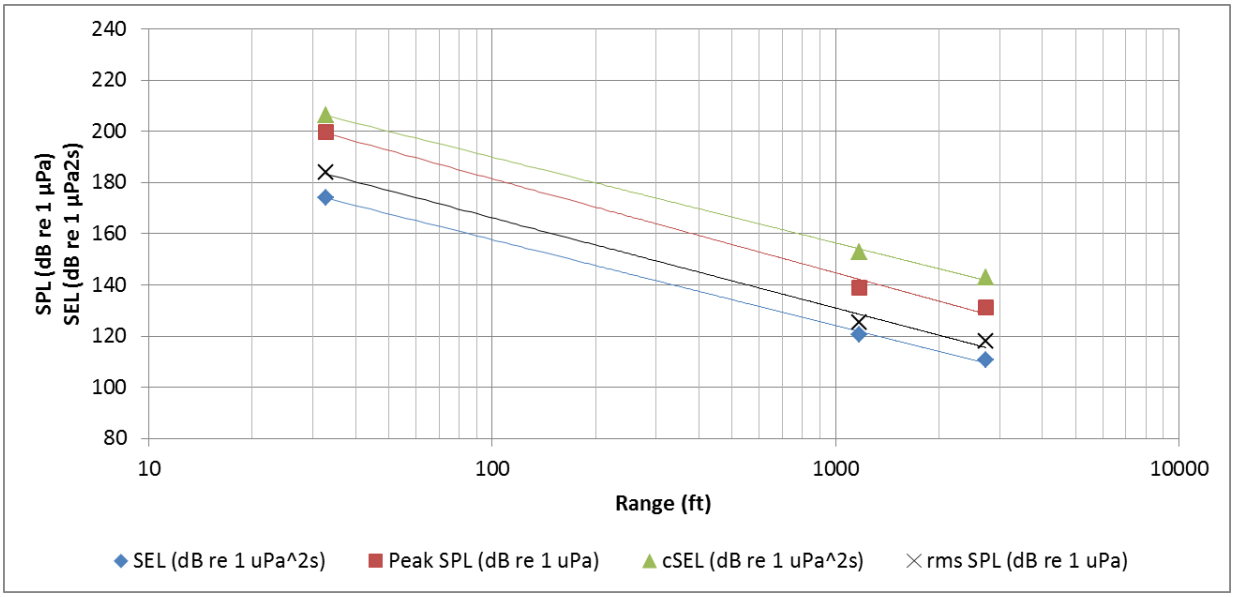

Figure 98. Measured acoustic quantities versus range for Test Pile 1B with NAS off. Lines show the best fit to the data, which was derived with linear regression.

Table 29. Estimates of the threshold ranges and spreading law coefficients for Test Pile 1B.

Threshold	Value	Mean Distance, ft	Minimum Distance, ft	Maximum distance, ft	Spreading Law Coefficient
NAS On					
cSEL	187 dB re 1 µPa^2·s	66.6	n/a	n/a	26.8
Peak SPL	206 dB re 1 µPa	5.5	4.6	7.5	28.1
rms SPL	150 dB re 1 µPa	132.0	125.3	146.5	26.5
NAS Off					
cSEL	187 dB re 1 µPa^2·s	122.6	n/a	n/a	33.6
Peak SPL	206 dB re 1 µPa	21.5	18.6	25.2	36.8
rms SPL	150 dB re 1 µPa	288.5	254.9	314.5	35.3

H.3. Test Pile 2A

At Test Pile 2A, impact piling was detected at Stations 4 and 8. Figures 99 and 100 plot the regression. Table 30 lists estimates of the threshold ranges and spreading law coefficients.

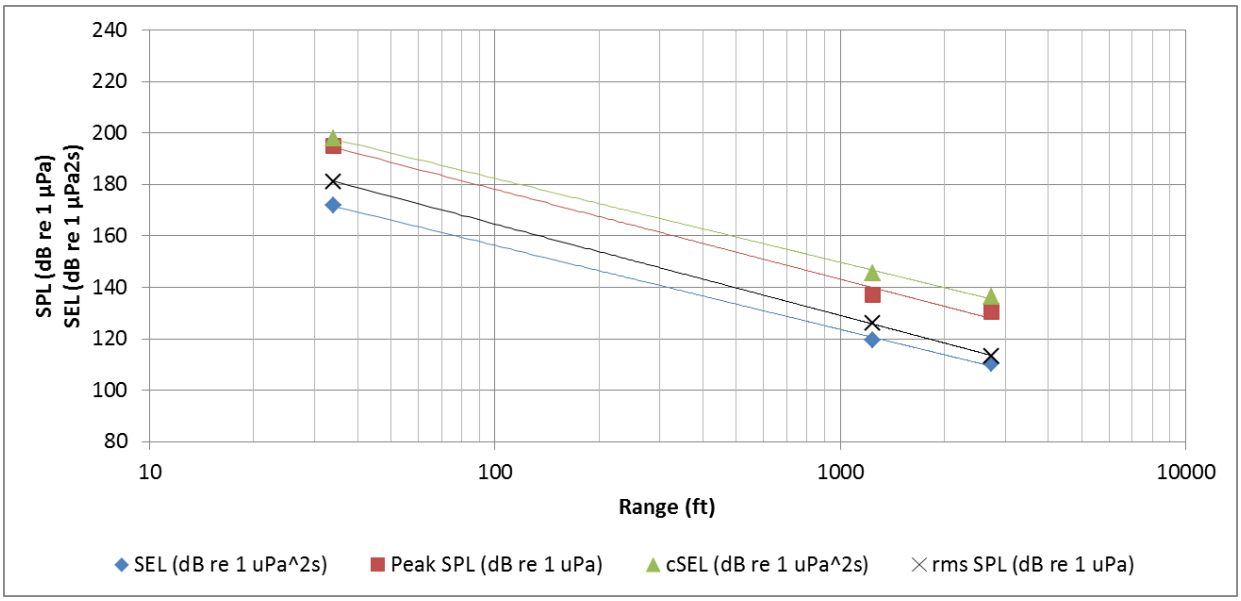

Figure 99. Measured acoustic quantities versus range for Test Pile 2A with NAS on. Lines show the best fit to the data, which was derived with linear regression.

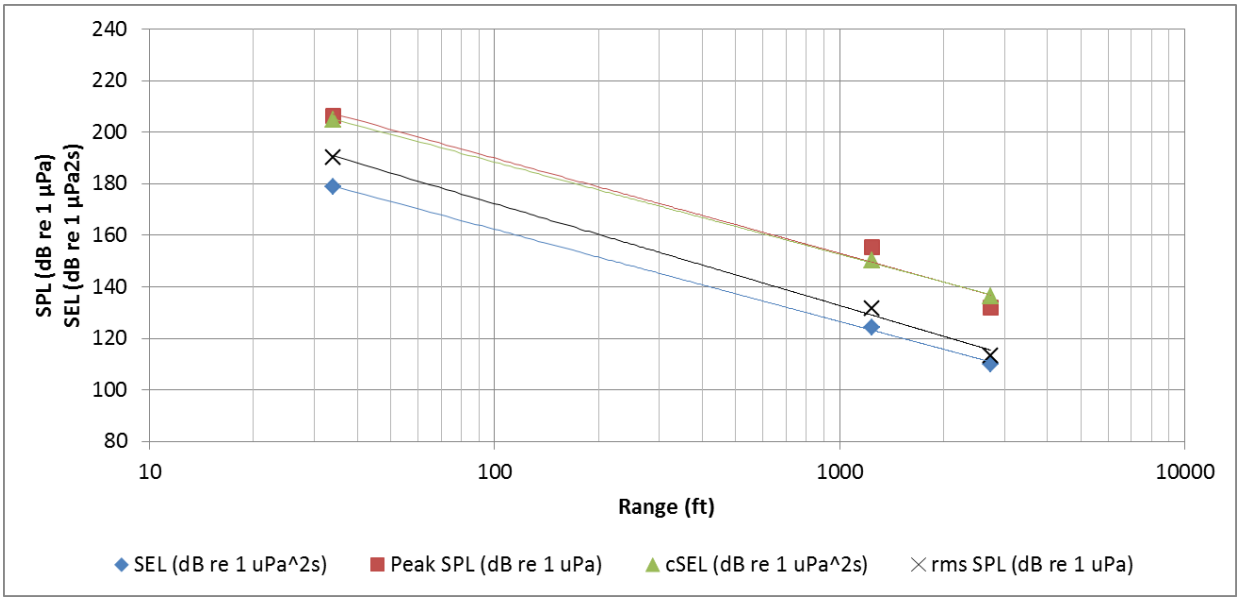

Figure 100. Measured acoustic quantities versus range for Test Pile 2A with NAS off. Lines show the best fit to the data, which was derived with linear regression.

Table 30. Estimates of the threshold ranges and spreading law coefficients for Test Pile 2A.

Threshold	Value	Mean Distance, ft	Minimum Distance, ft	Maximum distance, ft	Spreading Law Coefficient
NAS On					
cSEL	187 dB re 1 µPa^2·s	72.4	n/a	n/a	32.7
Peak SPL	206 dB re 1 µPa	15.9	12.4	19.6	35.0
rms SPL	150 dB re 1 µPa	257.8	232.4	289.6	35.6
NAS Off					
cSEL	187 dB re 1 µPa^2·s	109.6	n/a	n/a	35.8
Peak SPL	206 dB re 1 µPa	36.8	29.1	42.0	37.0
rms SPL	150 dB re 1 µPa	365.6	314.3	394.4	39.6

H.4. Test Pile 2B

At Test Pile 2B, impact piling was detected at Stations 4, 6, and 8. Figures 101 and 102 plot the linear regression. Table 31 lists estimates of the threshold ranges and spreading law coefficients.

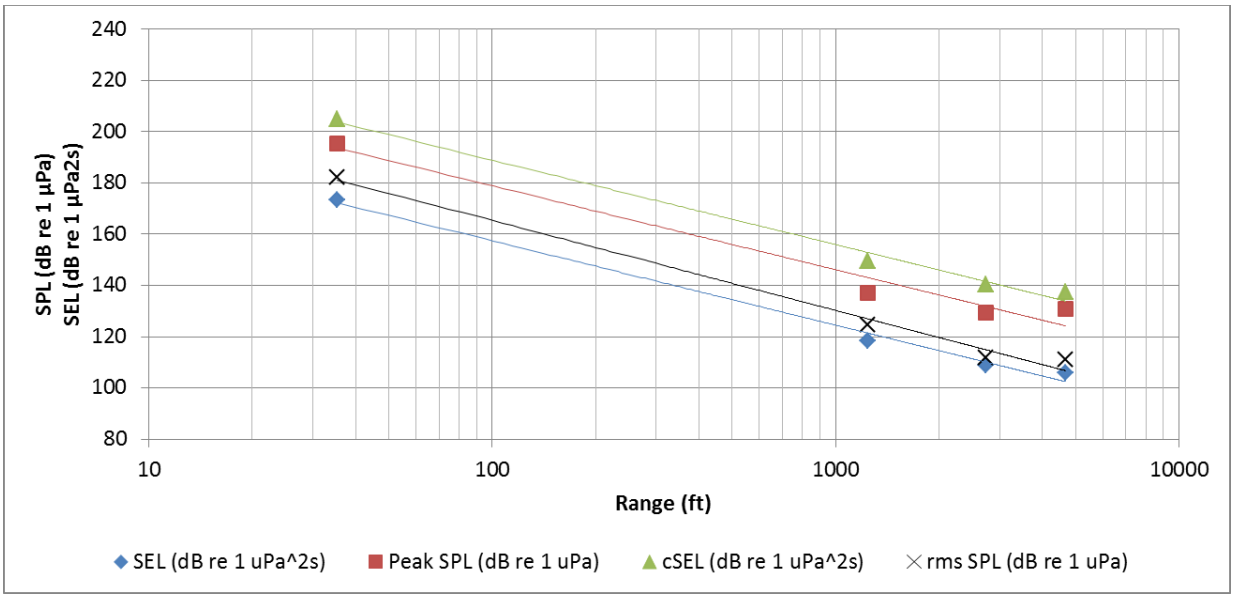

Figure 101. Measured acoustic quantities versus range for Test Pile 2B with NAS on. Lines show the best fit to the data, which was derived with linear regression.

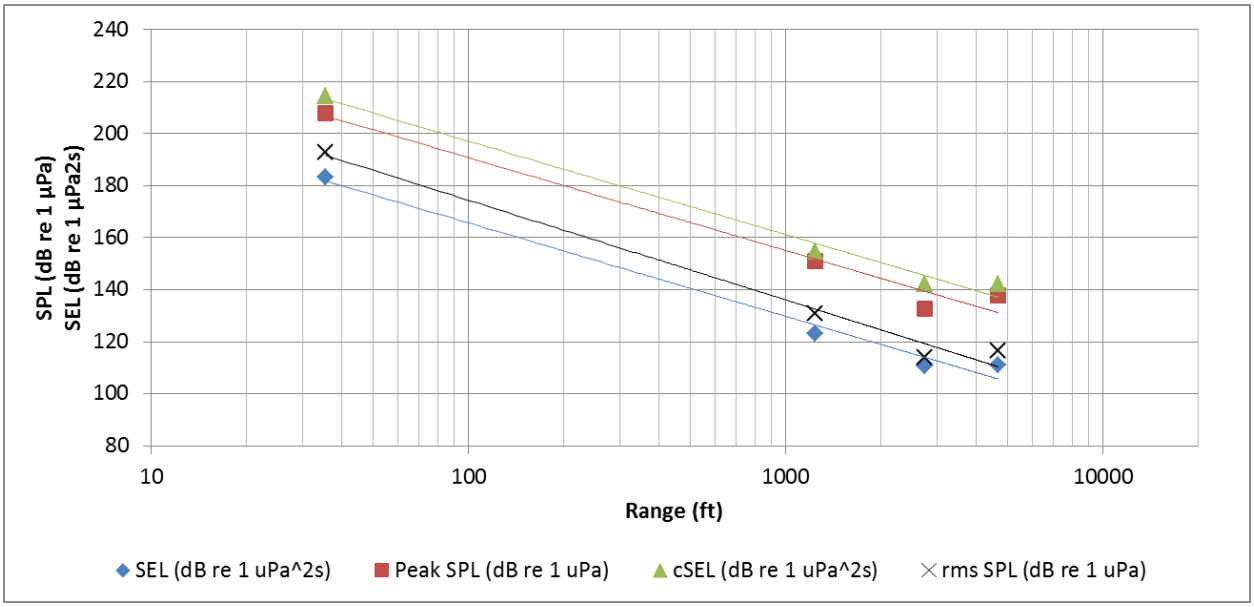

Figure 102. Measured acoustic quantities versus range for Test Pile 2B with NAS off. Lines show the best fit to the data, which was derived with linear regression.

Table 31. Estimates of the threshold ranges and spreading law coefficients for Test Pile 2B.

Threshold	Value	Mean Distance, ft	Minimum Distance, ft	Maximum distance, ft	Spreading Law Coefficient
NAS On					
cSEL	187 dB re 1 µPa^2·s	114.0	n/a	n/a	33.0
Peak SPL	206 dB re 1 µPa	14.8	13.6	17.0	32.7
rms SPL	150 dB re 1 µPa	273.8	256.4	306.0	35.1
NAS Off					
cSEL	187 dB re 1 µPa^2·s	191.5	n/a	n/a	35.9
Peak SPL	206 dB re 1 µPa	37.5	35.1	42.4	35.7
rms SPL	150 dB re 1 µPa	433.6	420.8	452.2	38.3

H.5. Test Pile 3A

At Test Pile 3A, impact piling was detected at Stations 6 and 7. Figures 103 and 104 plot sound levels versus range. Table 32 lists estimates of the threshold ranges and spreading law coefficients.

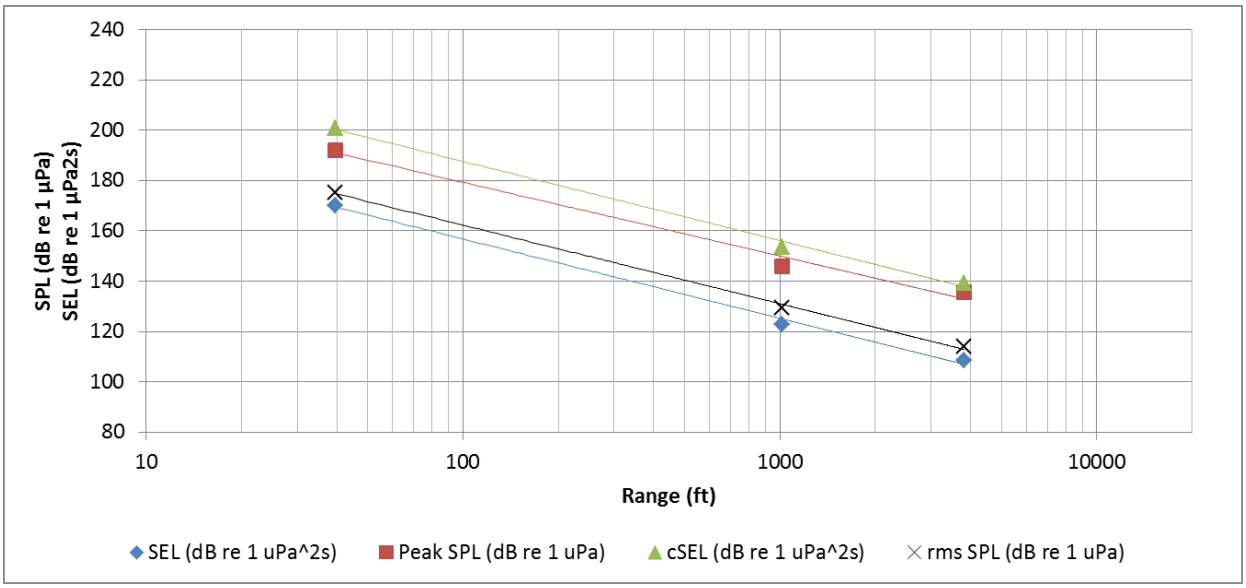

Figure 103. Measured acoustic quantities versus range for Test Pile 3A with NAS on. Lines show the best fit to the data, which was derived with linear regression.

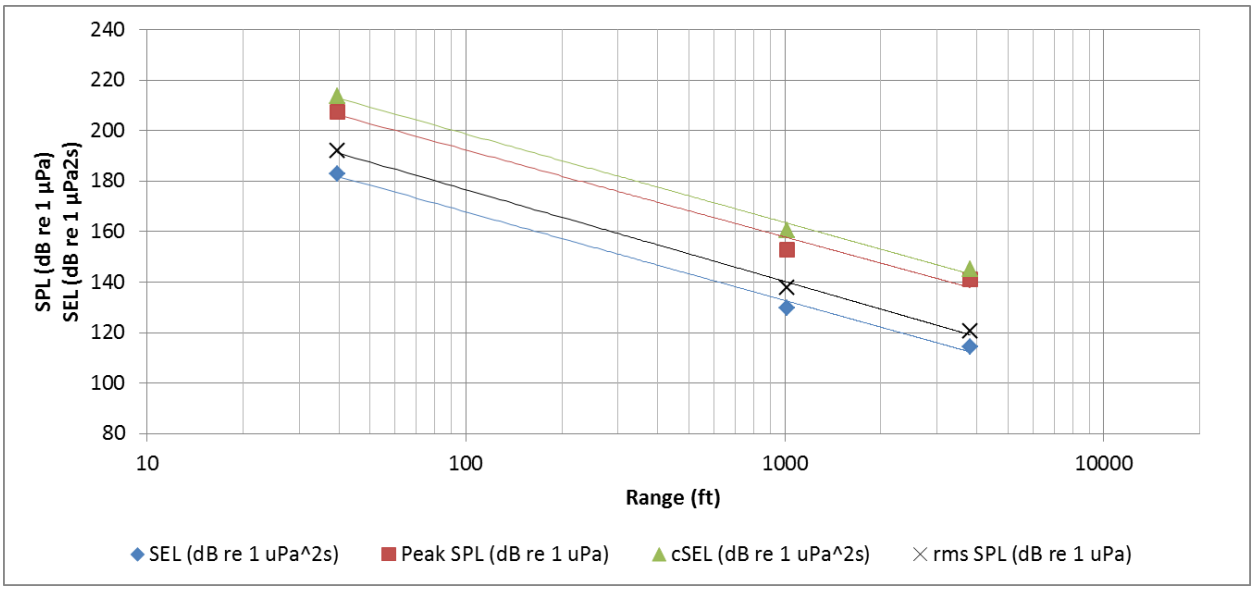

Figure 104. Measured acoustic quantities versus range for Test Pile 3A with NAS off. Lines show the best fit to the data, which was derived with linear regression.

Table 32. Estimates of the threshold ranges and spreading law coefficients for Test Pile 3A.

Threshold	Value	Mean Distance, ft	Minimum Distance, ft	Maximum distance, ft	Spreading Law Coefficient
NAS On					
cSEL	187 dB re 1 µPa^2·s	105.0	n/a	n/a	31.5
Peak SPL	206 dB re 1 µPa	12.3	7.2	16.0	29.3
rms SPL	150 dB re 1 µPa	247.4	168.7	332.1	31.3
NAS Off					
cSEL	187 dB re 1 µPa^2·s	216.0	n/a	n/a	35.1
Peak SPL	206 dB re 1 µPa	40.3	24.5	62.7	34.5
rms SPL	150 dB re 1 µPa	539.2	371.2	749.4	36.4

H.6. Test Pile 3B

At Test Pile 3B, impact piling was detected at Stations 6 and 7. Figures 105 and 106 plot the linear regression. Table 33 lists estimates of the threshold ranges and spreading law coefficients.

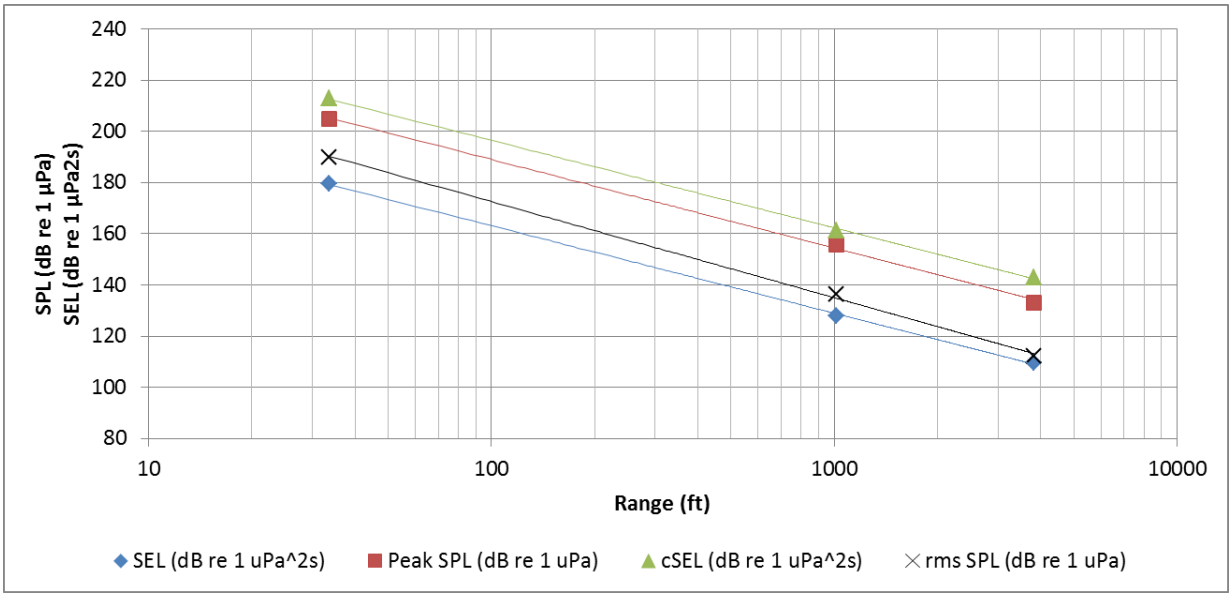

Figure 105. Measured acoustic quantities versus range for Test Pile 3B with NAS on. Lines show the best fit to the data, which was derived with linear regression.

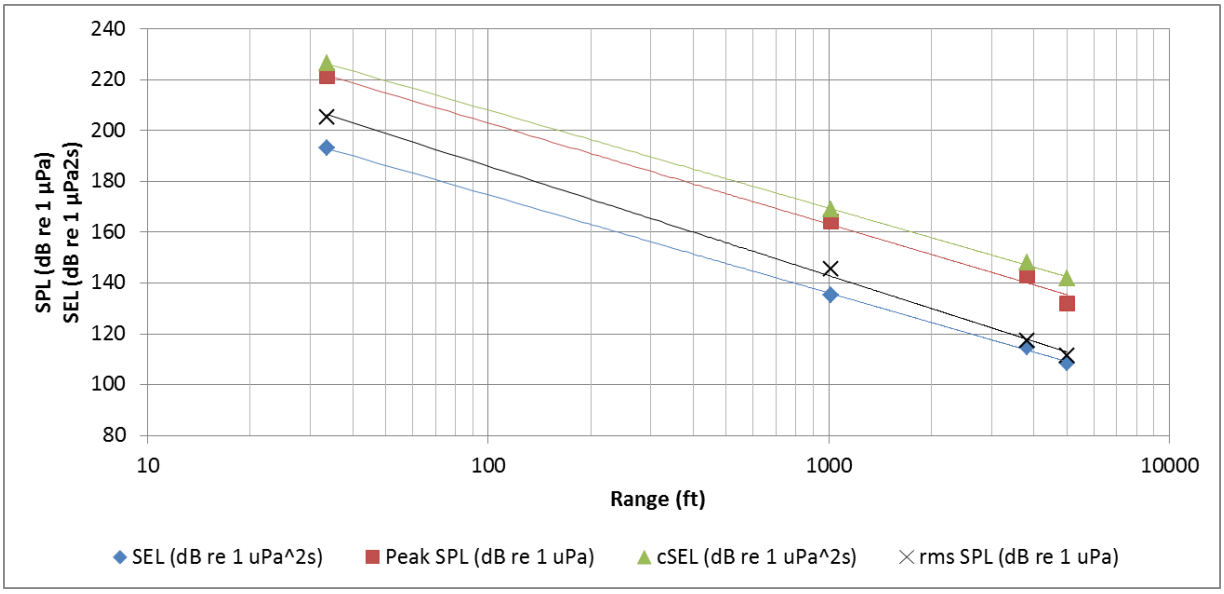

Figure 106. Measured acoustic quantities versus range for Test Pile 3B with NAS off. Lines show the best fit to the data, which was derived with linear regression.

Table 33. Estimates of the threshold ranges and spreading law coefficients for Test Pile 3B.

Threshold	Value	Mean Distance, ft	Minimum Distance, ft	Maximum distance, ft	Spreading Law Coefficient
NAS On					
cSEL	187 dB re 1 µPa^2·s	189.8			34.2
Peak SPL	206 dB re 1 µPa	32.4	19.8	37.8	34.6
rms SPL	150 dB re 1 µPa	398.7	286.3	461.8	37.6
NAS Off					
cSEL	187 dB re 1 µPa^2·s	351.2			38.6
Peak SPL	206 dB re 1 µPa	83.8	60.6	100.8	39.8
rms SPL	150 dB re 1 µPa	684.3	595.5	807.8	43.0

H.7. Test Pile 4A

At Test Pile 4A, impact piling was detected at Stations 2, 3, 6, and 7. Figures 107 and 108 plot sound levels versus range. Table 34 lists estimates of the threshold ranges and spreading law coefficients.

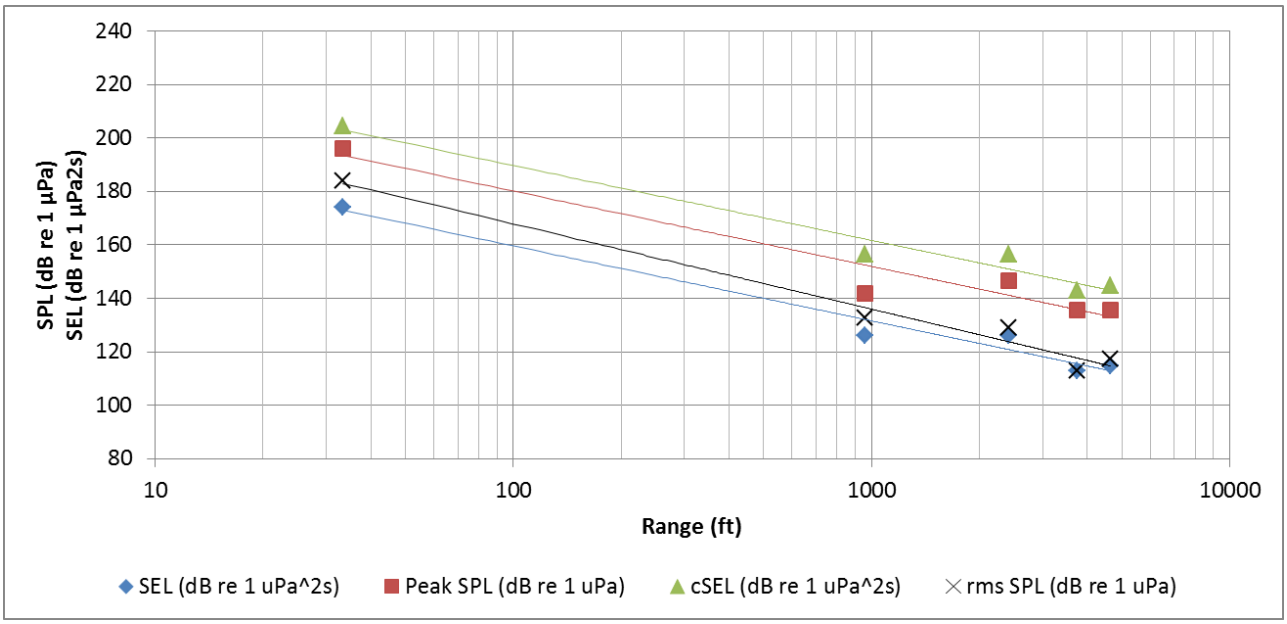

Figure 107. Measured acoustic quantities versus range for Test Pile 4A with NAS on. Lines show the best fit to the data, which was derived with linear regression.

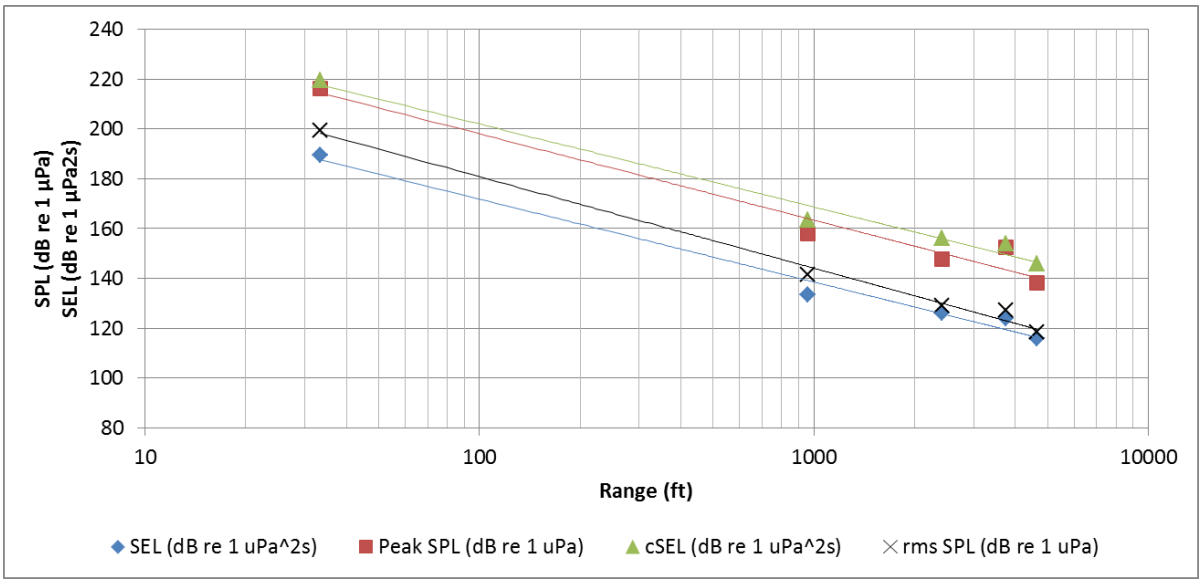

Figure 108. Measured acoustic quantities versus range for Test Pile 4A with NAS off. Lines show the best fit to the data, which was derived with linear regression.

Table 34. Estimates of the threshold ranges and spreading law coefficients for Test Pile 4A.

Threshold	Value	Mean Distance, ft	Minimum Distance, ft	Maximum distance, ft	Spreading Law Coefficient
NAS On					
cSEL	187 dB re 1 µPa^2·s	125.2	n/a	n/a	28.1
Peak SPL	206 dB re 1 µPa	12.1	9.4	14.4	28.2
rms SPL	150 dB re 1 µPa	362.8	307.3	428.3	31.9
NAS Off					
cSEL	187 dB re 1 µPa^2·s	281.5	n/a	n/a	33.4
Peak SPL	206 dB re 1 µPa	59.0	41.3	70.6	34.7
rms SPL	150 dB re 1 µPa	689.4	560.7	821.4	36.8

Appendix I. Vibratory Pile Driving Received Levels

This appendix contains plots of the received levels for each vibratory pile driving event. One set of plots shows the peak SPL, rms SPL, SEL, and cumulative SEL for the event. There are plots for short-range measurements and each long-range recorder that detected pile driving.

I.1. Test Pile 1A–Bottom Segment, ICE 66 Vibratory Driver

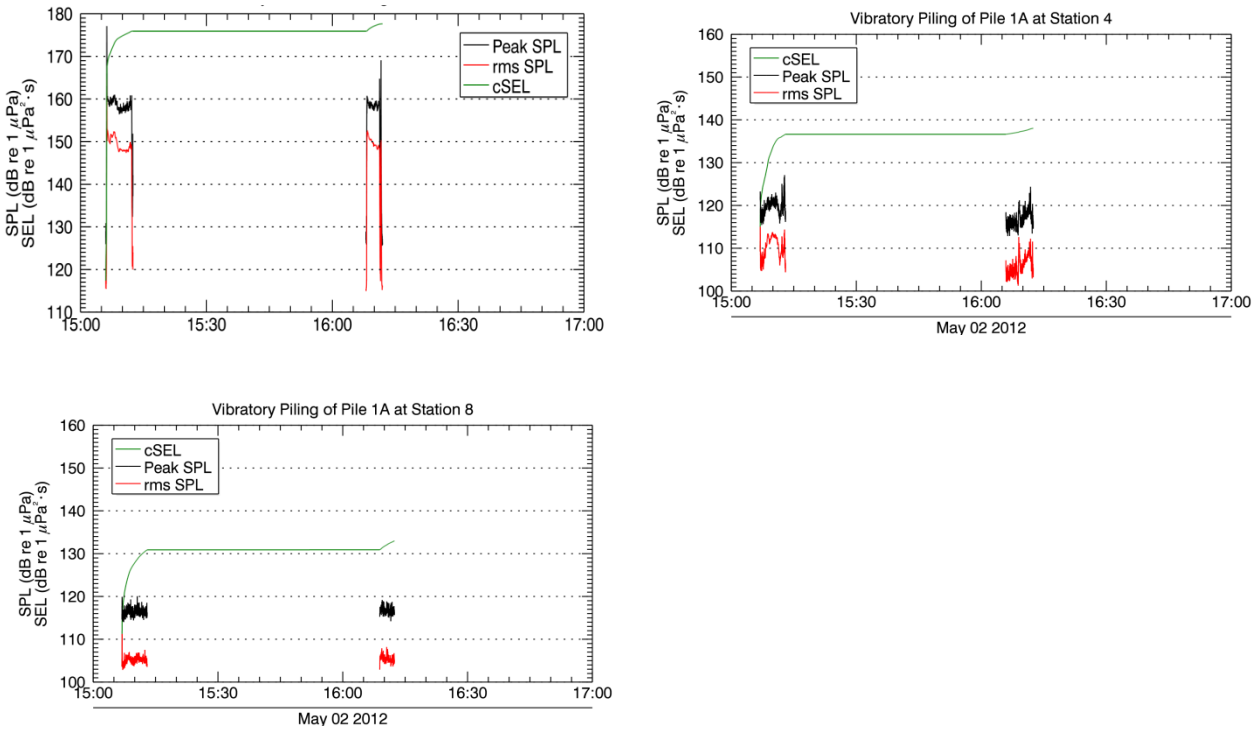

Figure 109. Plots of received sound levels for vibratory pile driving at Test Pile 1A, 2 May 2012. (Top Left) Short-range monitoring at 35.1 ft horizontal distance. (Top Right) Long-range monitoring at Station 4. (Bottom Left) Long-range monitoring at Station 8.

I.2. Test Pile 1B–Bottom Segment, ICE 66 Vibratory Driver

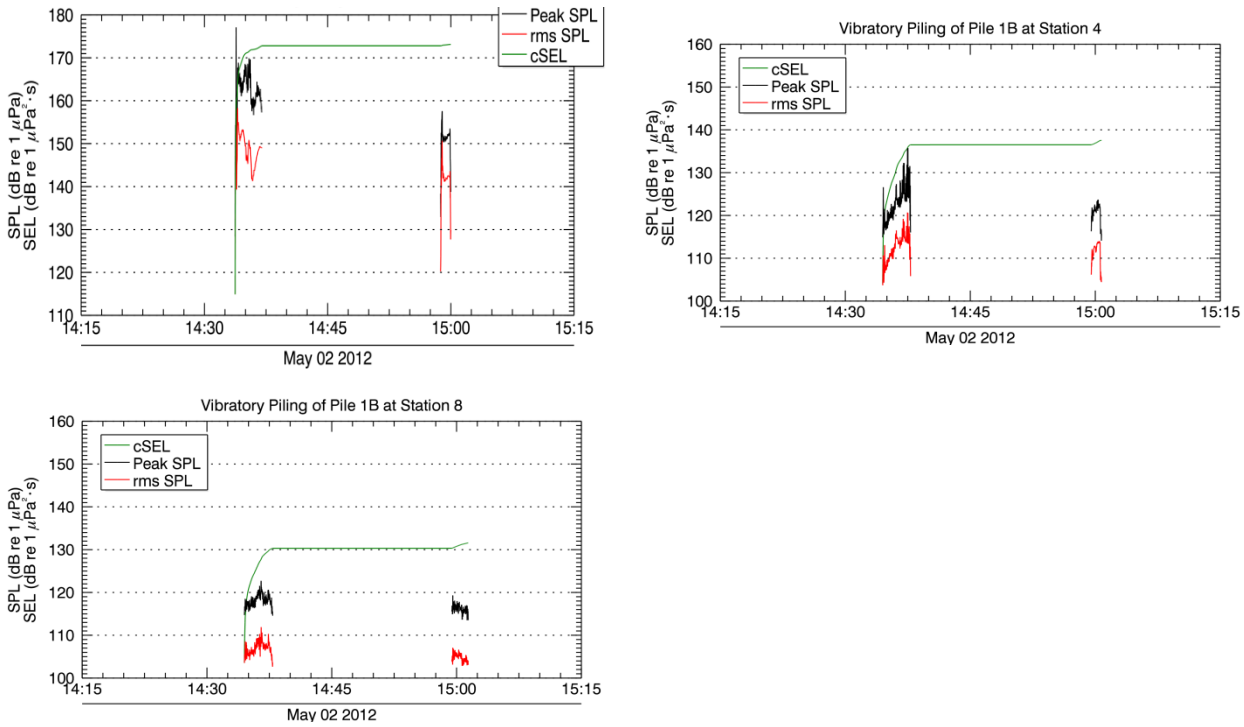

Figure 110. Plots of received sound levels for vibratory pile driving at Test Pile 1B, 2 May 2012. (Top Left) Short-range monitoring at 31.8 ft horizontal distance. (Top right) Long-range monitoring at Station 4. (Bottom Left) Long-range monitoring at Station 8.

I.3. Test Pile 1B–Top Segment, ICE 66 Vibratory Driver

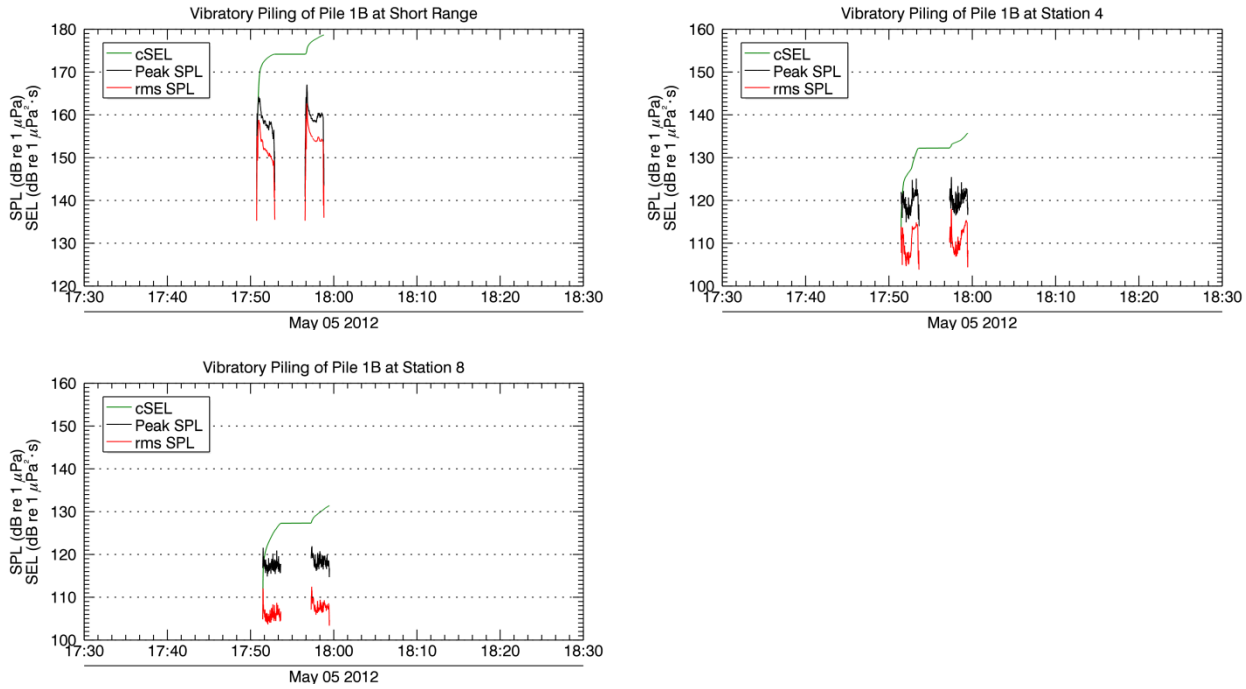

Figure 111. Plots of received sound levels for vibratory pile driving at Test Pile 1B, 5 May 2012. (Top Left) Short-range monitoring at 31.8 ft horizontal distance. (Top Right) Long-range monitoring at Station 4. (Bottom Left) Long-range monitoring at Station 8.

I.4. Test Pile 2A–Top Segment, ICE 66 Vibratory Driver

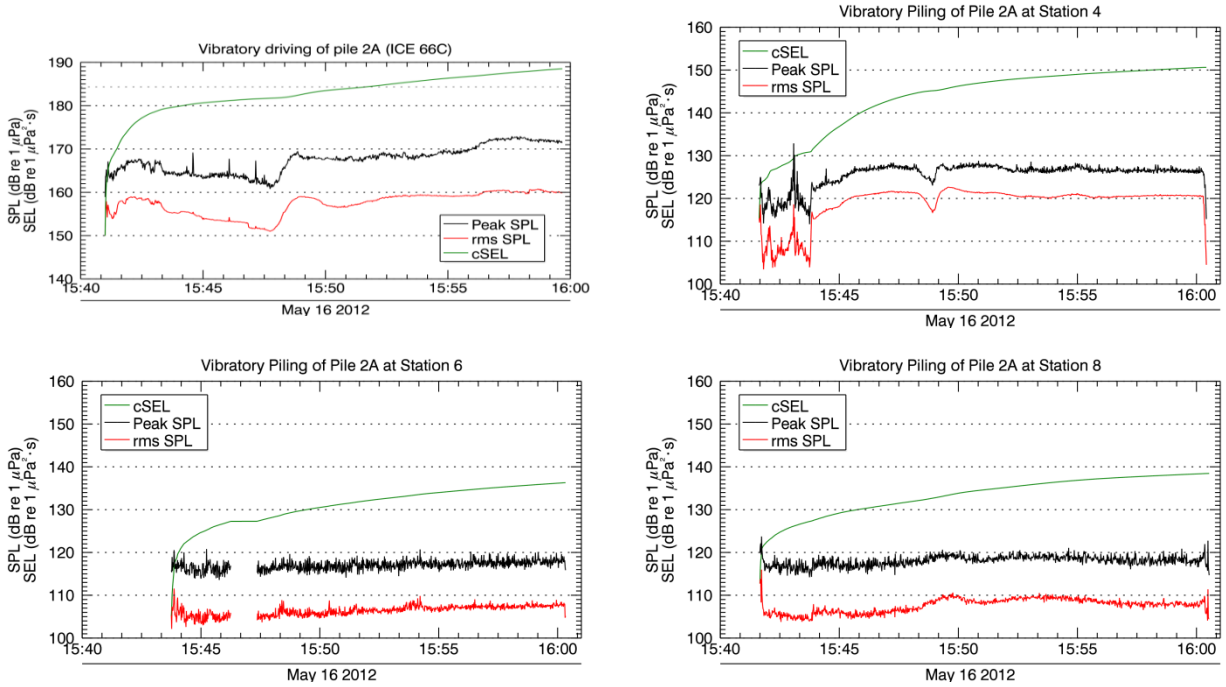

Figure 112. Plots of received sound levels for vibratory pile driving at Test Pile 2A, 16 May 2012. (Top Left) Short-range monitoring at 34.1 ft horizontal distance. (Top Right) Long-range monitoring at Station 4. (Bottom Left) Long-range monitoring at Station 6. (Bottom Right) Long-range monitoring at Station 8.

I.5. Test Pile 2A–Top Segment, Super Kong 600 Vibratory Hammer

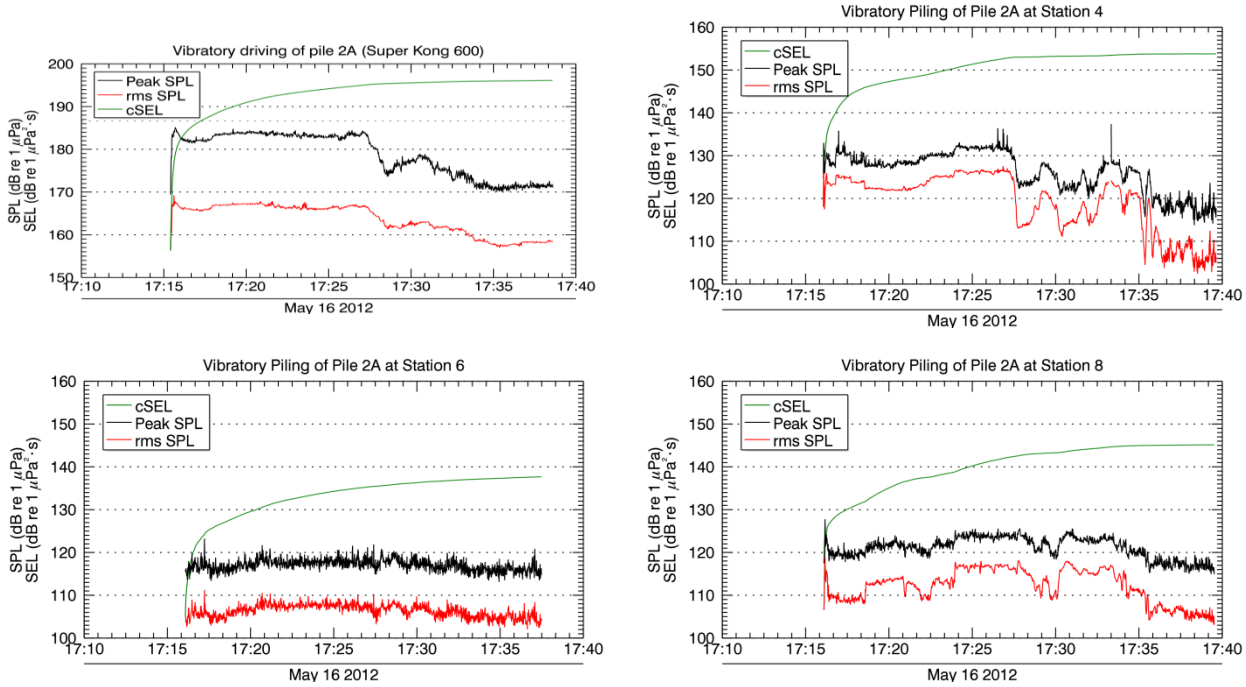

Figure 113. Plots of received sound levels for vibratory pile driving at Test Pile 2A, 16 May 2012. (Top Left Short-range monitoring at 34.1 ft horizontal distance. (Top Right) Long-range monitoring at Station 4. (Bottom Left) Long-range monitoring at Station 6. (Bottom Right) Long-range monitoring at Station 8.

I.6. Test Pile 2B–Top Segment, ICE 66 Vibratory Driver

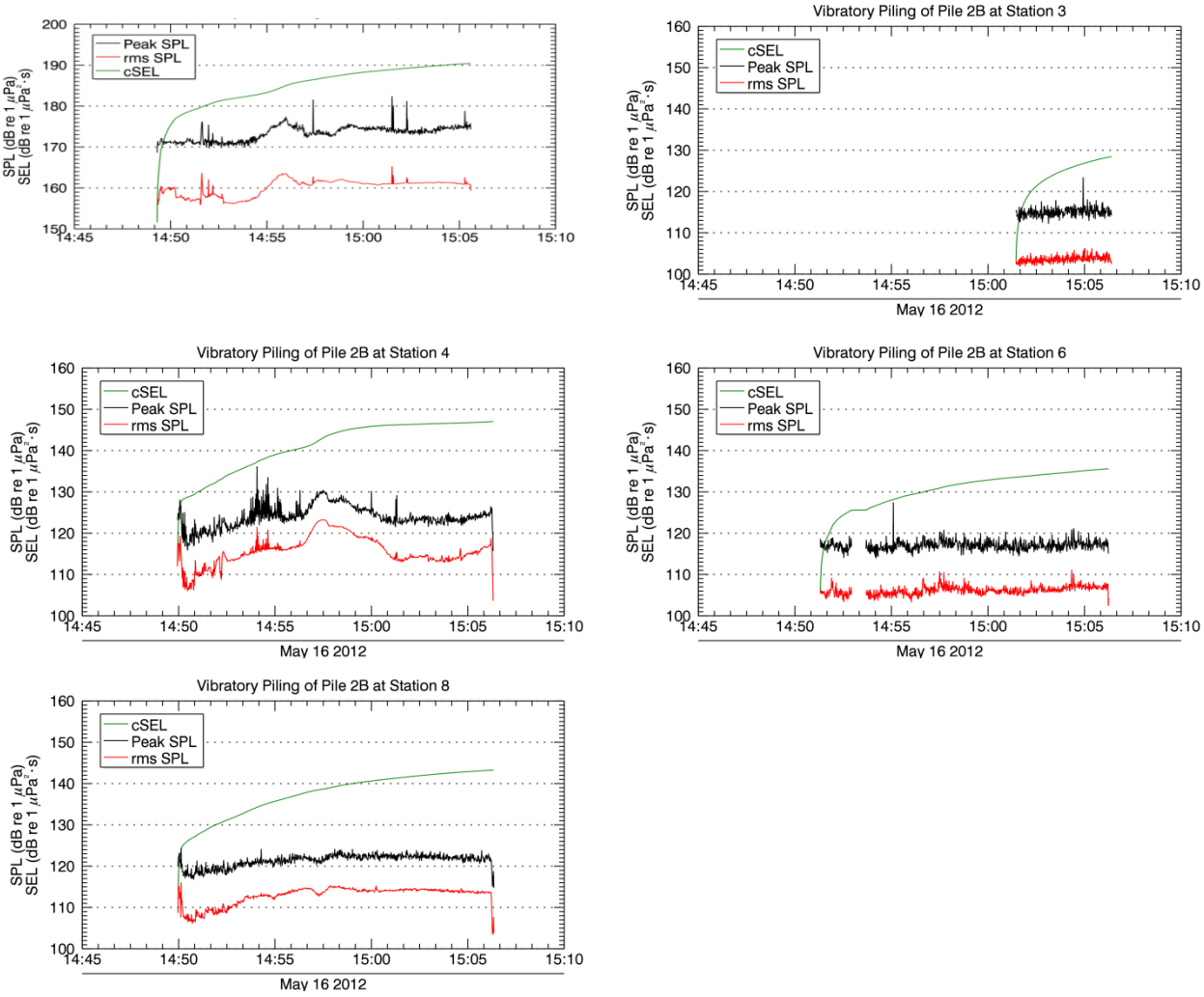

Figure 114. Plots of received sound levels for vibratory pile driving at Test Pile 2B, 16 May 2012. (Top Left) Short-range monitoring at 35.4 ft horizontal distance. (Top Right) Long-range monitoring at Station 3. (Middle Left) Long-range monitoring at Station 4. (Middle Right) Long-range monitoring at Station 6. (Bottom Left) Long-range monitoring at Station 8.

I.7. Test Pile 2B–Top Segment, Super Kong 600 Vibratory Hammer

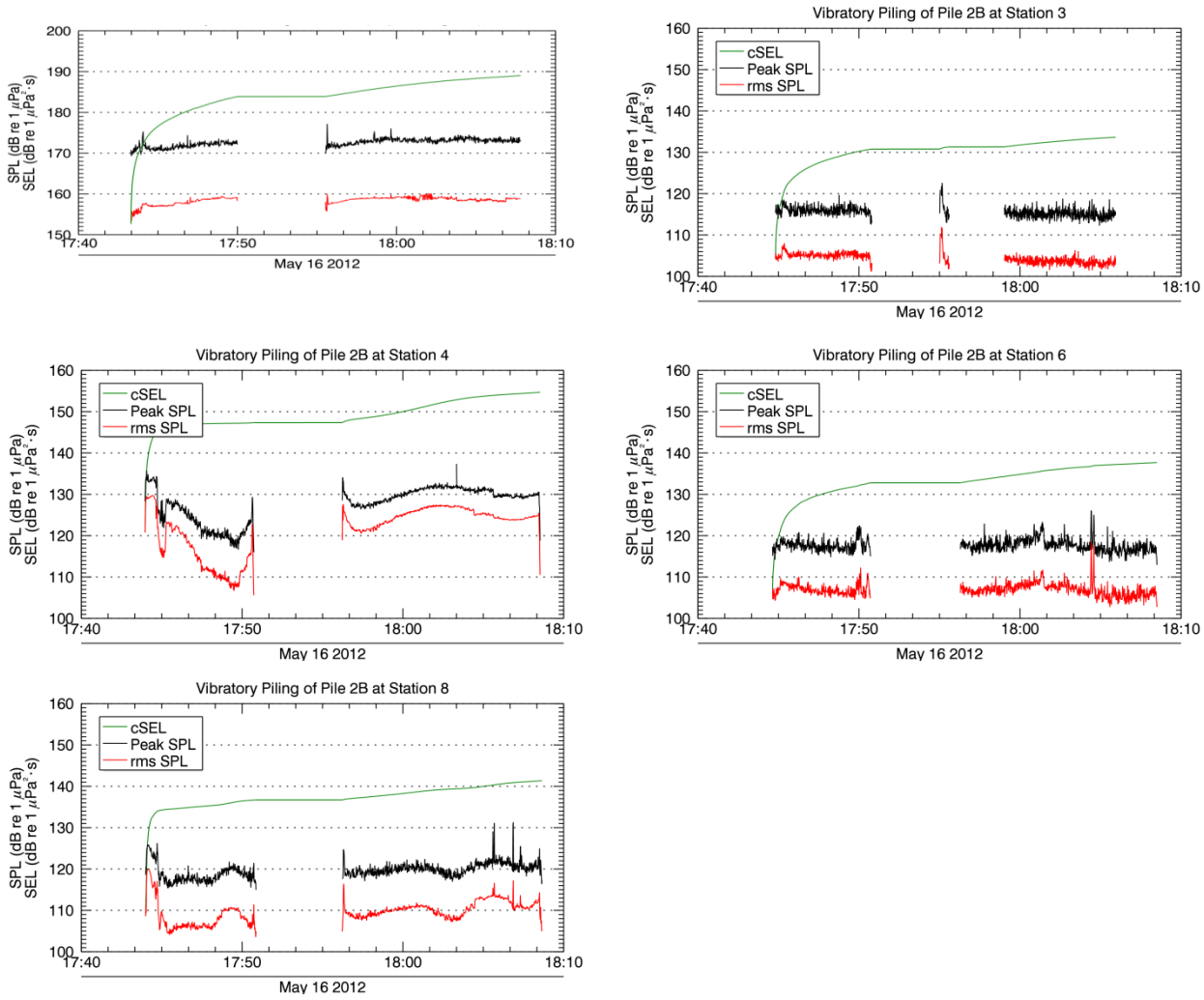

Figure 115. Plots of received sound levels for vibratory pile driving at Test Pile 2B, 16 May 2012. (Top Left) Short-range monitoring at 35.4 ft horizontal distance. (Top Right) Long-range monitoring at Station 3. (Middle Left) Long-range monitoring at Station 4. (Middle Right) Long-range monitoring at Station 6. (Bottom Left) Long-range monitoring at Station 8.

I.8. Test Pile 3A–Bottom Segment, ICE 66 Vibratory Driver

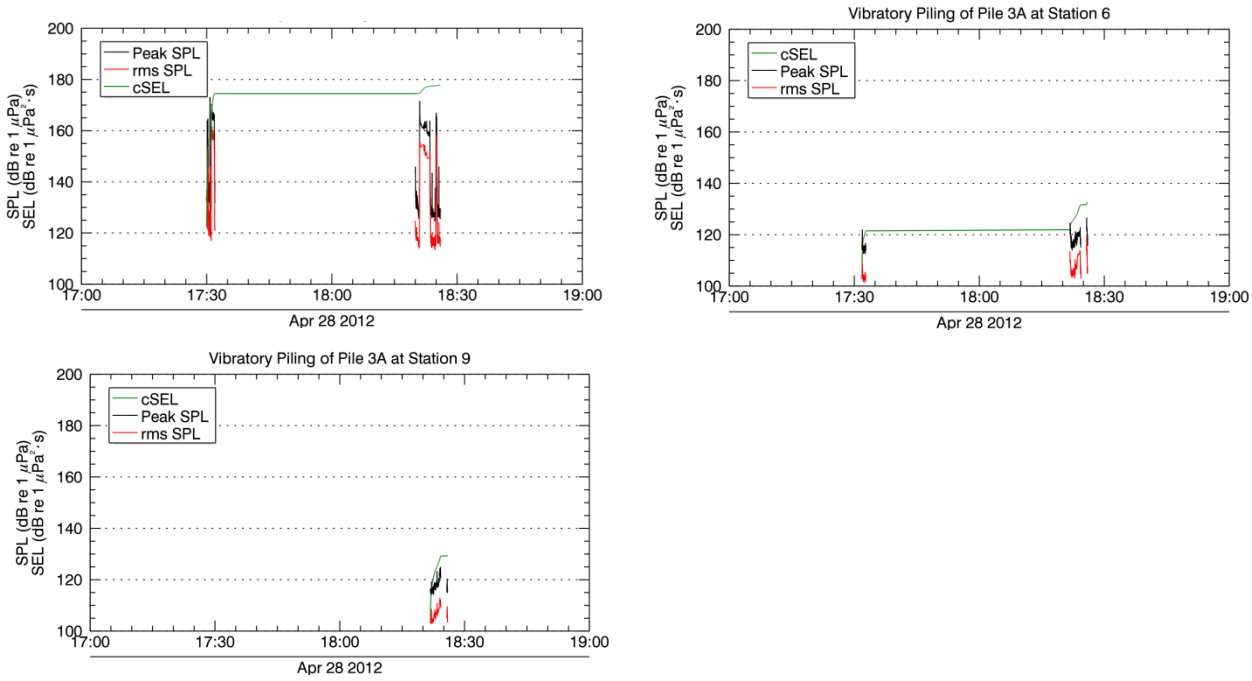

Figure 116. Plots of received sound levels for vibratory pile driving at Test Pile 3A, 28 Apr 2012. (Top Left) Short-range monitoring at 39.7 ft horizontal distance. (Top Right) Long-range monitoring data from Station 6. (Bottom Left) Long-range monitoring data from Station 9.

I.9. Test Pile 3B–Top Segment, Super Kong 600 Vibratory Hammer

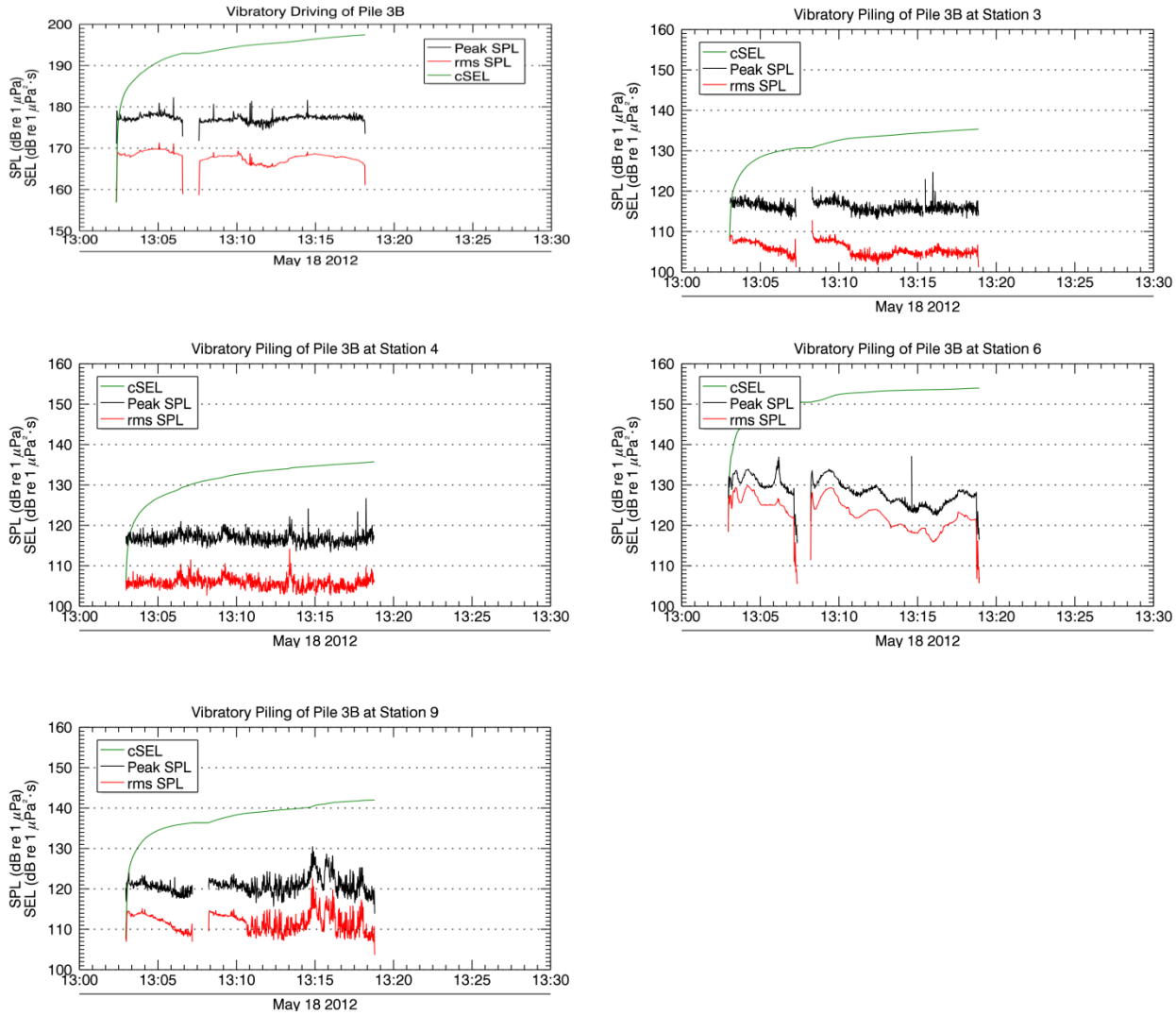

Figure 117. Plots of received sound levels for vibratory pile driving at Test Pile 3B, 18 May 2012. (Top Left) Short-range monitoring at 33.7 ft horizontal distance. (Top Right) Long-range monitoring data from Station 3. (Middle Left) Long-range monitoring data from Station 4. (Middle Right) Long-range monitoring data from Station 6. (Bottom Left) Long-range monitoring data from Station 9.

I.10. Test Pile 4A–Bottom Segment, Super Kong 600 Vibratory Hammer

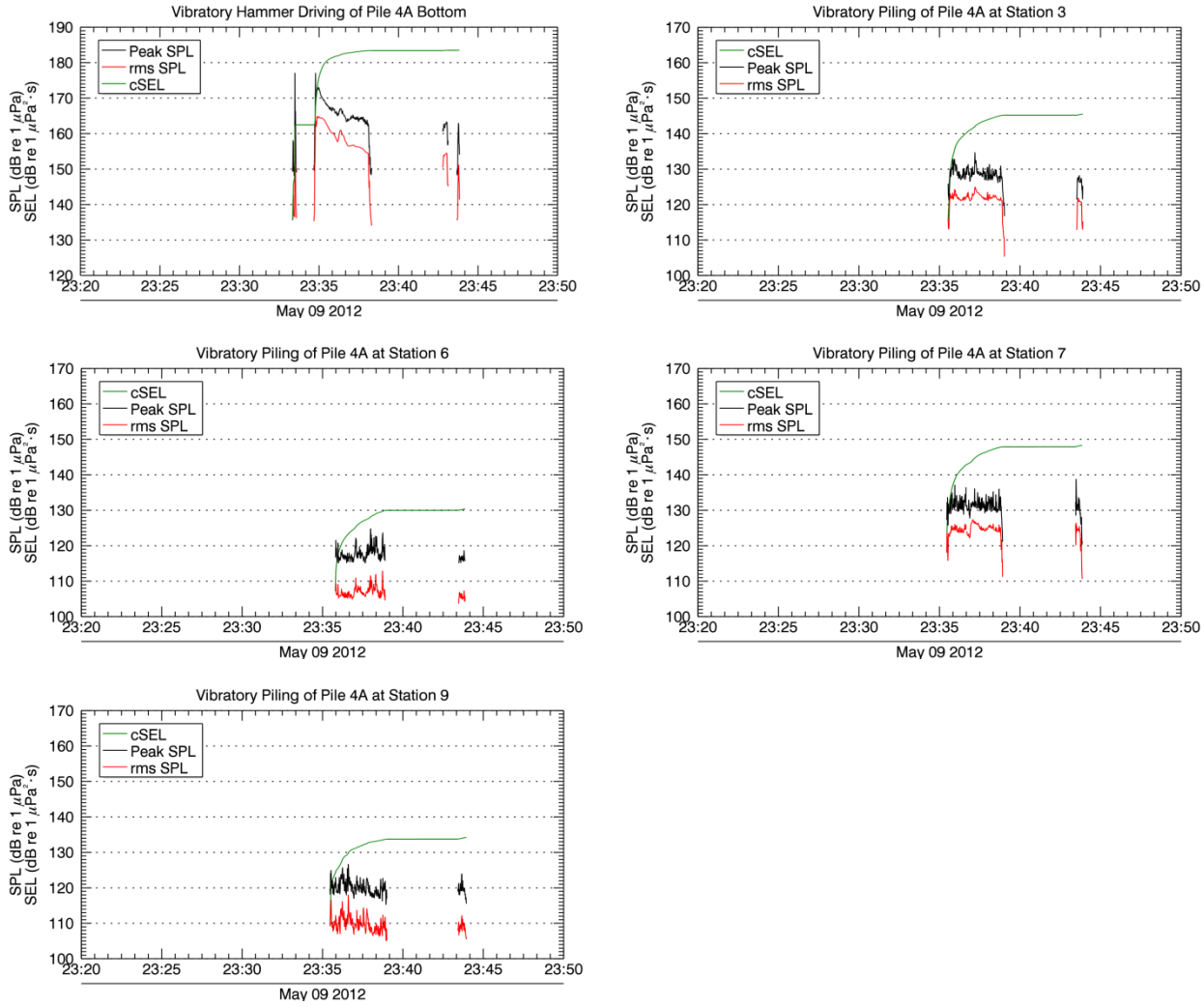

Figure 118. Plots of received sound levels for vibratory pile driving at Test Pile 4A, 9 May 2012. (Top Left) Short-range monitoring at 33.5 ft horizontal distance. (Top Right) Long-range monitoring at Station 3. (Middle Left) Long-range monitoring at Station 6. (Middle Right) Long-range monitoring at Station 7. (Bottom Left) Long-range monitoring at Station 9.